NASA CR-143667

EARTH OBSERVATORY SATELLITE SYSTEM DEFINITION STUDY

REPORT NO. 3: DESIGN/COST TRADEOFF STUDIES

- Appendix D: EOS Configuration Design Data
- Part 2: Data Management System Configuration

GRUMMAN

EARTH OBSERVATORY SATELLITE SYSTEM DEFINITION STUDY

REPORT NO. 3: DESIGN/COST TRADEOFF STUDIES

- Appendix D: EOS Configuration Design Data
- Part 2: Data Management System Configuration

Prepared For

NATIONAL AERONAUTICS AND SPACE ADMINISTRATION

GODDARD SPACE FLIGHT CENTER

GREENBELT, MARYLAND 20771

Prepared By

GRUMMAN AEROSPACE CORPORATION

BETHPAGE, NEW YORK 11714

NAS 5-20520

September 1974

CONTENTS

GENERAL AND SYSTEM CONFIGURATION

APPENDIX D.2 DATA MANAGEMENT SYSTEM

D.2.1 General and System Configuration

The EOS Data Management System (DMS) is composed of several subsystems (system elements) which because of their intrinsic complexity are, per se, systems. The system elements have basic purposes and are connected together so that the DMS can support the EOS Program by providing:

- o Payload Data Acquisition and Recording
- o Data Processing and Product Generation
- o Spacecraft and Processing Management and Control
- o Data User Services

Two types of data acquisition and processing configurations exist within the DMS: primary and secondary configurations. The primary or high-data rate configuration is composed of Primary Ground Stations (PGSs) and the Central Data Processing Facility (CDPF) elements. Three PGSs* are assumed to exist, but if the Tracking and Data Relay Satellite System (TDRSS) is used part of the TDRSS ground station becomes the PGS.

A secondary or Local User System (LUS) configuration also exists. The LUS includes the concept of the Low Cost Ground Station (LCGS), and the LUSs receive EOS edited (compacted) payload data at lower rates than do the PGSs. Data processing and analysis capabilities are incorporated within the LUS terminals. A potential population of 10 to several-hundred LUSs can be assumed to exist without materially impacting the basic DMS concepts.

Basically the DMS contains the ground located EOS system operational elements that convey, handle, convert, distribute, and manage the high-rate and edited lower rate spacecraft (S/C) Earth sensing instrument generated payload data.

---

* Assumed to exist at the STDN stations in Alaske (ULA); Goldstone, California (GDS), and the GSFC Engineering Test Center (ETC) at Greenbelt, Maryland.

D.2.1.1 System Configuration

A conceptual EOS DMS configuration is shown in Figure D.2.1.1-1. The Earth Observatory Satellite (EOS), in sun-synchronous orbit around the Earth and under control of the PCC, directly delivers high-rate (to 240 Mb/s) payload data to the PGSs. The PGSs are modified STDN stations that provide the S/C and ground communications capability for commanding and receiving data from the S/C housekeeping systems at S-Band carrier frequencies, and for receiving the payload data at X-Band carrier frequencies and subsequently recording the baseband digital payload data.

A Digital Data Processing System (DDPS) and Spacecraft Command Encoder (SCE) located at each PGS are used to interface the NASCOM circuits to and from the PCC. During payload data reception times, a Status Formatter (SF) collects payload data receiving and recording systems' status information and formats the information so that it can be handled by the DDPS and transmitted through the NASCOM circuits to the PCC. In this way the PCC can receive a near-real-time indication of how well the EOS-to-PGS communications link and PGS data acquisition and recording equipment are operating.

The CDPF is composed of several facility equipment and personnel organizations. All EOS information and system management control are handled by the Information Management System (IMS), part of the Information Services System (ISS). Other elements of the ISS are the LUS Diagnostic and Equipment Laboratory (LDEL), the Applications Program Development Laboratory (APDL), payload data user terminal and personnel interfaces, the data product archive and shipping areas, and service personnel. The Central Processing System (CPS) performs payload data processing and archiving.

Figure D.2.1.1-2 provides an overview of the CDPF organizations. The APDL and LDEL form the centralized part of the LUS concept and are tradeable

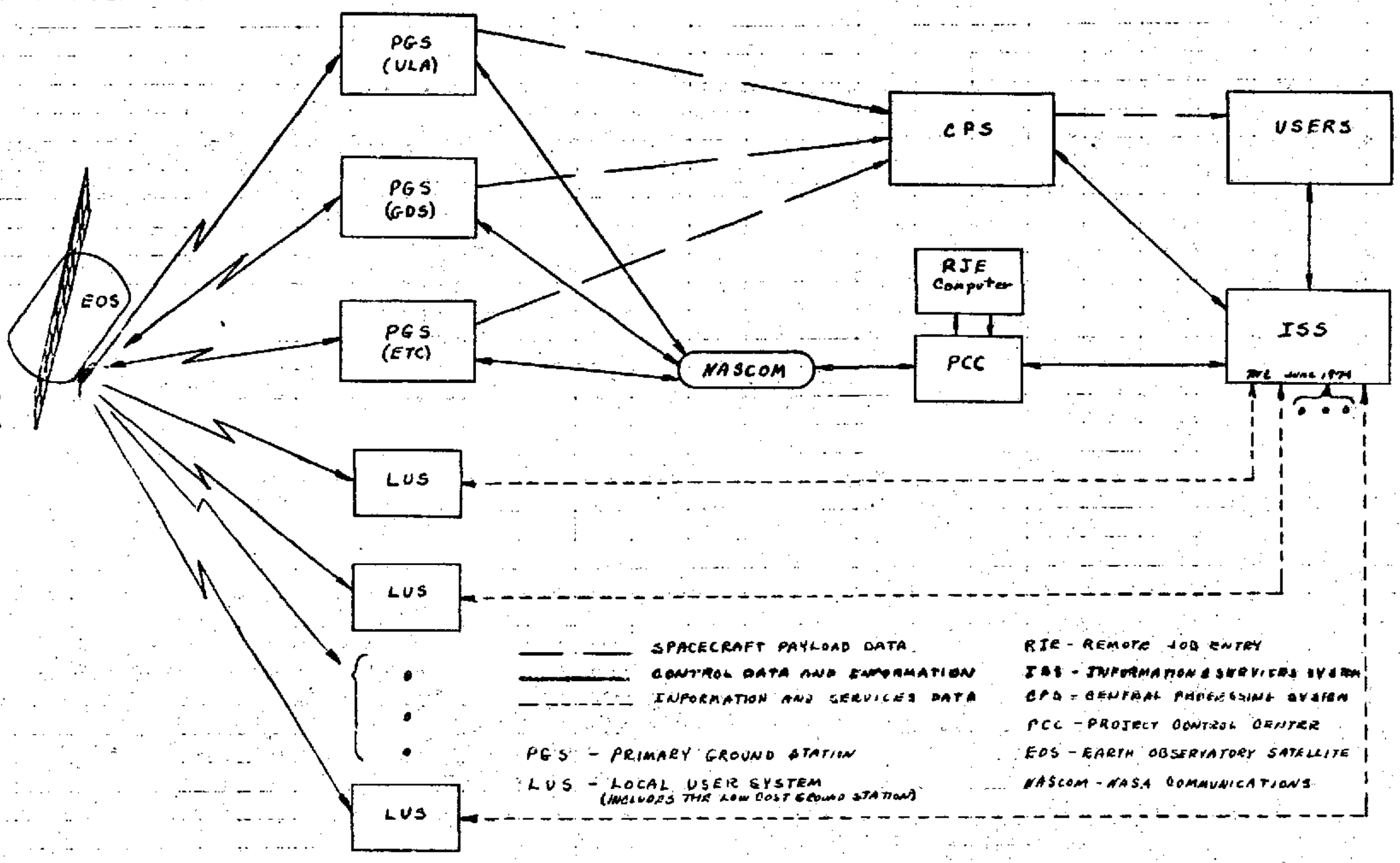

Figure D.2.1.1-1 EOS DATA MANAGEMENT SYSTEM (Data Communications, Control, Processing, and Information Services)

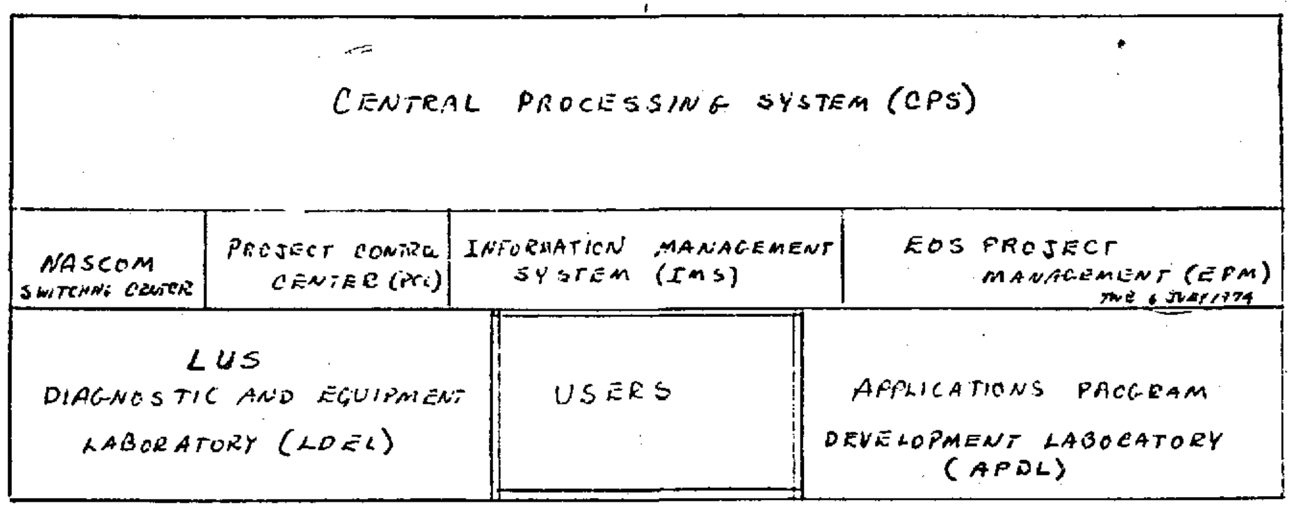

Figure 2.1-2 CENTRAL DATA PROCESSING FACILITY (CDPF) ORGANIZATION

items. Applications computer programs (data analyses programs) are developed and modified in the APDL for the LUSs operational personnel. The LDEL provides a centralized concept for remote LUS computerized equipment troubleshooting and operator support.

Existence of the APDL and the LDEL is predicated on the assumptions that (1) the LUS operators are primarily applications oriented, not computer operators or programmers, and (2) that the LUS equipment forms a family of configurations that is composed of basic equipment plus optional equipment for faster and greater data analyses activities, dependent on the particular local operators applications areas. If only a few LUSs are implemented the APDL and LDEL may not be cost-effective and hence, would not be considered as part of the DMS.

Centralized data processing is performed in the Central Processing System (CPS) It performs basic radiometric and geometric data processing corrections, archives the processed data, and produces digital and photographic payload data products for data users.

Data users that prefer to receive EOS edited data at lower transmission rates than possible at the PGSs can have LUSs. The concept for LUSs includes the EOS-to-LUS edited (compacted) direct payload data delivery LCGSs. The LCGS contains a programmed tracking capability to steer a small X-Band antenna on a line-of-sight path to the orbiting EOS. A local preamplifier, downconverter, and RF receiver are provided for data reception at rates to 20 Mb/s. Binary Phase Shift Keyed (BPSK) antipodal data signals are then fed to a demodulator and signal conditioner, and recorded. Recorded data are played through the LUS minicomputer and formatted on Computer Compatible Tape (CCT), and the data then may be displayed, processed, and analyzed as suites the particular LUS operator.

Note that the processing and display elements of the LCGS form an equipment subset that can be used independently for user data applications. Should other than the direct data delivery method be used to supply the LCGS with EOS payload data

then the processing and display equipment subset can be augmented with (for example) a computer-to-computer telecommunications interface and receive data from the CDPF or a regional facility in a relayed mode. Therefore, the LUS is a generalized data user concept in which the LCGS is only one of the possibilities for a local user equipment terminal.

The centralized control element for the DMS is the IMS. The IMS provides the CPS data users with an order entry into the DMS and a means to obtain order status information; and for the LUS operators, a digital and voice means of communicating their needs for EOS predicted and precision ephemeris and S/C attitude data, and planned compacted data transmission to the particular LCGS reception areas.

In turn, the IMS performs preliminary user data acquisition scheduling and CPS scheduling for the processing and handling of acquired payload data. Preliminary data acquisition schedules are forwarded to the PCC where the detailed EOS schedules are generated. The PCC provides the IMS with precision ephemeris and S/C attitude data that are forwarded to the CPS at the times needed to process PGS payload recorded data. Also the PCC operators review and send S/C and PGS systems' status information to the IMS so that this central element can be accessed to determine the total system state or the state of any system element.

The EOS DMS configuration described may be modified as the tradeoff study continues. For example, should the TDRSS be cost-effective to replace the PGS systems, or should a relayed data delivery method be used to supply the LUSs in place of the direct delivery LCGS concept, then changes would become necessary to the DMS configuration shown in Figure D.2.1.1-1.However, the basic information, processing, and control elements would still be included to a larger or lesser degree in the modified DMS configurations.

STDN MODS

D.2.2 STDN Modifications

The STDN modifications that have been considered to the network systems for acquiring and recording high-rate EOS payload data at the PGSs are discussed in these paragraphs. Basic modifications would be made at the ULA, GDS, and ETC sites, and they are necessary to accommodate the X-Band 240 Mb/s TM and HRPI composite data signals. Quadrature Phase Shift Keying (QPSK) data modulation is assumed where the TM data are modulated on the inphase (I) channel and the HRPI data are modulated on the quadrature (Q) channel.

Equipment modifications are of two types (i.e., those to the station RF/IF equipment, and those necessary for data handling and recording). These modifications include:

a. Replacing the existing S-Band antenna feed with a dual S/X-Band feed while retaining the existing 30/40 foot diameter reflectors (30' - ETC, 40' - ULS, 30' - GDS).

b. Providing a new uncooled X-band parametric preamplifier which yields an overall system noise temperature of 165° K.

c. Providing a new X-band down-converter and receiver with an approximately 200 MHz 3 dB bandwidth.

d. Providing a new 240 Mbps QPSK demodulator.

e. Providing either two 240 Mb/s data recorders or three 120 Mb/s recorded

f. Providing a Microcomputer Status Formatter.

D.2.2.1 RF/IF Modifications

Those mofications to the RF/IF station subsystem are shown in Figure D.2.2.1-1. Alternative configurations currectly being considered center around utilizing more of the existing STDN equipment in the X-band receiver e.g., the

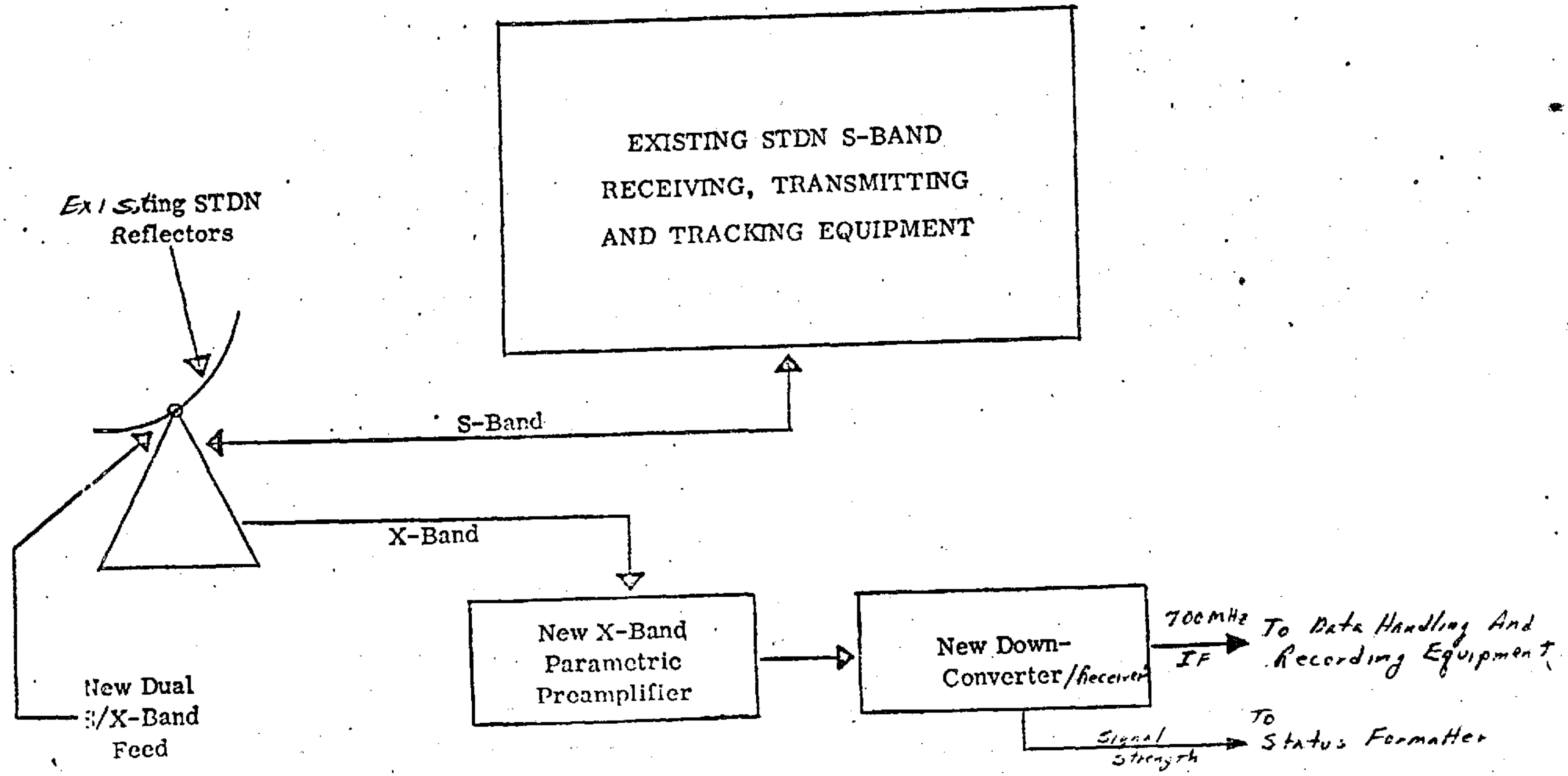

Fig. D.2.2.1-1 Network Modifications for Wideband (240 Mb/s) QPSK Link to STDN PGSs.
(Baseline Configuration)

reference oscillator. Following careful consideration of these possibilities, the ultimate configuration will be selected based on good engineering practice (i. e., maximizing reliability and performance; minimizing design risk and maintenance while meeting cost and schedule commitments).

Currently estimated costs for the RF/IF modifications are listed in Table D 2.2.1-1 It is expected that these estimated costs will change as the EOS system optimization continues. From the Table values, the total RF/IF modifications and subsystem O & M costs for 1-year of operation total $ 1,203. 5K for the three sites, and for 5-years total to $ 2,763. 5K.

D.2.2.2 Data Handling/recording Modifications

Two concepts have been considered for acquiring the EOS payload data at the PGSs. Figure 2.2.1-2 shows the currently favored method where channel ambiguity resolution (CAR) between the inphase (I) and quadrature (Q) demodulator channels occurs within the QPSK Demodulator and Signal Conditioner (QDSC) Unit. In this case the TM data streams are recorded on one 120 Mb/s recording unit and the HRPI data streams are recorded on a second 120 Mb/s recorder. A third recorder is provided as a backup in case either prime recorder is inoperative during a data acquisition pass. There is also a second QDSC Unit available as a backup.

The second concept, Figure D.2.2.1-3 indicates that the full 240 Mb/s data stream is recorded on one unit. Resolution between the TM & HRPI I & Q channels is not necessary because the full composite data stream can be transparently captured on a single recorder. As before, however, a second QDSC Unit and recorder are provided as a backup in case either prime unit was inoperative immediately prior to a data reception satellite pass.

For either concept a microcomputer SF is included. It receives signal strength indications from the RF/IF downconverter/ receiver, demodulator and signal conditioner lock indication from the QDSC units, and in the case of the CAR concept, an indicative TM/HRPI synchronization pattern count that also can be

Table D.2.2.1-1 Estimated Costs for RF/IF Modifications

Cost Elements	Nonrecurring ($K) plus Prototype Equipment		Recurring $K per Site for O & M	
			Per Modified Site	For Three Sites
Dual S/X-band feed		70.0	35.0	105.0
Uncooled Parametric Amp		60.0	30.0	90.0
Downconverter/ Receiver		70.0	35.0	105.0
Spares[1]			65.0	195.0
Subsystem Design	(12 mm)[2]	45.0	-	-
Subsystem Documentation	(6 mm)[2]	22.5	-	-
Installation, test, & Checkout (Misc. hardware)	(4 mm)[2] & $2K Misc. hardware	-	17.0	51.0
Operation & Maintenance (O&M) per year	(60 mm)[3] per year at $12.50/ hour	-	130.0	390.0
Subsystem totals for First Year		267.5	312.0	936.0
Including O&M for 5 years[4]		-	832.0	2496.0

1. Includes 1 paramp and 1 down converter/receiver for each site
2. Engineering and documentation cost per manmonth (mm) is $3.75K with overhead and fee
3. NASA Contract Labor Rate of $12.50 per hour assumed for O&M personnel
4. Includes 4 additional years cost for O&M personnel

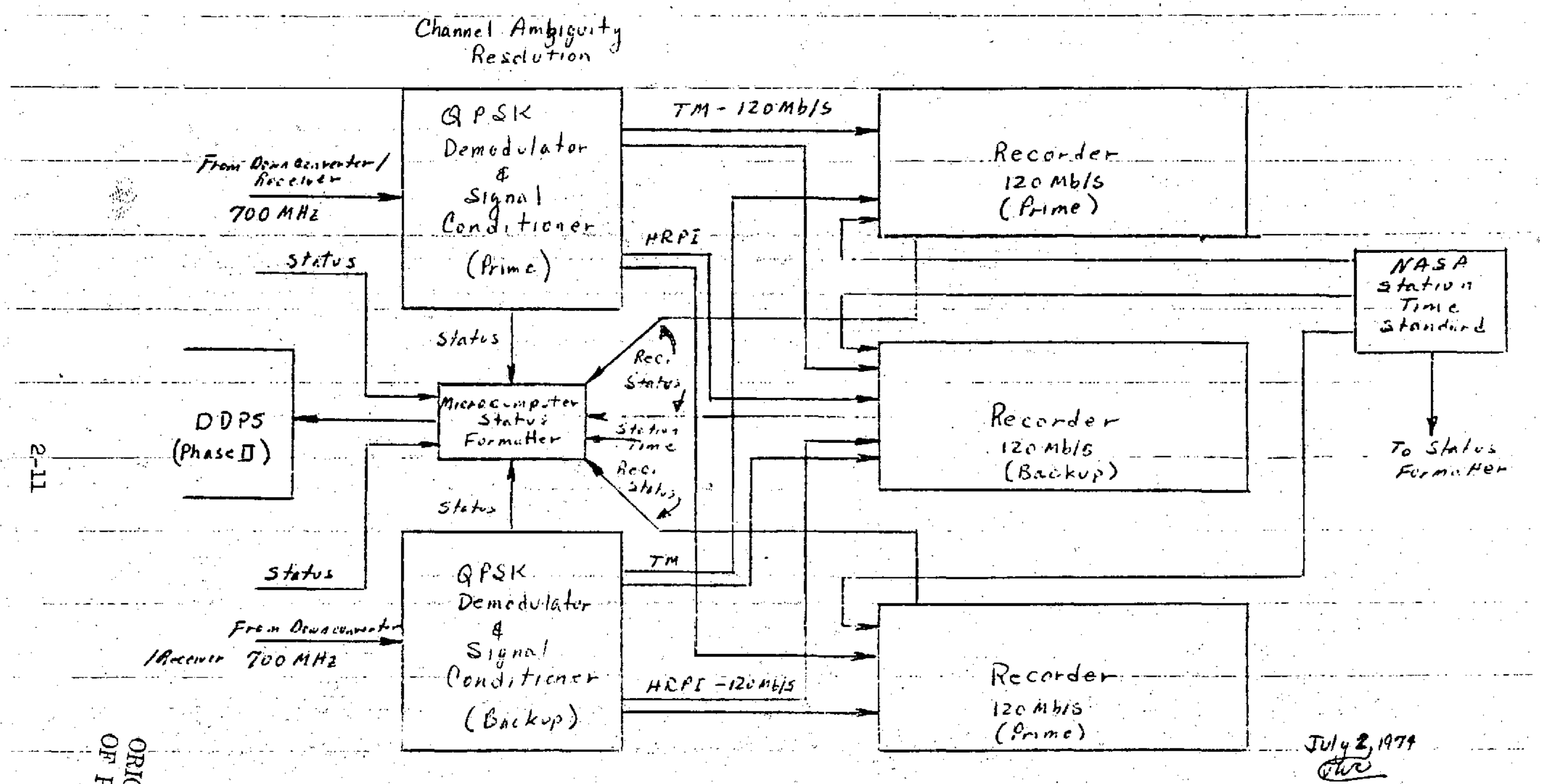

Fig. D.2.2.1-2 Primary Ground Station - 120 Mb/s Recording Station - Data Handling & Recording Mods

2-11

ORIGINAL PAGE IS OF POOR QUALITY

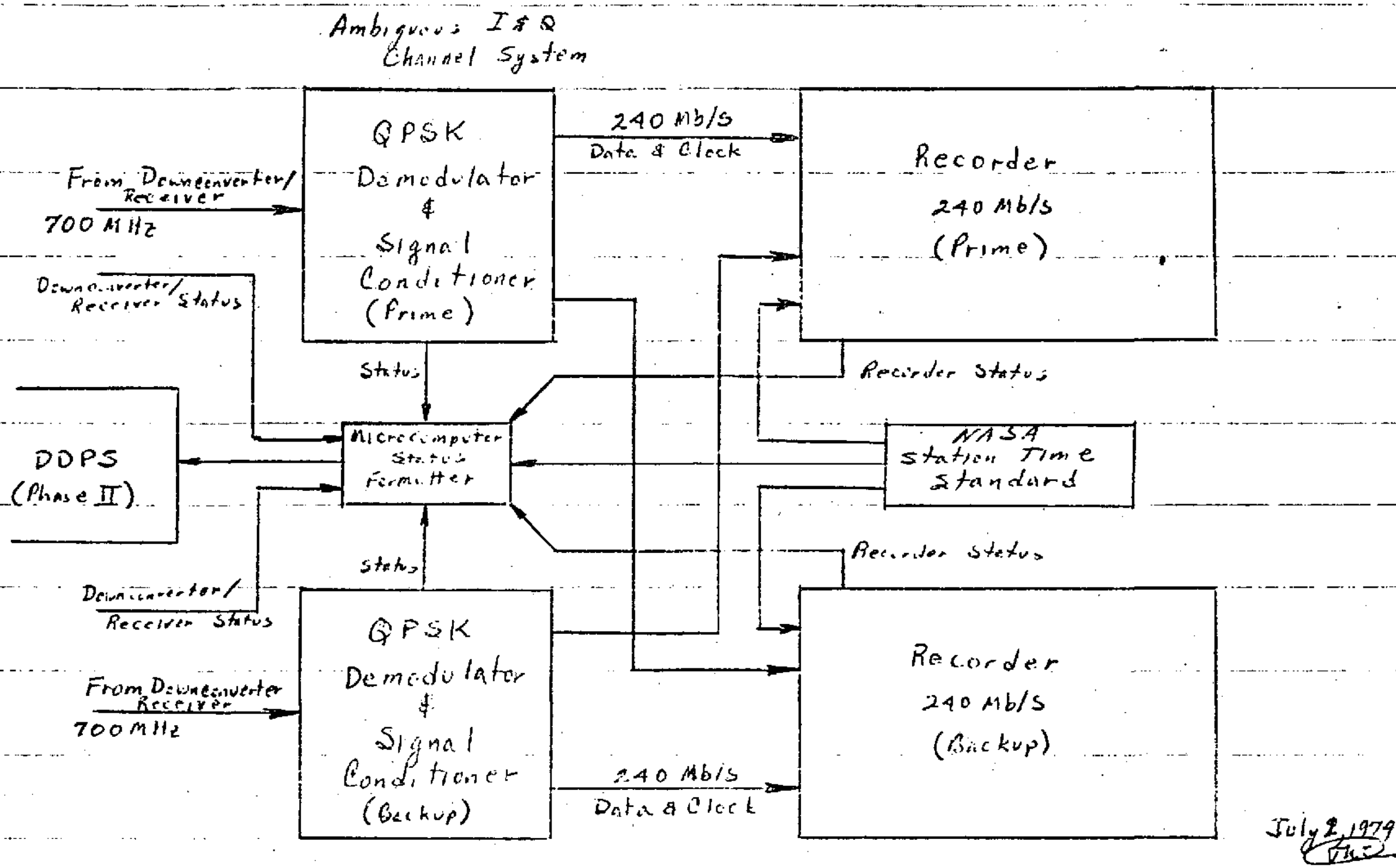

Fig. D.2.2.1-3 Primary Ground Station - 240 Mb/s Recording Station - Data Handling & Recording Mod

used for a cursory data quality estimator. Recorder status indications are also input to the SF which, with station time standard tags, formats 1200-bit NASCOM message data inputs to the DDPS for forwarding to the PCC.

The estimated development and operational costs for the data handling/recording modifications are listed in Table D.2.2.1-2 Note that we have included costs for development of the high-rate recording/reproducing tape recorders. These development costs are thus not included in the CPS costs where additional high-rate recorders are used for TM/HRPI data playback into the processing system. From the table values the total subsystem modification and O & M costs for 1-year of operation are estimated at $2,309.5K, and for 5-years of use total $3,869.5K for the currently preferred recording concept; and, respectively for 1 and 5 years, $2,387.5K and $3,947.5K for the 240 Mb/s recording concept at the lower ($520K) estimated development cost.

Table D.2.2.1-2 Estimated Costs for the Data Handling/Recording Modifications

Cost Element	Nonrecurring ($K) & Prototype Equipment		Recurring $K per Site and for O & M			
			Per Modified Site		For Three Sites	
	240 Mb/s	120 Mb/s	240 Mb/s	120 Mb/s	240 Mb/s	120 Mb/s
QPSK Demodulator and Signal Conditioner	145.0	155.0	37.0	39.0	111.0	117.0
Recording Units [1]	300.0 → 700.0	185.0	200.0 (1 unit)	270.0 (2 units)	600.0	810.0
Status Formatter	30.0	30.0	5.0	5.0	15.0	15.0
Spares [2]	-	-	237.0	174.0	711.0	522.0
Subsystem Design [3]	(6mm) 22.5	(6mm) 22.5	-	-	-	-
Subsystem Documentation [3]	(6mm) 22.5	(6mm) 22.5	-	-	-	-
Installation, test, and Checkout & Misc. Hardware [3]	(3mm) & $ 2K Misc. -	(3mm) & $2K Misc. -	13.5	13.5	40.5	40.5
O & M Per Year [3]	60 mm/year -	60mm/year -	130.0	130.0	390.0	390.0
Subsystem Totals for First Yr.	520.0 → 920.0	415.0	622.5	631.5	1867.5	1894.5
Including O&M for 5 Years	-	-	1142.5	1151.5	3427.5	3454.5

1. Cost estimates for 240 Mb/s units from RCA, for 120 Mb/s from Amplex. Quantity discounts, if any, not applied for the current estimates.
2. One QDSC and Recorder Unit assumed per station.
3. Engineering, documentation, and O&M costs assumed the same as indicated for Table 2.10.4-1.

D.2.2.3 Modification Summary Costs

Cost estimates developed in the two preceding paragraph sections are summarized in Table D.2.2.1-3in terms of development and installed costs and O & M costs for 1 and 5 years. The decision to use two 120 Mb/s recorders with a spare unit per site is based on the lower total system cost estimate of $ 2733. 0K as opposed to the higher 240 Mb/s recording systems cost of $ 2811. 0K, where the lower 240 Mb/s recorder and prototype development cost of $ 300. 0K has been assumed (Table D.2.2.1-2 The 120 Mb/s recording systems choice is also influenced by input elements and the costs therefore of the CPS (Paragraph 2. 10. 4. 5).

The O & M costs include one full time RF/IF subsystem operator (4 shifts) for 24-hour per day operation and one maintenance person on a standard 40-hour per week shift. Similar personnel costs are assumed for the Data Handling/Recording Subsystem operation and maintenance activities.

However, it is most reasonable to assume that the site O & M EOS personnel would be shared with those personnel normally associated with the STDN stations' operations. For this sharing activity, it is assumed that one-fourth of the O & M cost would be accountable to the EOS program and the remaining three-fourths of the O & M cost would be borne by the STDN operational budget. Based on the cost sharing assumption, the STDN modification and operational costs are estimated as $2 , 783. 0K for installed, tested, and documented equipment with spares with a yearly O & M cost of $ 195. 0K (1/4 x $ 780. 0K) and a 5-year O & M budget of $ 975. 0K (1/4 x $ 3900. 0K).

Table D.2.2.1-3 STDN Modification Summary Costs

Cost Elements	Equipment Dev. & Installed ($K) at 3 stations with Spares	O & M ($K)[2]	
		for 1 yr.	for 5 yrs.
RF/IF Modifications	813.5	390.0	1950.0
Data Handling/Recorder Modes			
240 Mb/s Recorders[1]	1997.5	390.0	1950.0
120 Mb/s Recorders	1919.5	390.0	1950.0
Subsystem Totals			
240 Mb/s Recs.	2811.0	780.0	3900.0
120 Mb/s Recs.	2733.0	780.0	3900.0

(1) Lower nonrecurring cost of $520.0K assumed for 240 Mb/s systems.
(2) With cost sharing only 0.25 of O&M accountable to EOS Program.

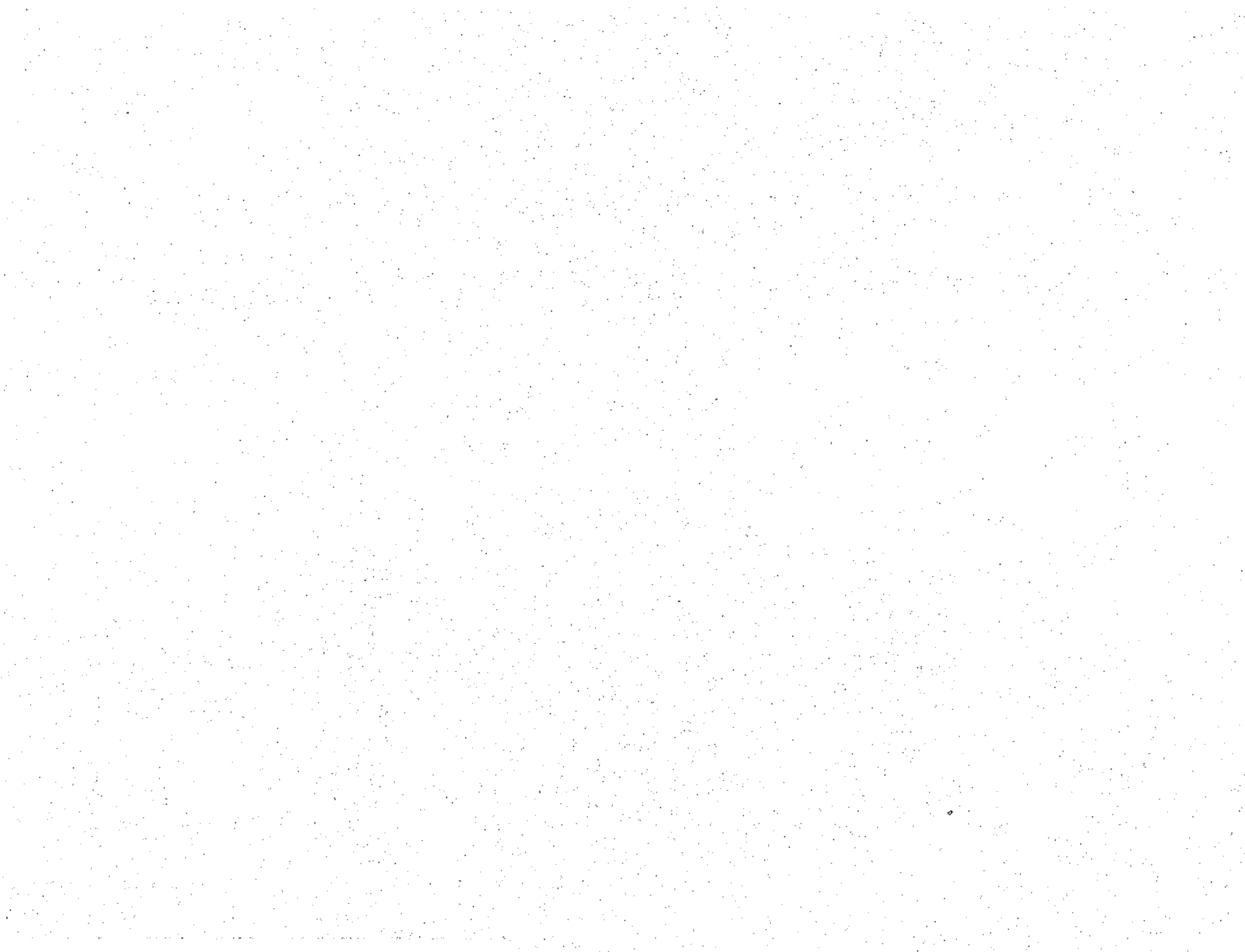

GENERAL STRUCTURE

D.2.3. Central Data Processing Facility

D.2.3.1. General Structure

The general structure of the central data processing facility (CDPF) is shown in Fig. D.2.3.1-1. Each of these areas will be discussed in the following sections to the extent necessary to define the major functions and to quantitatively define the parameters that affect size or throughput rate. A general subdivision into functional area is:

- o storage or archival of the image data
- o process of the image data
- o management of the data (information management system, IMS) including cataloging, retrieval, interface with users.
- o product generation & distribution

Each of these functional areas has an impact on system cost and each has its particular problem areas associated with the handling of the data volume planned for EOS and the required throughput rates that follow from these volumes.

D.2.3.1.1 Levels of Processing

The data received from the EOS spacecraft must be processed to correct for both internal and intrinsic system errors and natural errors (e.g. earth curvature and earth rate) before the final products are generated. Three levels of processing have been identified which are:

TYPE I — Radiometric Calibration and one-dimensional scan line correction

TYPE II — Geometric correction, using the best estimates of S/C attitude and orbit, including two-dimensional resampling of the data to place it in the format of the selected grid.

TYPE III — Precision Geometric correction is, identical to Type II, expect that ground control points are located in the images so that a more precise resampling grid can be determined.

The general flow of data through the various processing steps is shown in Fig. D.2.3.1.-2. As shown, the composite data in a scene is separated by bands, and by detectors within each band to perform radiometric correction. Immediately following this one dimensional line ccan correction is performed using data available on the scanner nonlinearities. Upon completion of the Type I processing, the data would be archived and some products may be generated from this data.

A resampling grid is computed to map the desired map projection into the coordinate system of the scanner. This mapping makes use of orbit and attitude data as well as standard transformations which account for earth curvature, and earth rate. If this computed grid is accurate enough (accuracy is determined by system characteristics and/or users requirements) the image data is resampled according to this computed grid and the Type II processing is completed. If the grid is NOT accurate enough, it is corrected by locating ground control points (GCP's) in the scene (probably in only one band). The image data is then resampled according to this improved grid. For either Type II or Type III processing, a choice must be made of the interpolation algorithm for resampling. A by-product of the Type III processing is improved attitude and orbit estimates which update the auxilliary date that accompanies (in a header) the video scan lines.

A final step is the remerging and possibly reformatting of the multispectral data.

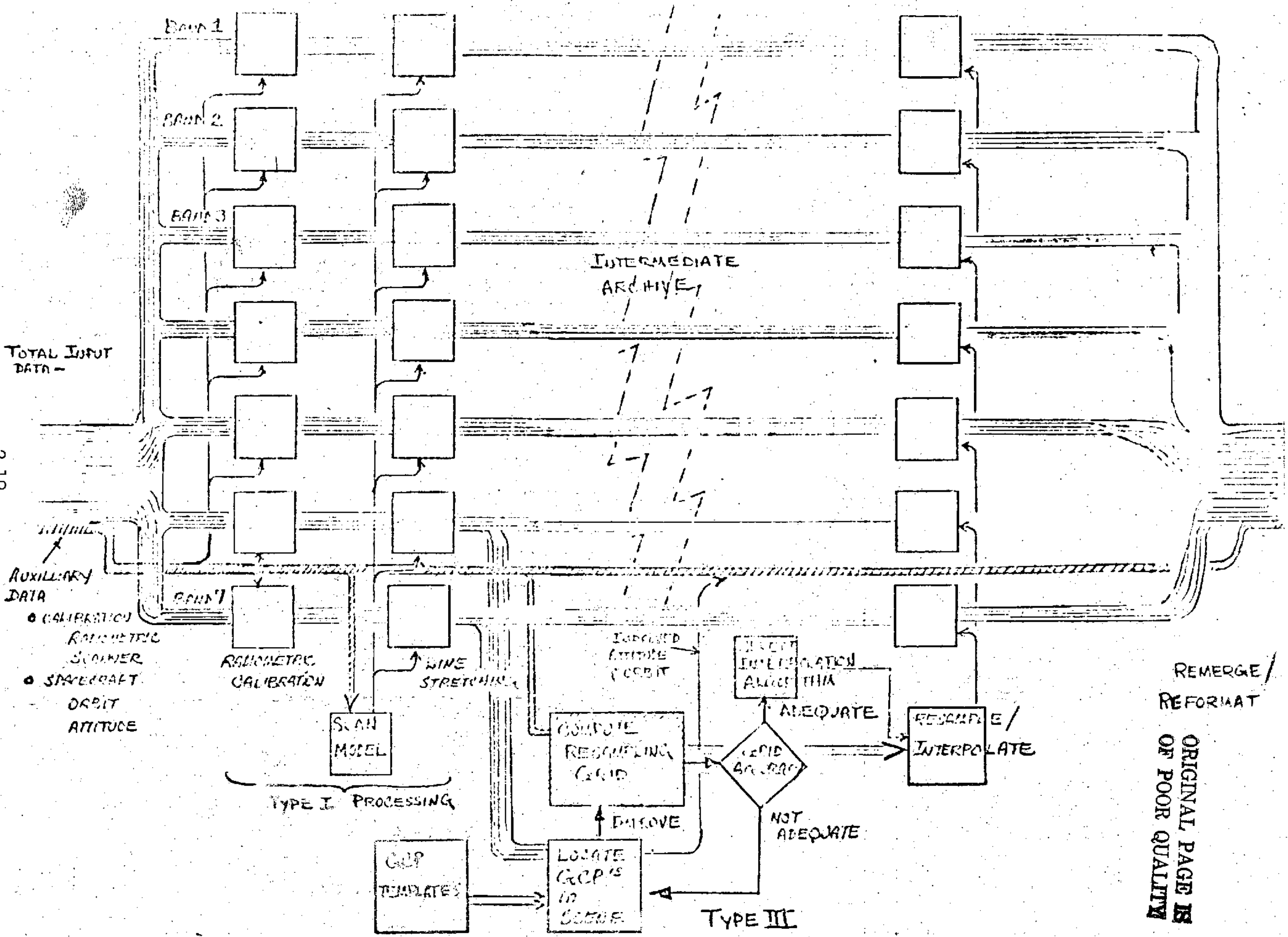

FIGURE D.2.3.1-2 CDP DATA FLOW

TYPE I PROCESSING

D.2.3.2. TYPE I Processing

D.2.3.2.1 Radiometric Corrections

By radiometric corrections, we refer to the amplitude corrections that are made to the individual picture samples. These corrections can be required for one or more of the following reasons:

1. A detector channel (in the group of 16 in one band) may have a different gain than the others.
2. A correction for atmospheric effects (may vary with spectral band) may be desirable for a particular scene. Basically, the reflectance (high resolution) bands measure the sunlight reflected from the surface of the earth. This measurement may be inaccurate due to attenuation or backscatter along the viewing path. A measurement of conditions in the local area will be necessary to predict this effect.
3. A correction may be desirable for slight differences in sun angle for various scenes.
4. A radiometric correction is usually made to picture samples before a film output is produced (the so-called "gamma correction" to match the characteristics of the film to be used).
5. Radiometric corrections may be required to "undo" any nonlinear A/D conversion which was done at the sensor. For example, logarithmic or square-root compression of the sensor outputs may be performed at the sensor to optimize signal-to-noise ratio. This is fairly common with PMT's (photomultiplier tubes). If this nonlinearity is introduced at the source, an inverse mapping must be done at the ground to remove it.

Regardless of the source of radiometric errors, the correction procedure amounts to a simple table look-up. When dealing with 6-bit samples (64 levels, 0 to 63), for example, only a 64-word table is needed to map input to output. Such a table is required for each detector in each of the spectral bands.

For (1) and (5) above, these corrections would be made routinely. The table for (1) would be updated occasionally (once per scene, possibly). Correction (4) would also be made for all film outputs. Correction (2) is, of course, dependent on the availablility of correction data, and

it appears that (2) and (3) would not be made routinely.

In most cases, the radiometric corrections must be made before any geometric corrections. This is because such geometric corrections as interpolation (one or two dimensional) must be made with radiometrically-correct values.

Corrections for radiometric errors utilize a simple table look-up procedure. One 6-bit word is used to produce another 6-bit word to correct for improper gains, or any of the other radiometric errors noted above. The real question seems to be the number of tables that must be stored.

It will be assumed that radiometric corrections for calibration errors are performed to all samples as these are put onto the high-density storage medium. However, at a later point, it may be necessary to correct again. RFP Reference 1.3.6 (page 43) considers the following numbers:

Six high resolution channels -- 8820 x 6300 pixels

One thermal channel -- 1900 x 1350 pixels

Total of -- 3.36×10^8 pixels/scene

Number of machine operations (equivalent of fixed point add) to perform radiometric corrections-4.69×10^8 instructions/scene.

Dividing the number of operations by the number of pixels gives 1.4 instrucions/pixels for table look-up.

D.2.3.2.2 One Dimensional Line-Scan Correction

(1) General Description

One of the simpler forms of geometric correction is line-stretching. It is perhaps useful to describe the one-dimensional error process rather carefully since some of the terminology will be useful later.

Consider the simplified scanning situation shown in Figure D.2.3.1-3. A scanner located at I begins scanning elements on a surface below the sensor. The scanner begins at angle $+\theta$ at time t=0 and sweeps at a constant angular rate across the scene. In synchronism with this process is a sampling clock that produces pulses spaced every Δ seconds. For this process to be perfect, several conditions must be met:

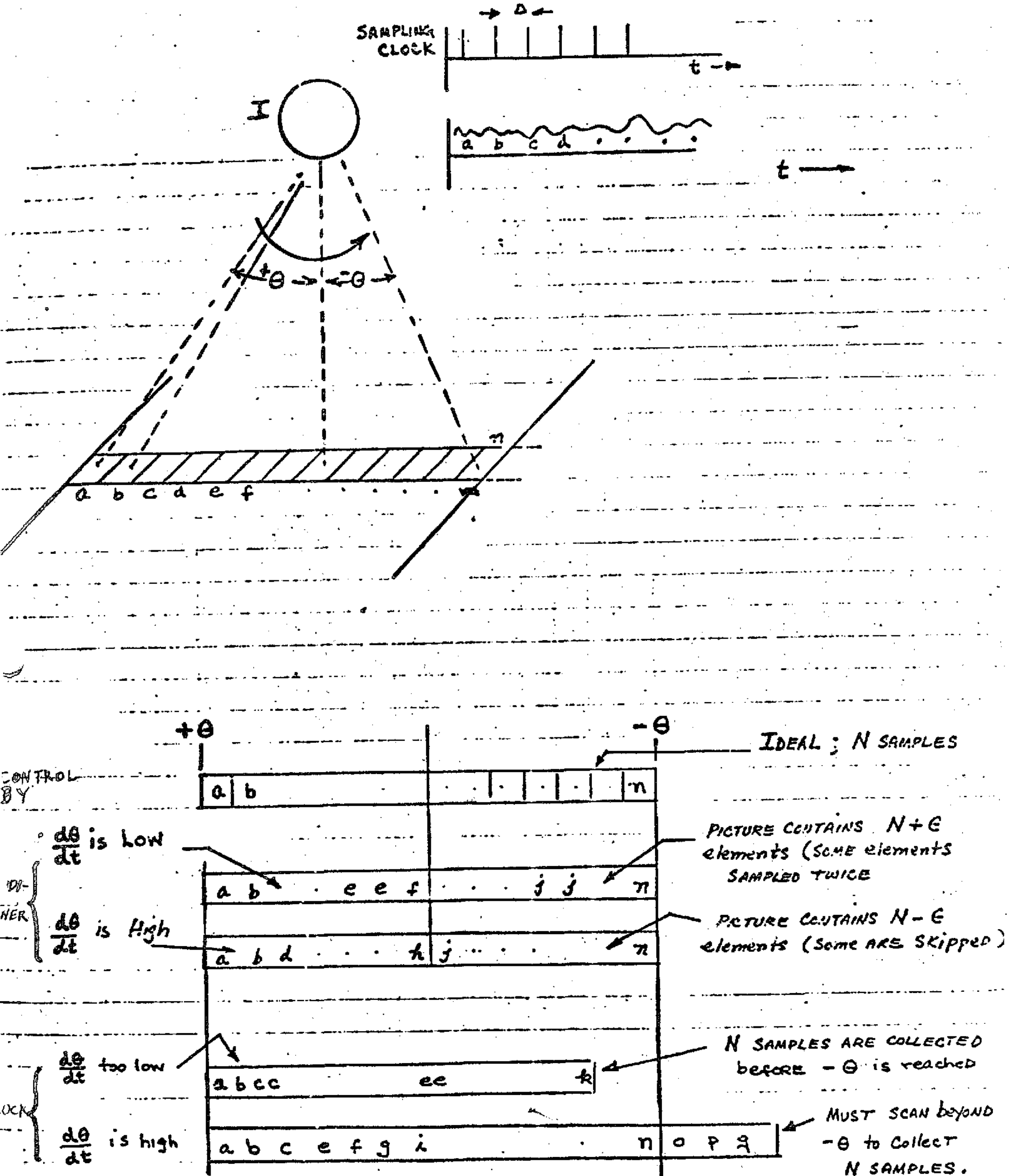

Fig. D.2.3.1-3 The Effect of Scan Errors

1. Each element on the ground must be equidistant from the scanner, for example, the scanner could be located very far from a flat surface (which will be assumed, for now).
2. The scanner must be fixed with respect to the array of elements to be scanned (roll or yaw motion of a S/C, for example, would violate this).
3. The array of elements must be fixed with respect to the scanner (earth rotation, for example, violates this).
4. The scanning itself ($d\theta/dt$) must be constant.
5. The sampling clock (which in effect supplies dt in (4) must be perfect.

Most of the conditions above are violated in practice. Some, however, are negligible and others (such as earth rotation) are known and can be corrected for.

One source of error in a system of this type is the imperfection in scan rate relative to the sampling clock. Given that the clock is perfect, and that start of scan ($+\theta$) can be made to coincide with t=0, then an error in scan rate will cause too few (scanning is too fast and $-\theta$ is reached early) or too many (scanning slow) samples to be collected during the scan interval. This situation of collecting a variable number of samples assumes that the process is controlled by the scanner, for example, by creating a stop-scan mark when $-\theta$ is reached. An alternative would be to have scanning controlled by the clock by counting a fixed number of samples, in which case errors would cause the scan lines to be short (scanning too slow) or long (scanning fast) relative to the true image.

These two situations are shown at the bottom of Figure D.2.3..1-3. With respect to the "true" situation on the ground (the top figure) we see that four types of error situations can occur depending on the method of limiting the scan width (sensing $-\theta$, or counting samples) and the type of error ($d\theta/dt$ high or low). Each situation produces a slightly different distortion of the true picture. To correct the picture, the basic procedure is to obtain equal angle samples from the equal time samples. This procedure, generally, requires interpolation and resampling.

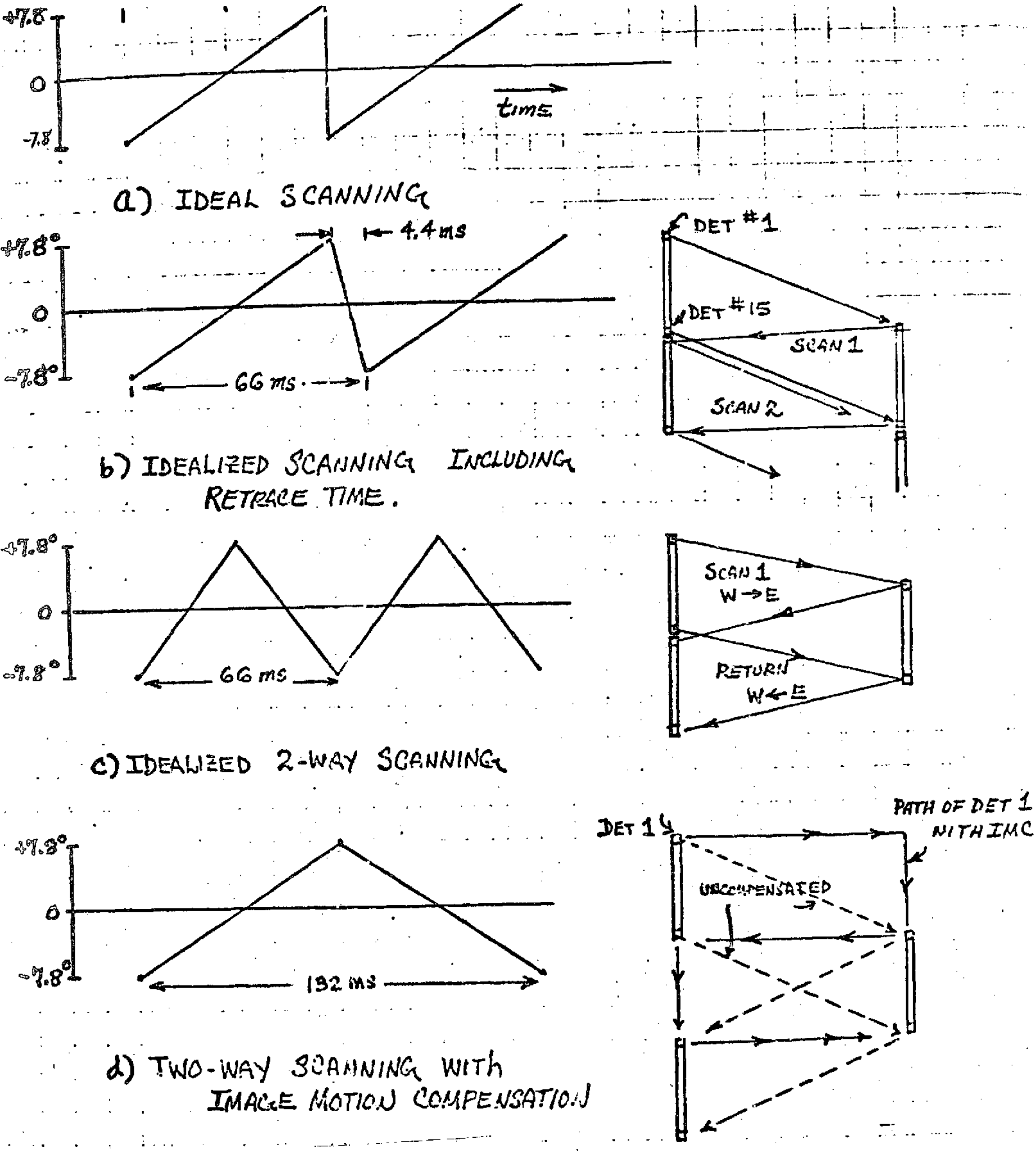

Fig. D.2.3.1-4 Idealized Scanning Patterns

(2) Assumed Scanning Characteristics

As an example of true one-dimensional scan correction procedure, we consider a particular baseline design for the Thematic Mapper, the Hughes' design.

The latest information on the Hughes Thematic Mapper (TM) indicates that a scan linearity of only approximately 1 percent will be achieved. However, a calibrated wheel can be provided with the scan mirror to provide an equal-angle clock which can be used to correct for this scan nonlinearity. This correction could be performed in the S/C or at the ground station. A general concept for line stretching is given to correct these errors.

We assume a 680km orbit with a ground-track velocity (v_g) of 6.811km/s. The scanner oscillates about the ground track and to achieve the swath width the scanner must oscillate ±7.8° (approximately) about the roll axis as the S/C moves in its orbit. An idealized scan pattern is shown in Figure D.2.3.1.-4a., the scanner traces out a linear pattern of angle versus time and retraces in zero time to begin the next scan.

In practice, the earth is scanned with a set of N contiguous (in N-S direction) detectors and each detector has an instantaneous field of view of 30 meters. If N = 15, then the swatch has a North-South dimension of approximately 450 meters. To avoid missing any of the ground elements, such a scanner must traverse the 185 km swath in the time required for the 15 detectors to advance in the along-track direction by 450 meters, or a time 450/6.811 = 66.069 ms. With such a scheme, the retrace must be accomplished in a time 30/6.811 = 4.404 ms so that dectector #1 on scan two commences 30 meters to the south of detector #15 on the first scan. This is shown in Figure D.2.3.1-4b. Note that this example yields a scan efficiency of 66/70.4 = 93.7 percent. An efficiency this high cannot be obtained with a scanner of this type because the scanner cannot be retraced fast enough.

In Figure D.2.3.1-4c, we show another idealized scanning pattern where the set of 15 detectors are scanned first from west-to-east and then from east-to-west. This type of scan is unsatisfactory since much of the gound is sampled twice and the data rate from the instrument is approximately doubled. This overlap is eliminated in the Hughes' design by an "image motion compensator" (IMC) which bends the west-to-east scan lines upward and the return scans downward to produce an accurate, nonoverlapping scan pattern. For the purposes here, we will assume that the IMC performs its function

perfectly. The resultant scan pattern is shown in Figure D.2.3.1-4d.

Because of the large physical size of the oscillating mirror, the scanner cannot be stopped and started in zero time. Therefore, the retrace or turn-around times cannot be as short as Figure D.2.3.1-4 would imply. For adjacent scans to be exactly contiguous, the constraint is that a complete cycle (west to east followed by east to west) be completed in the time required for the S/C to advance (2N + 1) resolution elements. For N = 15, this distance amounts to 930 meters which is traversed in 136.543 ms. To achieve this, the scanner must over-scan the swatch slightly to allow for the turn around time. This is shown in Figure D.2.3.1-5. A requirement is that the scan cycle repeat every 136.543 milliseconds. This interval contains two reversal periods (t_r) and two active periods (t_s). For the scan to be 80 percent efficient $t \,(t_r + t_s) = 0.8$ therefore, $t_s = 54.617$ ms and $t_r = 13.654$ ms. Using these numbers, $1.4 \; \frac{185{,}000}{30} = 8633$ samples must be taken in 54.617 ms for a sampling rate of 158,964 samp/sec. Assuming 6 bits/samples, this gives a data rate of 103 Mbps.

One west-to-east scan cycle is shown at the right of Figure D.2.3.1-5. Roughly, we can model the nonlinear scanning as

$$\theta(t) = -\,7.8^{\circ} + \frac{15.6\ t}{54.617\ \text{ms}} - \epsilon\ 7.8 \sin\left(\frac{2\pi t}{54.617\ \text{ms}}\right);\ 0 < t < 15.617\ \text{ms}$$

where ϵ is the departure from linearity expressed as a function of full scale. Since 15.6 degrees corresponds to 8633 pixels, a departure of 0.2 percent from linearity corresponds to errors of $\pm$ 8.6 pixels. A 1 percent departure from linearity results in errors of $\pm$ 40 pixels.

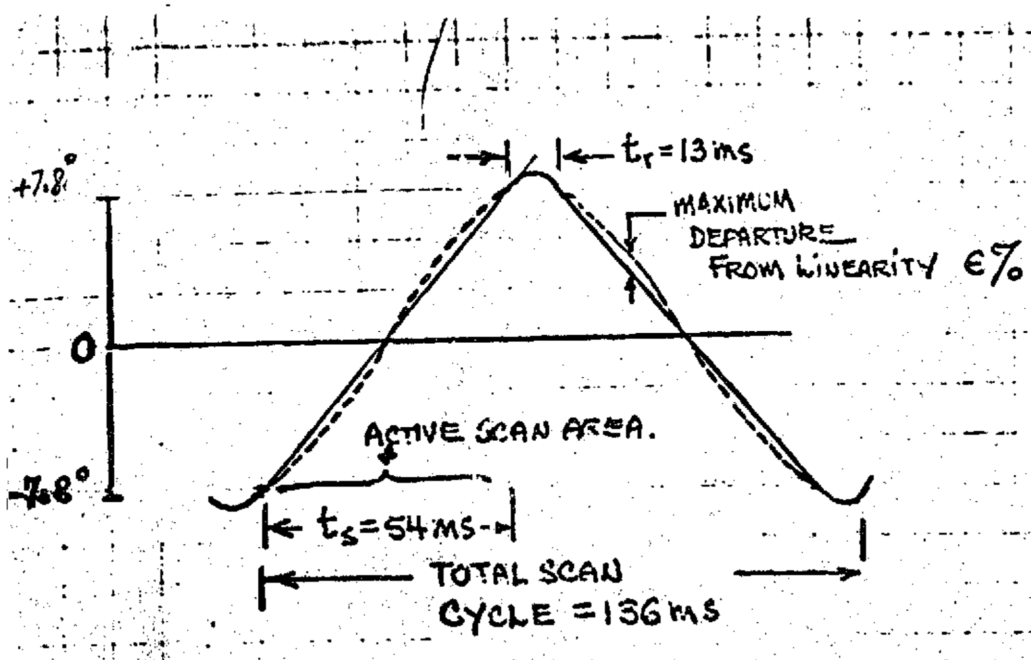

Fig. D.2.3.1-5 Actual Two-Way Scan Pattern 2N

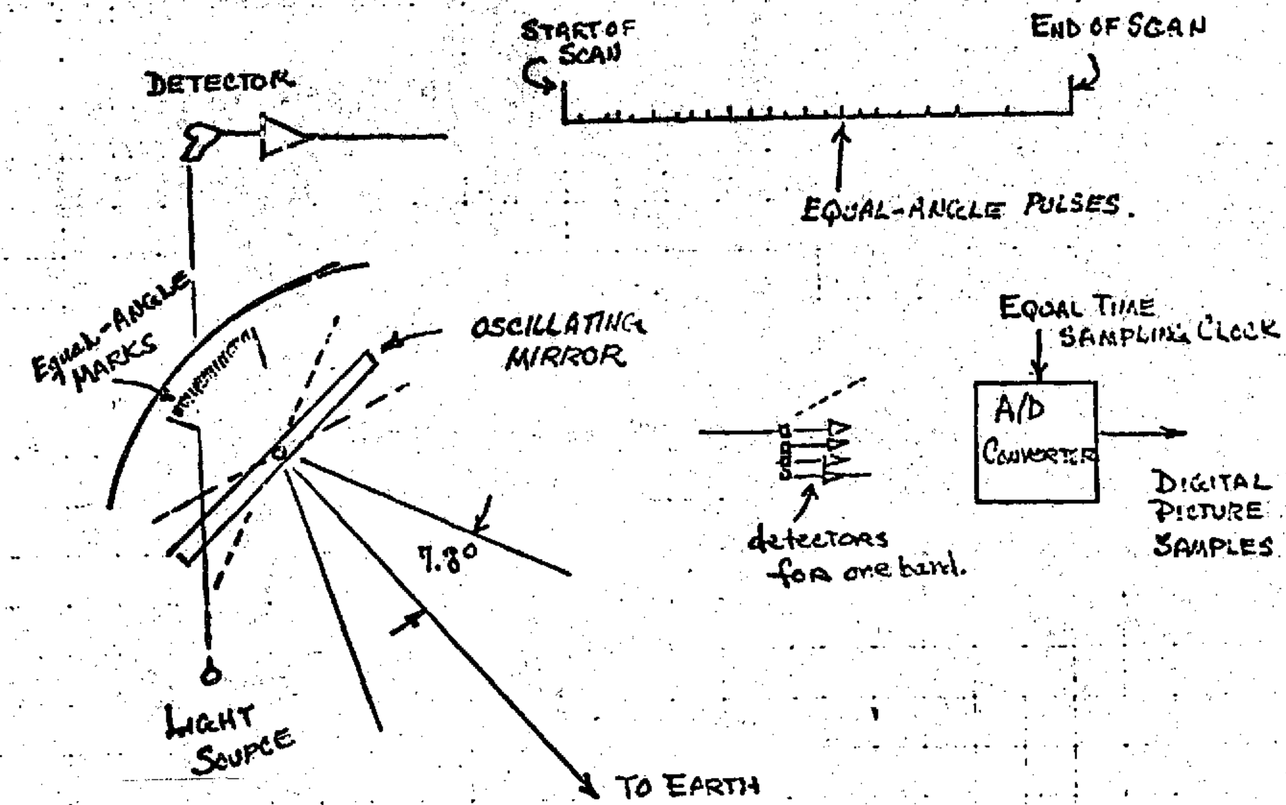

Fig. D.2.3.1-6 Concept for Obtaining Equal-Angle Scan Pulses.

ORIGINAL PAGE IS
OF POOR QUALITY

(3) Correction for Scan Nonlinearities

For 30 meter ground resolution, at an orbit altitude of 680 km, the resolution of the system is 44.117 μ radians. If the detectors are sampled 1.4 times per IGFOV, a sample is taken every 31.512 μ radians. Total mirror travel is 15.587 degrees.

In Figure D.2.3.1-6 we show (conceptually) a calibrated wheel that is rigidly attached to the oscillating mirror. The wheel has precise equal-angle marks and also distinguishable start-of-scan and end-of-scan markings. We assume that these markings on the wheel can be converted to a sequence of pulses as the scanner traverses the $\pm 7.8°$ interval. If the scanner moves in a nonlinear manner, this will be converted to non-uniform spacings of the pulses. In other words, nonuniformity in the angle-versus-time function will be converted to a nonuniform time spacing between the equal-angle pulses. Since the scanner nonlinearity is a fairly regular, somewhat predictable, function the nonlinearity will appear as a gradual position (or phase) modulation of the pulse train.

To correct for the scanner nonlinearity, the following considerations apply:

1. Scan errors manifest themselves as pulse position modulation on the Equal Angle (EA) pulses.

2. The sampling and A/D conversion of the video data is performed by an Equal Time (ET) sampling clock - presumably this clock is derived from a very precise frequency source and it is also related to the clock that modulates the transmitter (i.e., the bit clock).

3. The time varying phase information in (1) must be used to advance or retard a clock (to be in synchronism with the equal angle clock) so that the video samples can be interpolated and resampled to produce equal-angle (rather than equal time) samples.

There are several possible approaches for accomplishing this:

1. Use the scan-calibration information to correct the sampling clock before the samples are taken. This may be very difficult (probably impossible) because the clock must be corrected with almost zero time delay. Also, it may be undesirable to change the frequency to this clock (since the bit clock may be tied to it).

2. Use the scanner data to derive a resampling clock and resample the data immediately (i.e., in the S/C). Such corrections must be performed at the sampling rate (approximately 150 kHz).

3. Send the scan calibration data to the ground where a resampling clock is derived to resample the data. These corrections would not have to be done at the high sampling rate.

In the following, we will assume that the correction must be performed after the fact, i.e., after the samples are taken (option 1 is eliminated). Figure D.2.3.1-7 is a conceptual diagram of the sampling/correction/resampling system. We assume 6 visible + 1 IR bands with 15 detectors in each of the high resolution bands. We show A/D converters in each channel; with this approach the corresponding samples in the different bands could be taken simultaneously. A control loop is shown which servos the mirror oscillation to cause the scan period (on the average) to be precisely 136.543 ms/2 (scan rate = 14.6474 scans/second). This loop senses the start-of-scan pulses from the photo detector and converts these to standard-width pulses. These pulses are compared to the output of a counter that divides a standard 1.129028 MHz clock*. The standard width pulse is selected to the wide enough to give a linear indicator of error over the range of scan period jitter expected. For example, if the individual scans are accurate to ± 1 pixel** (± 8.857 μsec) then the standard width

* Selected to give one clock count = 0.1 resolution element.

** This may be optimistic - it may be possible to control mirror scanning so that the long term average is quite accurate; errors on any given scan may, however, exceed 1 pixel.

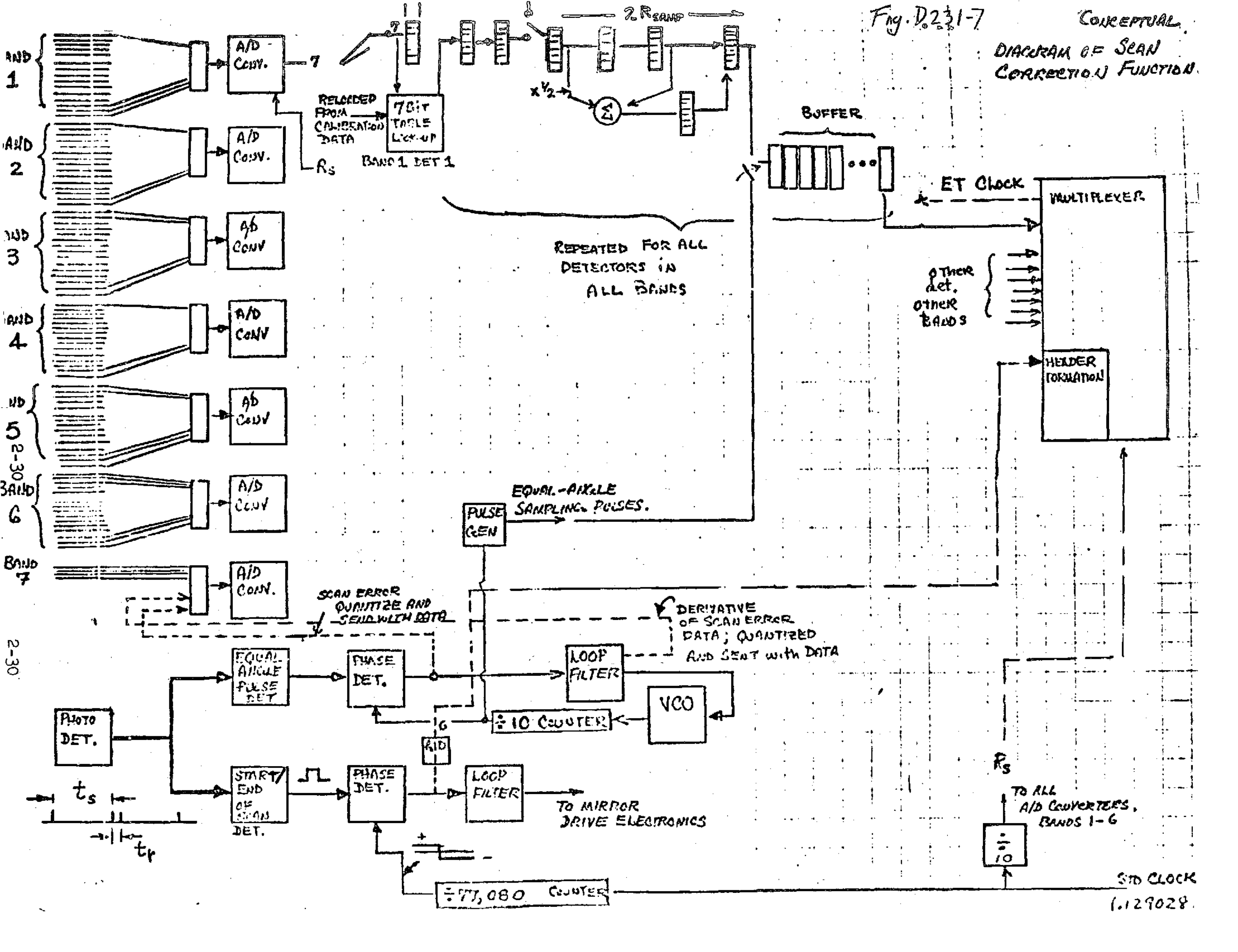

Fig. D.2.3.1-7 CONCEPTUAL DIAGRAM OF SCAN CORRECTION FUNCTION

pulse should have a width 17.7 μseconds. To quantize the loop error signal with an error < 0.1 pixel, it will be necessary to A/D convert the error to at least 5 bits. This digitized error signal will be included in the header data that precedes each scan line.

We should emphasize at this point that two phase locked loops are actually needed to correct the scanner. The first, discussed above, servos the mirror on a long-term basis to maintain the scan rate constant. This loop would have a relatively narrow bandwidth, possibly a fraction of a Hz, and will average over many scans.

A second PLL is to be used to track variations in the equal-angle reference pulses within one scan. This represents a fairly difficult problem for several reasons. First, the loop must have a relatively wide bandwidth so as to track the nonlinearities with little or no delay. Secondly, this second loop must, in some way, coast through the turn-around periods or, alternatively, it must reacquire the scan calibration pulses on each scan. Thirdly, the loop must provide an accurate enough subdividion of the scan cycle to linearize the scan to within 0.2 pixel.

To see how this second PLL might work, consider the simplified diagram as shown in Figure D.2.3.1-8. At the top of the diagram, we show a sequence of pulses from the calibration source. After the start of scan pulse, the scanner starts out slowly with the equal-angle pules too far apart. At mid scan, the mirror is moving too fast and the equal-angle pulses are too close together. Near the end of the scan, the scanning again slows down as end-of-scan is approached.

A voltage-controlled oscillator (VCO) with a nominal frequency of 1.129028 MHz is used in the loop. This loop produces pulses which drive a divide-by-10 counter. Counter reset (change in the most significant bit) supplies a + to - transition to the phase detector. A second input to the phase detector are the equal-angle pulses from the photo detector. These pulses have been normalized to standard width. With no time error between the input pulses and the output of the divide-by-10 counter, the counter output bisects the input pulse and, when integrated, yields zero error signal.

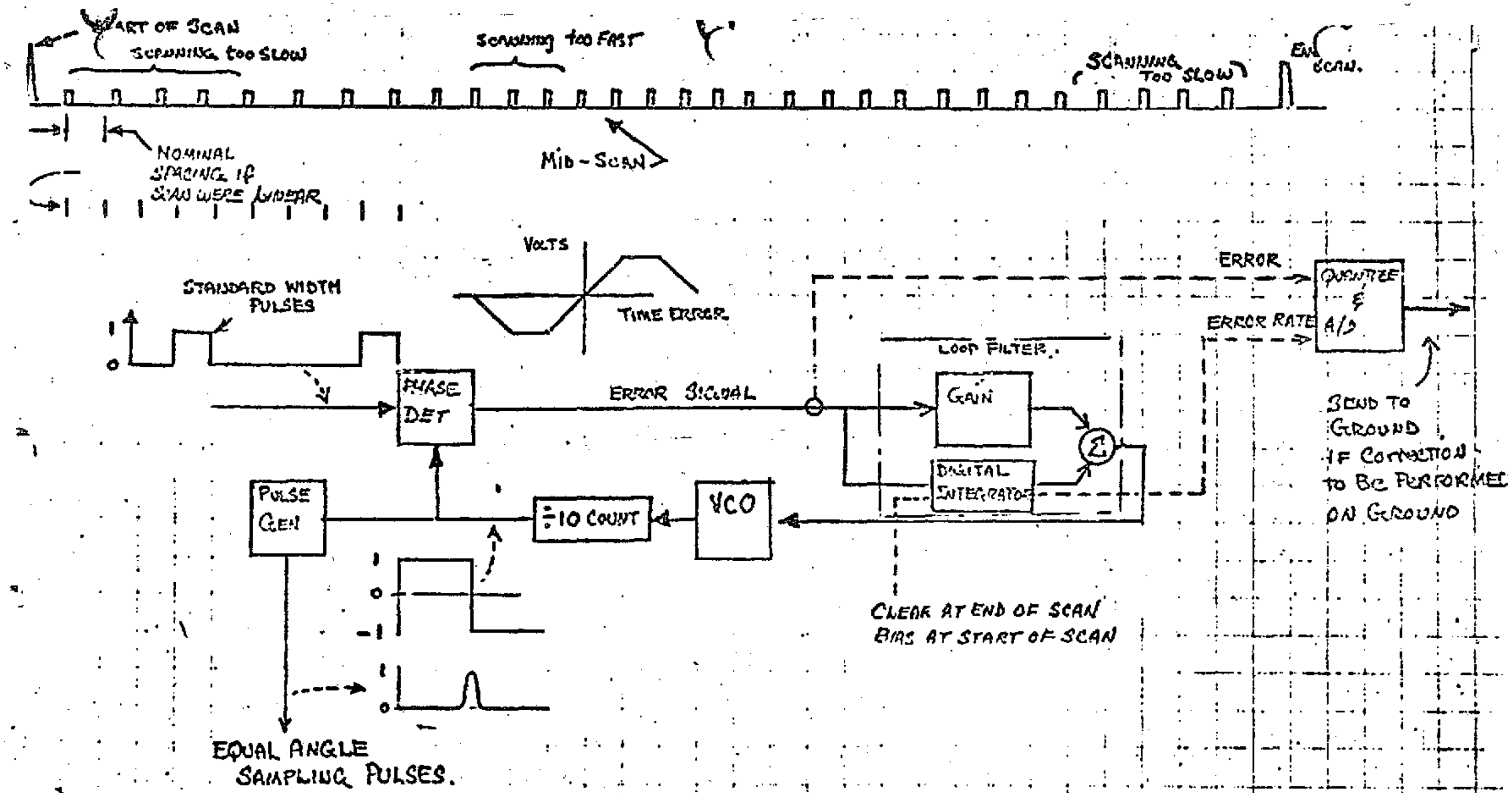

Fig. D.2.3.1-8 Scan Tracking PLL.

Leading or lagging time errors produce positive or negative error voltages which speed up or slow down the VCO to zero the error. A second order loop filter is used so that the VCO follows the "phase modulation" on the input pulse train with an acceptably small time lag. In effect, the loop bandwidth must be wide enough to lag by no more than 0.2 pixel for the maximum acceleration on the input nonlinearity (maximum acceleration occurs at 1/4 and 3/4 scan for the nonlinearity shown in Figure D.2.3.1-5. Note that the digital integrator in the loop filter must be cleared at the end of scan and reset (with the best estimate of scan rate) at the start of the next scan. For now, we will not be concerned with reacquisition of the loop from scan-to-scan.

The main output of the "fast" PLL is an equal-angle clock which tracks the equal-angle calibration marks on the scan wheel. This loop can, of course, be implemented on the ground using the loop error and error rate signals, which are sent with the video data. Alternatively, the correction can be made in the S/C as shown in Figure D.2.3.1-7.

Returning to Figure D.2.3.1-7, we show how the resampling would be performed in the S/C. The first step in the correction consists of a table look-up operation where the 7-bit (or 6-bit) sample from detector 1 of Band 1 is corrected radiometrically by using the 7-bit word as the address to a table that yields a 7-bit output word. The corrected sample is supplied as input to an interpolator. As shown, the interpolator operates at twice the sampling rate ($2R_s$) so that on alternate clock pulses, true samples or zeros are entered into the delay line. The delay line is shifted to produce, alternately, true or interpolated samples at its output. The interpolated sample is mid way between true samples. The equal-angle resampling clock is used to select the sample which happens to appear at the output of the interpolator at each clock time. Since the equal-angle clock is not in synchronism with the equal time clock, these samples will "drift" from ture to interpolated and back.

For the corrected picture samples to be outputted at a constant rate, the equal-angle samples must be buffered. It appears that 50, 7-bit words of storage* will be required for each detector of each channel (this is strictly a function of the amount of nonlinearity in the scan). Furthermore, the buffer must be loaded with the equal-angle samples prior to

* Words of buffer storage ≈ peak error in pixels, + 25 percent margin.

commencing read-out (assuming that the scanning is slow at the start). For an error of 1 percent, the scan nonlinearity amounts to ± 40 pixels. Assume that the scan starts out too slow as shown in Figure D.2.3.1-5. The read out at the sampling rate is too fast so that the buffer must be filled before read-out commences. With the buffer full, the ET sampling clock removes samples faster than they are entered by the FA clock so that the buffer tends to empty. At mid scan, however, the EA clock has caught up with and then exceeds the rate of the ET clock and the buffer tends to fill again. However, the EA clock slows down near end of scan, and the ET clock can empty the buffer. A delay in the video of 50 samples (316 μ sec) is incurred if the correction is performed in the S/C. Also, 4750 words of 7 bit storage are required for the buffers. Also, 95 128 word memories (mostly read, write infrequently) are required for the radiometric table look-up.

Conceptually, it seems possible to perform Type I processing, which includes radiometric correction and one-dimensional scan correction, with special purpose digital hardware. If performed in the S/C the logic must operate at a maximum of 2 times the sampling rate (about 300 kHz) for an interpolator that produces one interpolated value mid way between true values. The interpolation interval can, of course, be subdivided into smaller intervals with a proportional increase in logic rate in the interpolator. Interpolation will have some effect on system MTF; this effect remains to be determined.

The scan tracking PLL must be simulated to determine its ability to yield a (corrected) scan linearity of ± 0.2 pixel. Also the acquisition behavior must be determined.

If these corrections are performed on the ground, a PLL error signals must be sent with the video so that a second loop can be implemented on the ground to do the actual EA resampling. Quantization of the error signal must be resolved and also, the acquisition process may become more difficult.

TYPE II PROCESSING

D.2.3.3 TYPE II Processing

D.2.3.3.1 The Problem

The basic problem in the Type II processing is to resample the sensor data according to a grid that one wishes to use for the output image. This process is shown in Figure D.2.3.1-9 & 10. The original data exists as rows

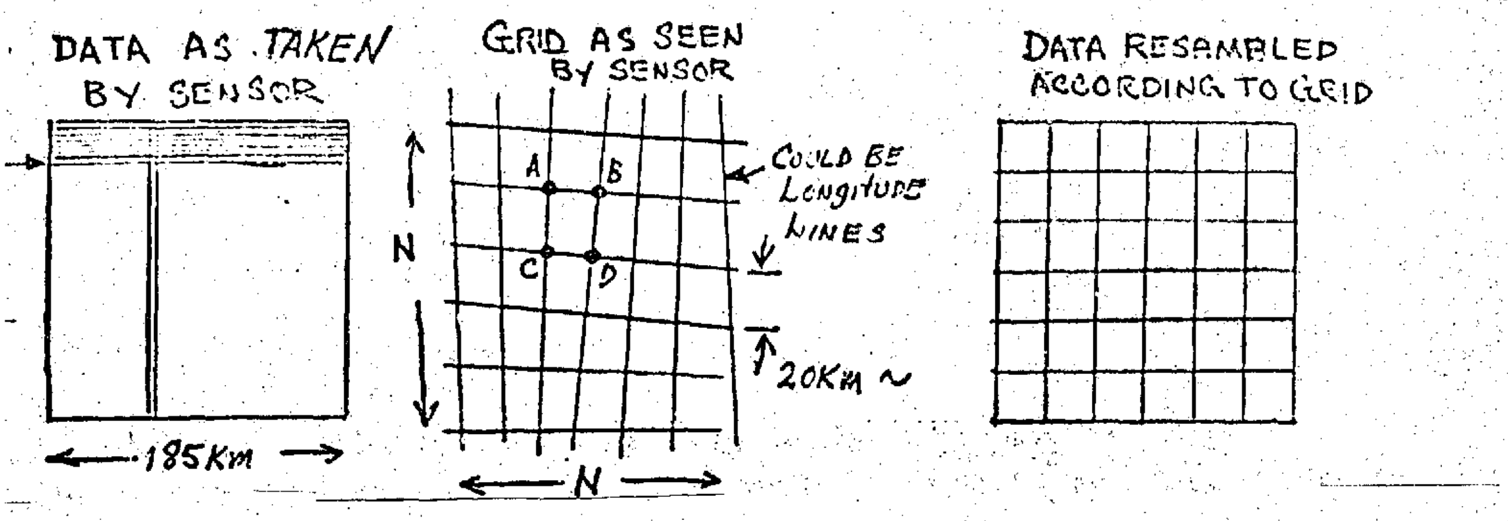

Fig. D.2.3.1-9 Overall Relationship of Resampling Grid to Original Data

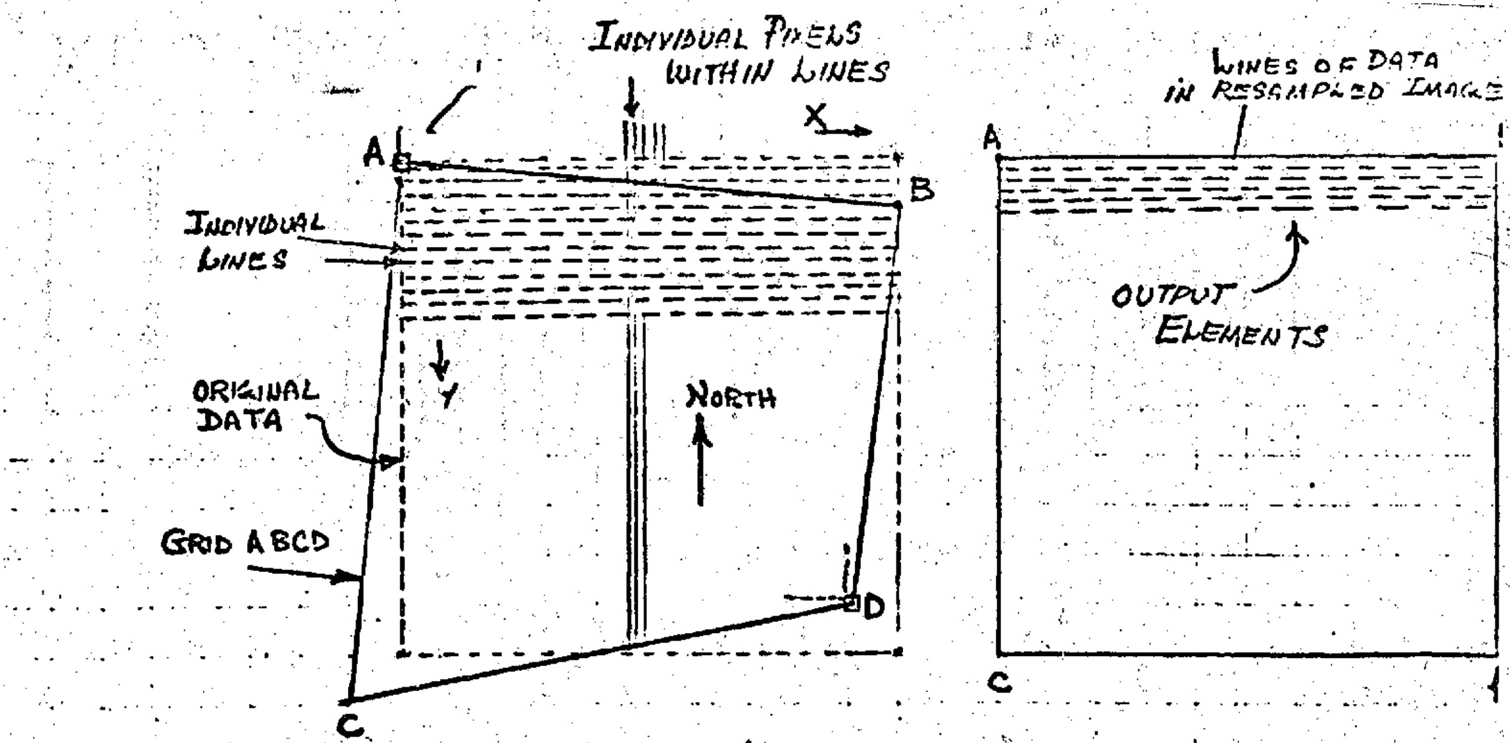

Fig. D.2.3.1-10 Detail of Grid Square ABCD

of pixels (intensity values) that were taken by the scanner. The pixels are sensed by the scanner at the point that the sensor views the earth at any particular instant of time. The scanning traces out some path with respect to the grid that will eventually be used to make the image (one can envision this grid as a series of lines that are painted on the earth). These grid lines are distorted as seen by the scanner because of S/C attitude and orbit errors, earth curvature and earth rate, and the fact that the S/C ground track does not follow a north-south line. Given that this grid is computed, say in the form of a 10 by 10 array of points, then the latitude and longitude of certain pixels in the original data will be identified. As an illustration, assume that the corners ABCD identify one of the N^2 sub-squares within the grid. IF N = 10, the grid would subdivide the image into 863 by 616 pixel squares (approximately). Assuming that corner "A" is located at θ_A degrees of latitude and ϕ_A degrees of longitude, the corners might be identified as:

	Latitude, Longitude	Pixel, Row Number, Pixel Within Row
A	θ_A , ϕ_A	1232 , 1726
B	$\theta_A - \delta$, ϕ_B	1242 , 2589
C	$\theta_C - \alpha$, $\phi_A + \beta$	1868 , 1700
D	$\theta_C + \gamma$, $\phi_B + \epsilon$	1838 , 2570

If we assume that corner A is located at pixel 1726 within row 1232, then the remaining 3 corners are displaced in the rectangular data array from their ideal* locations if the grid were square. For example, corner C is located 10 pixels (or rows) to

* The use of the term "ideal" here is bound to be confusing. Perhaps an ideal scanner can be envisioned that is skewed or adjusted as necessary to view precise lines of latitude (or whatever grid is desired in the final map) during each west-to-east sweep, and advances or retards subsequent lines to compensate for earth rate and the fact that the S/C ground track does not follow the vertical grid (lines of longitude).

the south, and 26 pixels to the west of its "ideal" location.

To resample the image, therefore, three basic steps must be performed.

(1) The resampling grid must be calculated which subdivides or sections the original image data.

(2) the coordinates of the desired output points must be computed relative to the input data

(3) the output points are obtained by selecting, or interpolating between, the true input put points.

Each of these steps will be discussed below.

D.2.3.3.2 Computation of Resampling Grid

The calculation of the resampling grid consists of a series of coordinate transformations and notations that map the latitude and longitude of points on the earth's surface to points in the coordinate system of the data taken by the scanner. The latter coordinate system for the Thematic Mapper would consist of the line and element numbers of a particular element in the rectangular array of data. The steps in the process are shown conceptually in Fig. D.2.3.3.11. Note that the overall objective of this procedure is to map points on the earth into the rectangular array of image data. If the original points correspond to the intersections of grid lines in the desired map projection, then the mapping of multiple points will locate the desired grid in the output image. This grid is then used to resample and interpolate the original data to produce the final output product.

Given the steps shown in Fig. D.2.3.3.-11, we can estimate the time required to map one grid point into the following equivalences:

Floating Point Multiply	= 5 x	integer add time
Floating Point Divide	=11.0x	integer add time
Trigonometric Function	= 22 x	integer add time
Floating Point Add	= 3 x	integer add time

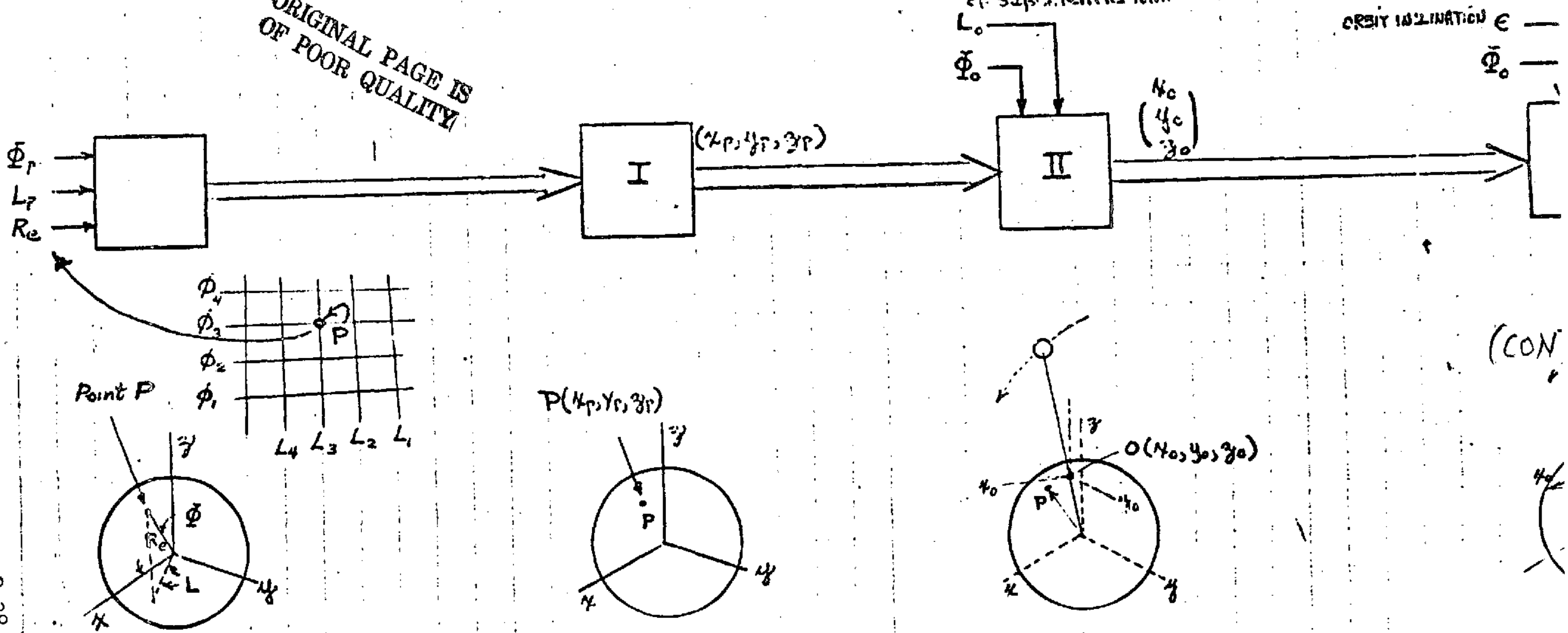

START with P (A Point on the earth)
SPECIFIED BY
LATITUDE – Φ_p (degrees NORTH OF EQUATOR)
LONGITUDE – L_p (degrees west or East of 0° Meridian)
EARTH RADIUS – km., R_e

TRANSFORMATION # 1.
TRANSFORM FROM EARTH-CENTER SPHERICAL COORDINATES TO EARTH-CENTER CARTESIAN COORDINATES

$$x_p = R_e \cos\Phi_p \cos L_p$$
$$y_p = R_e \cos\Phi_p \sin L_p$$
$$z_p = R_e \sin\Phi_p$$

TRANSFORMATION # 2
TRANSFORM FROM EARTH-CENTER CARTESIAN TO SUB-satellite CENTERED CARTESIAN

$$x_o = x_p \pm \Delta x$$
$$y_o = y_p \pm \Delta y$$
$$z_o = z_p \pm \Delta z$$

$$\Delta x = R_e(\cos\Phi_p \cos L_p - \cos\Phi_o \cos L_o)$$
$$\Delta y = R_e(\cos\Phi_p \sin L_p - \cos\Phi_o \sin L_o)$$
$$\Delta z = R_e(\sin\Phi_p - \sin\Phi_o)$$

TRANSFORMA
Rotate x_o, y_o
1) new axis u is i
track (rotatio
2) Rotate by Φ
about y_o ;

$$\begin{vmatrix} u \\ v \\ w \end{vmatrix} = \begin{vmatrix} \cos H_s \\ -\sin H \\ 0 \end{vmatrix}$$

H_s
ϵ -

FIG. D.2.3.1-11
RESAMPLING GRID STEPS

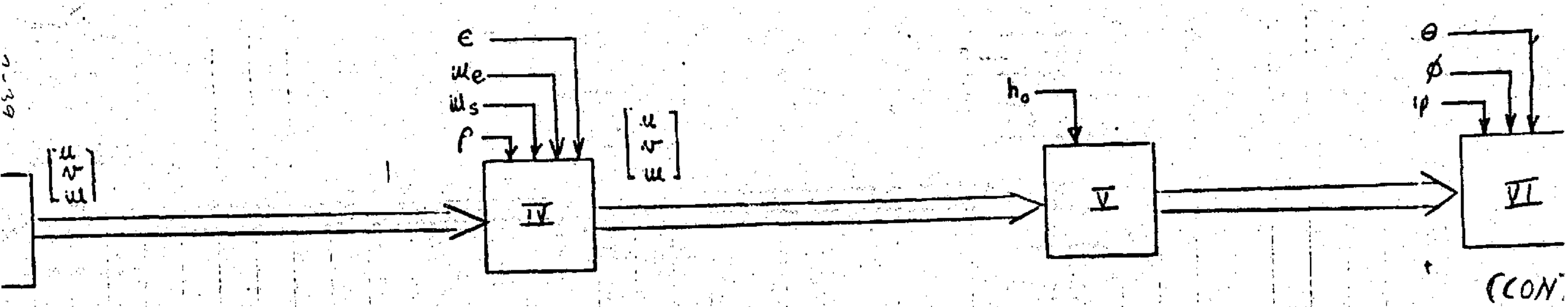

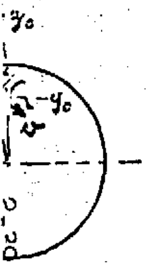

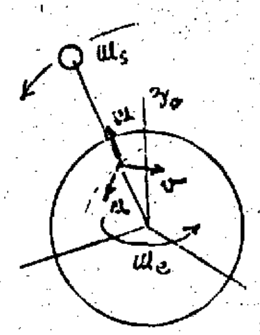

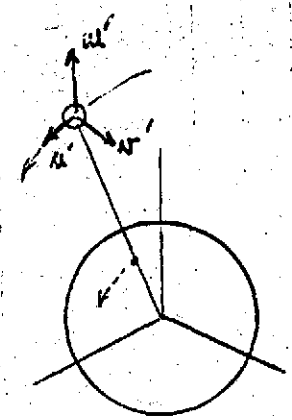

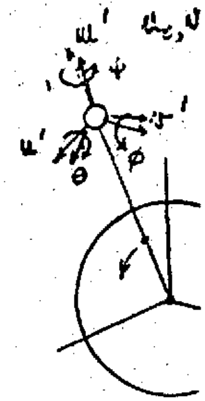

#3

...axes so that
...ction of satellite ground
... H_s about z_0)
...titude of subsatellite point)
v axis is in scan direction

$$\left|\begin{matrix} \cdot H_s & 0 \\ \cdot H_s & 0 \\ 0 & 1 \end{matrix}\right| \left|\begin{matrix} \cos\Phi_0 & 0 & -\sin\Phi_0 \\ 0 & 1 & 0 \\ \sin\Phi_0 & 0 & \cos\Phi_0 \end{matrix}\right| \left|\begin{matrix} x_0 \\ y_0 \\ z_0 \end{matrix}\right|$$

$$\sin^{-1}\left\{\frac{\sin\epsilon}{\cos\Phi_u}\right\}$$

TRANSFORMATION #4

CORRECT FOR EARTH'S ROTATION

ΔH_s = heading deviation due to earth's rotation $= \tan^{-1}\left\{\frac{\omega_e}{\omega_s}\cos\epsilon\sin\rho\right\}$

ρ = orbital travel angle from vertex of orbit
ϵ = polar inclination of orbit
ω_e = earth rate
ω_s = angular rate of satellite

$$\begin{vmatrix} u \\ v \\ w \end{vmatrix} = \begin{vmatrix} 1 & \tan\Delta H_s & 0 \\ 0 & \frac{1}{\cos\Delta H_s} & 0 \\ 0 & 0 & 1 \end{vmatrix} \begin{vmatrix} u \\ v \\ w \end{vmatrix}$$

TRANSFORMATION #5

TRANSLATE TO ORBIT ALTITUDE

$u' = u$
$v' = v$
$w' = w + h_0$
h_0 = ORBIT ALTITUDE

TRANSFORMATION

ROTATE ONS into 3/k...
FRAME TAKING INTO...
PITCH (ψ), ROLL (θ),...
YAW ERRORS.

$$\begin{vmatrix} u_s \\ v_s \\ w_s \end{vmatrix} = \begin{vmatrix} \cos\psi & 0 & \sin\psi \\ 0 & 1 & 0 \\ -\sin\psi & 0 & \cos\ldots \end{vmatrix}$$

$$\begin{vmatrix} \cos\phi & -\sin\phi \\ \sin\phi & \cos\phi \\ 0 & 0 \end{vmatrix}$$

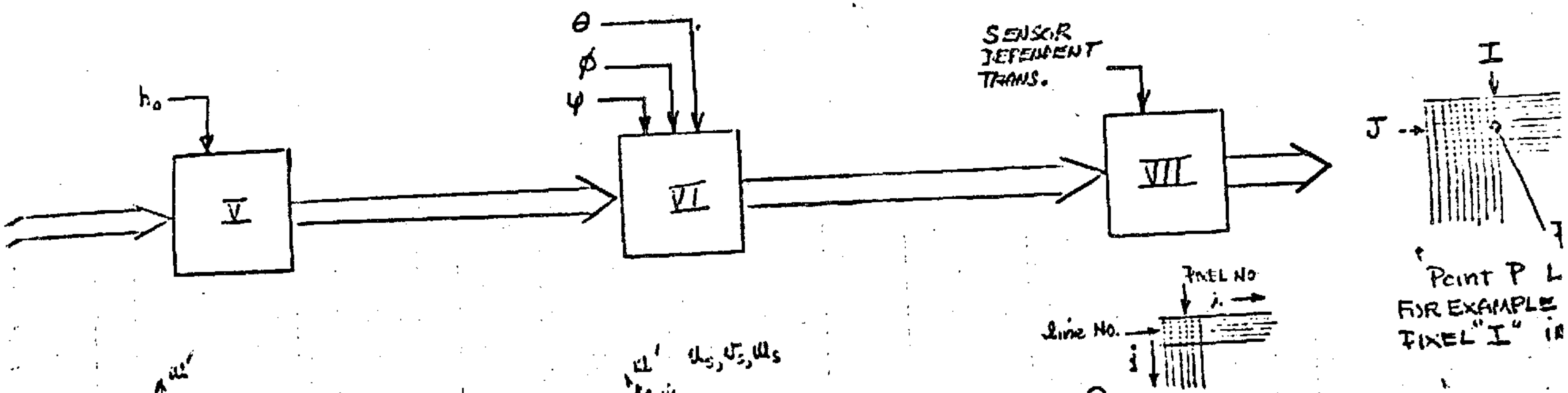

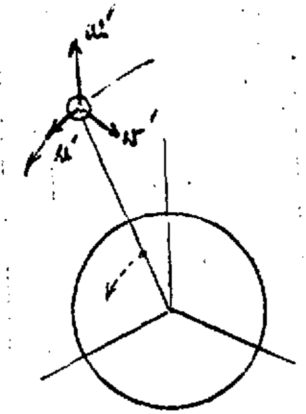

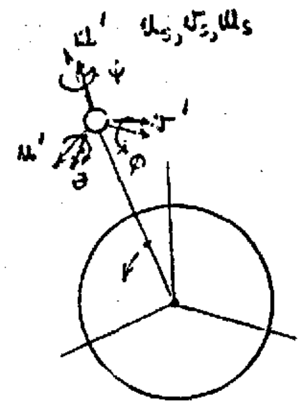

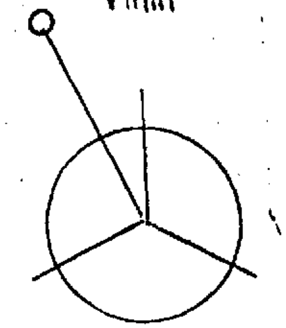

TRANSFORMATION # 5

TRANSLATE TO ORBIT ALTITUDE

$u' = u$

$v' = v$

$w' = w + h_o$

$h_o \equiv$ ORBIT ALTITUDE

TRANSFORMATION # 6

Rotations into S/C Frame taking into account Pitch (ϕ), roll (θ), and Yaw Errors.

$$\begin{vmatrix} u_s \\ v_s \\ w_s \end{vmatrix} = \begin{vmatrix} \cos\psi & 0 & \sin\psi \\ 0 & 1 & 0 \\ -\sin\psi & 0 & \cos\psi \end{vmatrix} \begin{vmatrix} 1 & 0 & 0 \\ 0 & \cos\theta & -\sin\theta \\ 0 & \sin\theta & \cos\theta \end{vmatrix}$$

$$\begin{vmatrix} \cos\phi & -\sin\phi & 0 \\ \sin\phi & \cos\phi & 0 \\ 0 & 0 & 1 \end{vmatrix} \begin{vmatrix} u' \\ v' \\ w' \end{vmatrix}$$

TRANSFORMATION # 7

Final Translation into Image Plane, i.e. into the coordinate system defined by pixel number within scan line and scan line number. (Will be function of scanner, in general)

Using these multiplicative factors, and Fig. D.2.3.1-11 we obtain the number of machine operations required to compute one grid point as shown below:

Operations Required to Determine
Grid Points

TRANS	NUMBER MULT.	NUMBER DIVIDE	NUMBER ADD	TRIG	OPERATIONS MULT	OPERATIONS DIVIDE	OPERATIONS ADD	OPERATIONS TRIG	TOTAL OPERATIONS
1	7			5	35			110	165
2	7		6	10	35		18	220	273
3	36	1	24	12	396	11	72	264	743
4	12	2	6	5	60	22	18	110	210
5			1		0	0	3	0	3
6	81	0	54	12	405	0	162	264	831
7(ESTIMATED)									(700)
TOTAL									2925 operations

This estimate of approximately 3×10^3 total operations (for all points) should probably be multiplied by at least 10 to obtain a final estimate. Such an increase is probably justified by the fact that extended-precision calculations would be performed, and also that iterations may be required for some of the calculations. A better, somewhat conservative estimate, therefore might be 3×10^4 machine operation per grid point.

D.2.3.3.3. <u>Coordinate Computation</u>

Once the coordinates of the resampling grid are completed, the next step is to compute the coordinates of the <u>desired</u> data samples as one moves through the true samples. This is shown in more detail in Figure D.2.3.1-12. To resample the line AB, the first step is to compute the coordinates of the desired points (circles in Figure D.2.3.1-12) relative to the coordinates of the original points (squares in Figure D.2.3.1-12).

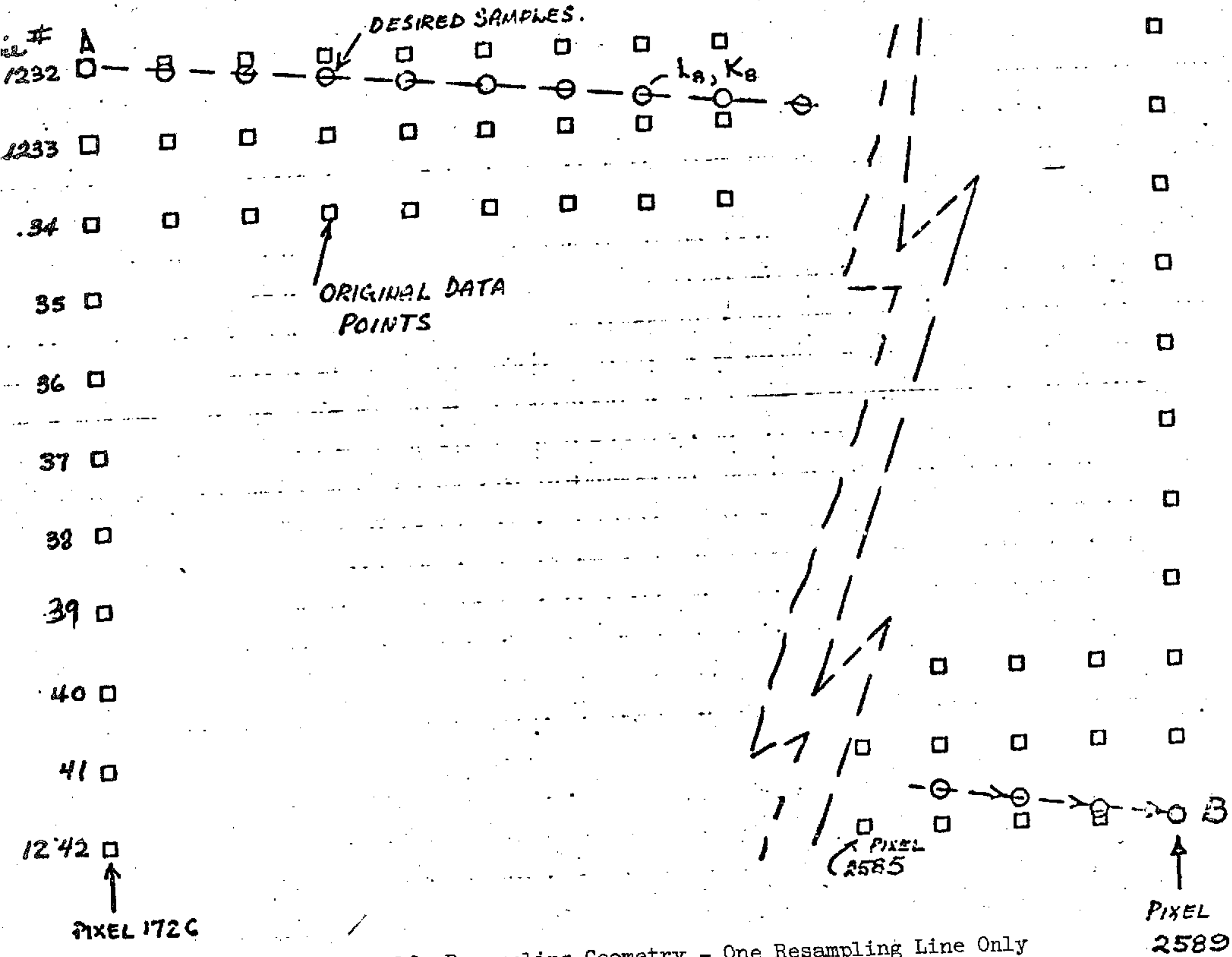

Fig. D.2.3.1-12 Resampling Geometry - One Resampling Line Only

Denote the original samples as P (I,J) where I denotes the row number and J the pixel number within the row. Since point B coincides exactly with row 1242, pixel 2589, there is no correction required in the east direction. The coordinates K, L of the desired samples can therefore be obtained recursively as*

$$L_{j+1} = L_j + 1 \quad \text{(pixel number progresses across row)}$$

$$L_1 = 1726$$

$$K_{j+1} = K_j + \frac{10}{863} \quad \text{(row number picks up an extra 10 after progression through 863 pixels)}$$

$$K_1 = 1232$$

If this simple recursive algorithm is used to resample only the first line in the output image, we could envision the input array P(I, J) as being accessed by the coordinates L, K. As we move across the line, both L and K are incremented, the pixel number L_j by exactly 1 and the row number K by a small fraction. After 83 or 84 steps, the "address" moves downward by one row; after 863 pixels, it has moved downward by exactly 10 rows.

To perform this coordinate computation in a linear manner over the total image, both ΔL and ΔK will be functions of position in the image. Returning to Figure D.2.3.1-10, we see that the line spacing is compressed at the right side of the image as compared to the left. This can be accounted for with simple second differences that change the increments as one moves down the rows. For example, row number for line AB changes according to $K_{J=1} = K_j + 10/863$. However, in progressing across line CD

the row number must change as $K_{j+1} = K_j - 30/863$; at point D, one is reading a pixel from a position in the original data 30 rows above point C.

* This simple linear recursive procedure applies only to the linear scanners. For a conical scan pattern, the coordinate computation becomes more complex.

We will assume for now that some simple recursive equations can be developed to compute the coordinates of a desired resampled point R(K, L). These equations would require only fixed point additions (with possibly some shifts) to compute L and K to accuracies of possibly 1/64 of a resolution element. A total of 14 bits (pixels 1 - 8630) + 10 bits (accuracy to 2^{-10} pixel) may be adequate to represent each of these coordinates. This must be verified, however, since an integrated error will be incurred in the recursive algorithms.

D.2.3.3.4 <u>Interpolation Algorithms</u>

In this section, we will describe the basis algorithms used to interpolate the original or true data complex to obtain the desired output samples $I(\underline{\underline{x}},\underline{\underline{y}})$ = light intensity at position $(\underline{\underline{x}},\underline{\underline{y}})$. Three types of interpolation algorithms are considered:

1. Nearest neighbor interpolation (uses the data sample closest to $(\underline{\underline{x}},\underline{\underline{y}})$)
2. Bilinear interpolation (uses the 4 data samples closest to $(\underline{\underline{x}},\underline{\underline{y}})$)
3. Cubic convolution (uses the 16 data samples closest to $(\underline{\underline{x}},\underline{\underline{y}})$)

The interpolation algorithms will be compared in terms of the computer operations required for the interpolation computations in fixed point arithmetic (data transfer in/out of memory is excluded from this time) and 2) compute the Machine Instructions per Pixel (MIPPS) required for the interpolation computations.

The geometry used for the nearest neighbor and the bilinear interpolation is shown in Figure D.2.3.1-13 and that for the cubic convolution in Figure D.2.3.1-14. Shaded squares indicate the positions (pixels) where the data samples were taken and dark circle indicates the position (x,y) where an output sample is required. The x-axis refers to the N-S direction (track direction) and the y-axis the W-E direction (scan direction) on the earth's surface. Since the data samples are obtained at regular intervals during the scan, the positions of the data samples can be expressed in terms of integers (i,j) such that

$$\text{Position of a sample} = (i\Delta x,\ j\Delta y)$$

However, the position (x, y) will be, in general, such that

$$i\Delta x \le x < (i+1)\Delta x$$

$$j\Delta y \le y < (j+1)\Delta y$$

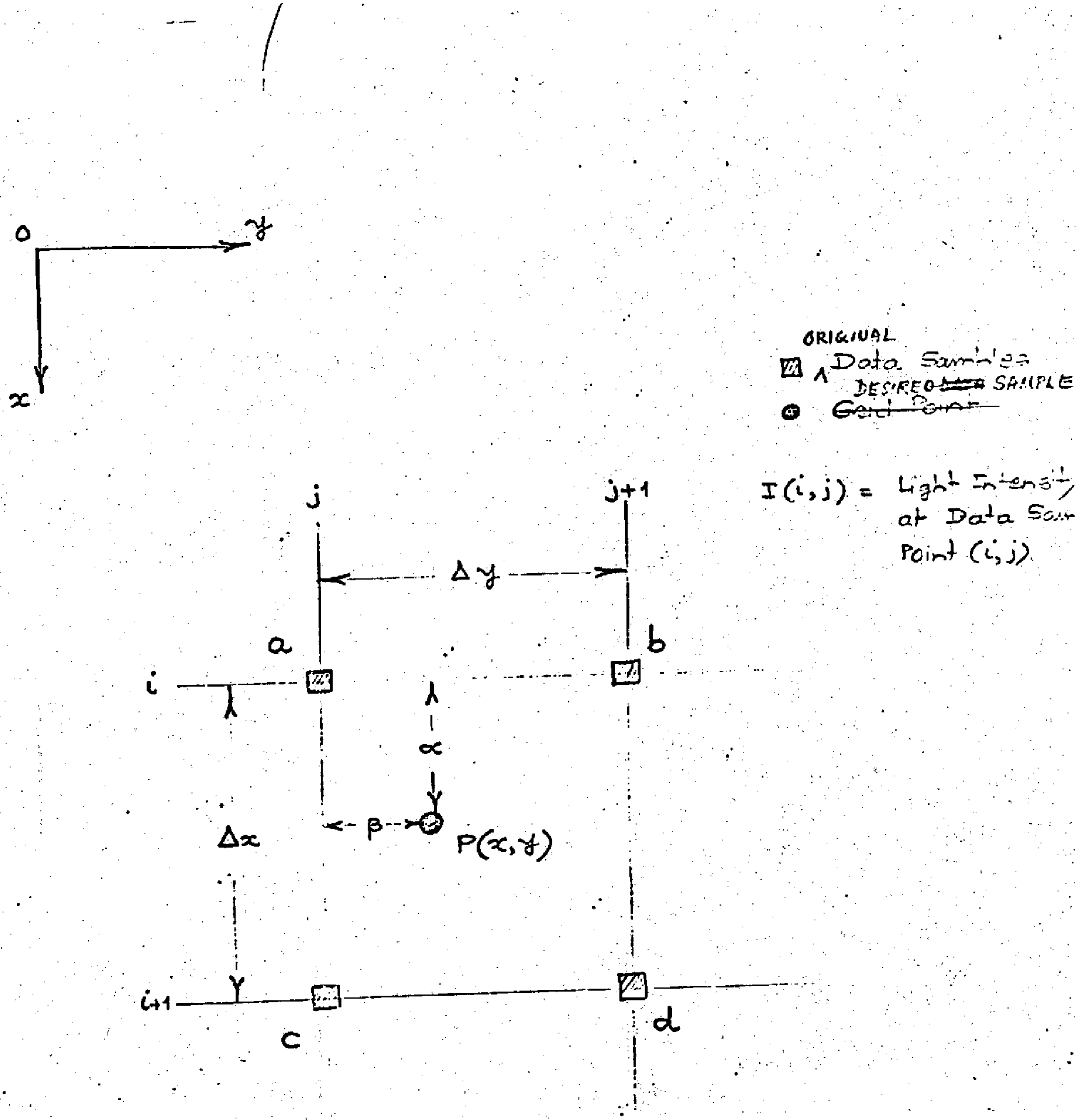

Figure D.2.3.1-13. Geometry for Nearest Neighbor and Bilinear Interpolations

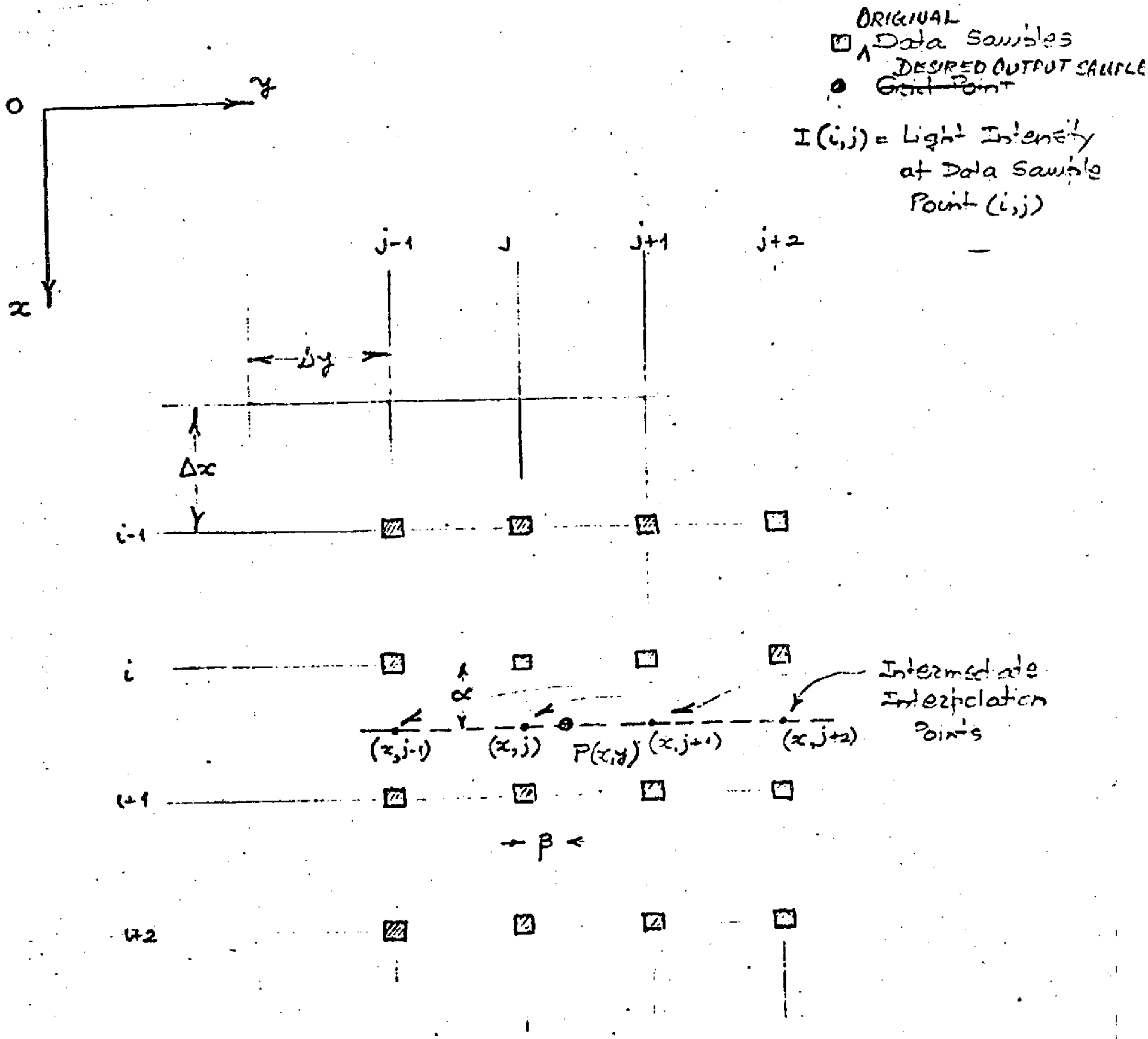

Fig. D.2.3.1-14 Geometry for Cubic Convolution

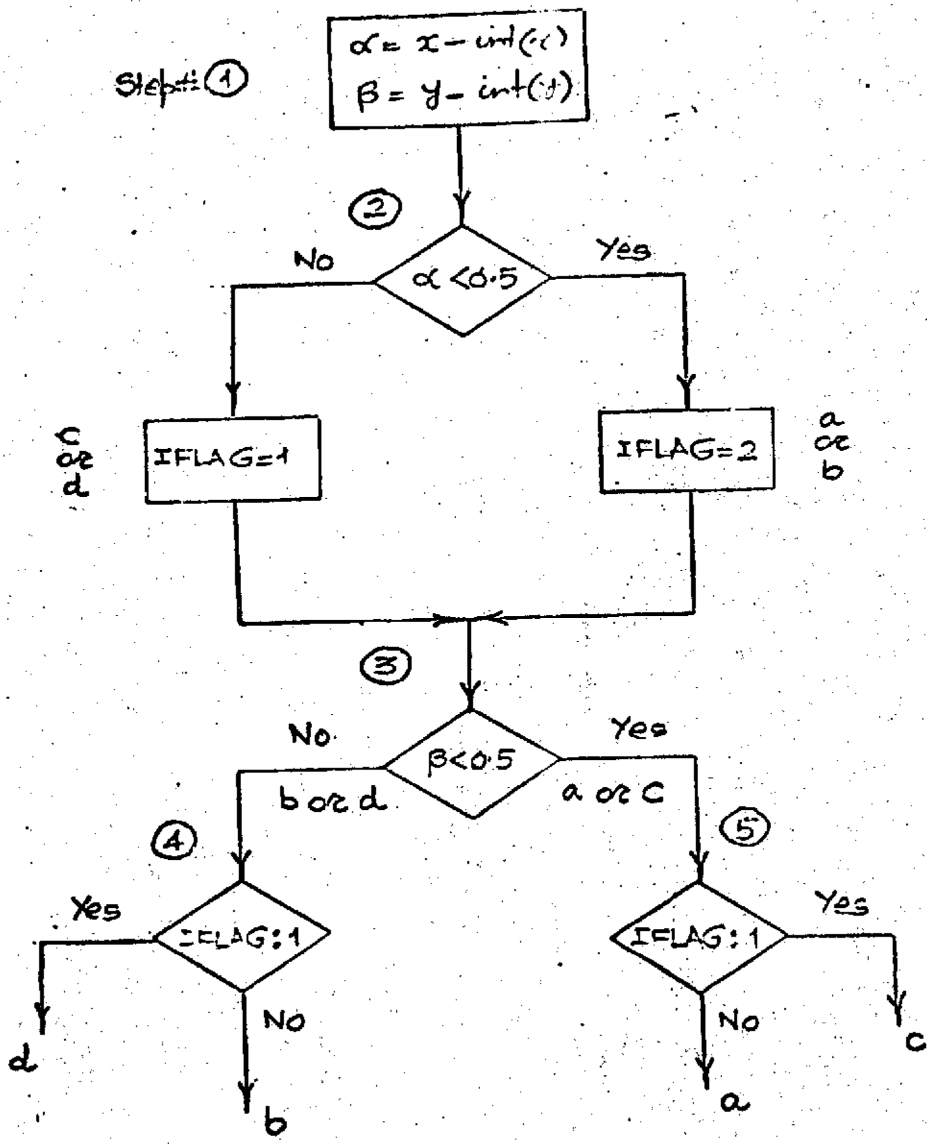

Fig. D.2.3.1-15 Nearest Neighbor Interpolation (I) Computations

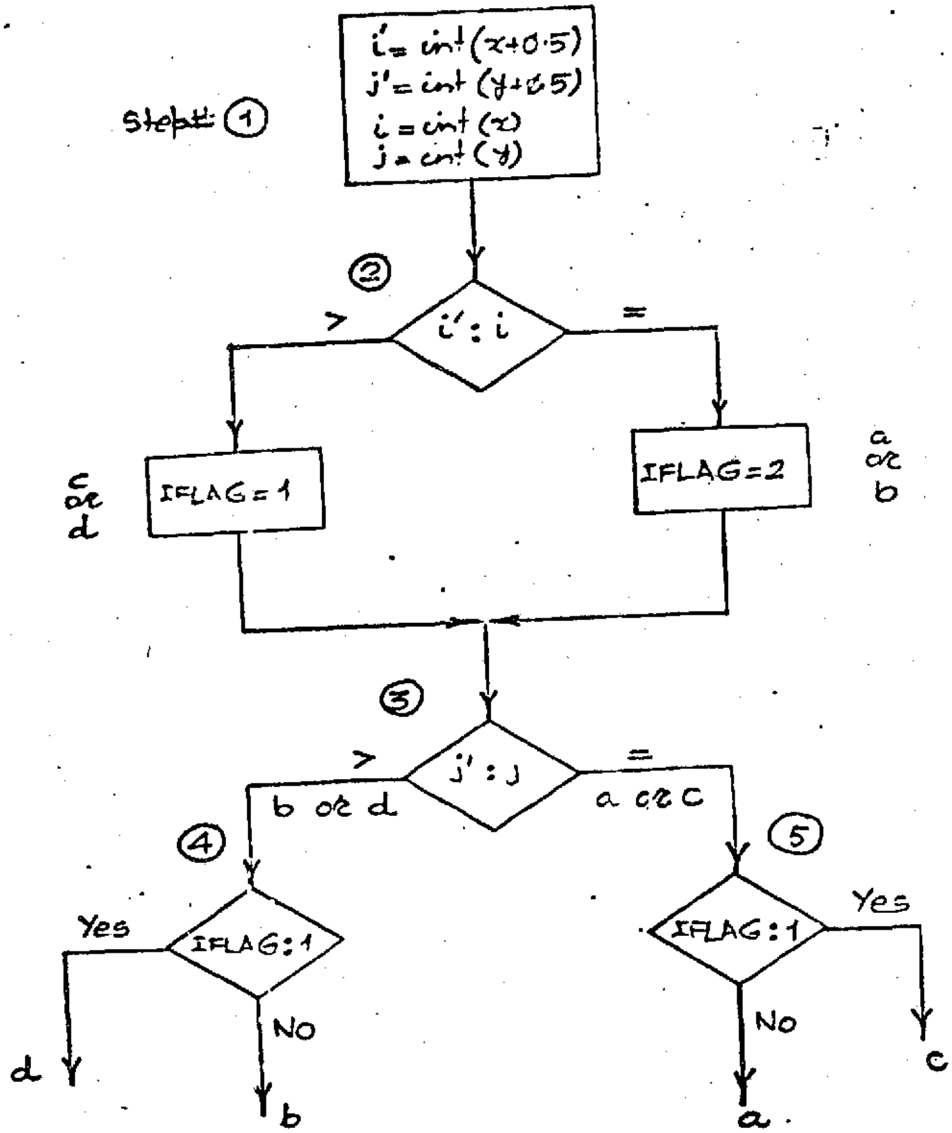

Figure D.2.3.1-16 Nearest Neighbor Interpolation (II) Computations

Table D.2.3.3.4-1 Computer Operations for Nearest Neighbor Interpolation

Interpolation Type	Step No.	Adds	Subs	Multis	Divs	Compare & Branch
Nearest Neighbor (I)	1	0	2	0	0	0
	2	0	0	0	0	1
	3	0	0	0	0	1
	4	0	0	0	0	1
	5	0	0	0	0	1
	1-5	0	2	0	0	4
Nearest Neighbor (II)	1	2	0	0	0	0
	2	0	0	0	0	1
	3	0	0	0	0	1
	4	0	0	0	0	1
	5	0	0	0	0	1
	1-5	2	0	0	0	4

(1) Nearest Neighbor Interpolation

This interpolation involves finding the data sample closes to (x,y) and transferring the light intensity of that sample to (x,y). That is

I (x,y) = intensity of light at the nearest neighbor found (1)

Figures D.2.3.1-15 and D.2.3.1-16 give two versions of the nearest neighbor interpolation algorithms and Table D.2.3.3.4-1 summarizes the computer operations required for this interpolation.

(2) Bilinear Interpolation

This interpolation algorithm involves the finding of 4 data samples closest to (x,y) and obtaining I (x,y) as a weighted sum of the intensities of light of these 4 samples. I(x,y) is given by

$$I(x, y) = (1 - \beta)\left[(1 - \alpha)I(i, j) + \alpha I(i + 1, j)\right] + \beta\left[(1 - \alpha)I(i, j+1) + \alpha I(i+1, j+1)\right] \quad (2)$$

where

$$\left.\begin{aligned} i &= \mathrm{int}(x) \\ j &= \mathrm{int}(y) \\ \alpha &= x - i \\ \beta &= y - j \end{aligned}\right\}$$

Figure D.2.3.1-17 shows the bilinear interpolation algorithm and Table D.2.3.3.4-2 summarizes the computer operations required for this algorithm.

(3) Cubic Convolution

Cubic interpolation uses 16 original data samples to obtain each output sample.

The algorithm is basically an approximation to ideal (sinx/ x) interpolation and one implementation of time algorithm is shown in Figure D.2.3.1-14. In time implementation, we first interpolate an x-direction to obtain 4 numbers giving the intensities of light at positions; (x,j-1), (x,j), (x,j+1), (x, j+2). Then we interpolate in the y-direction to obtain the light intensity at (x,y). The interpolation function is given by

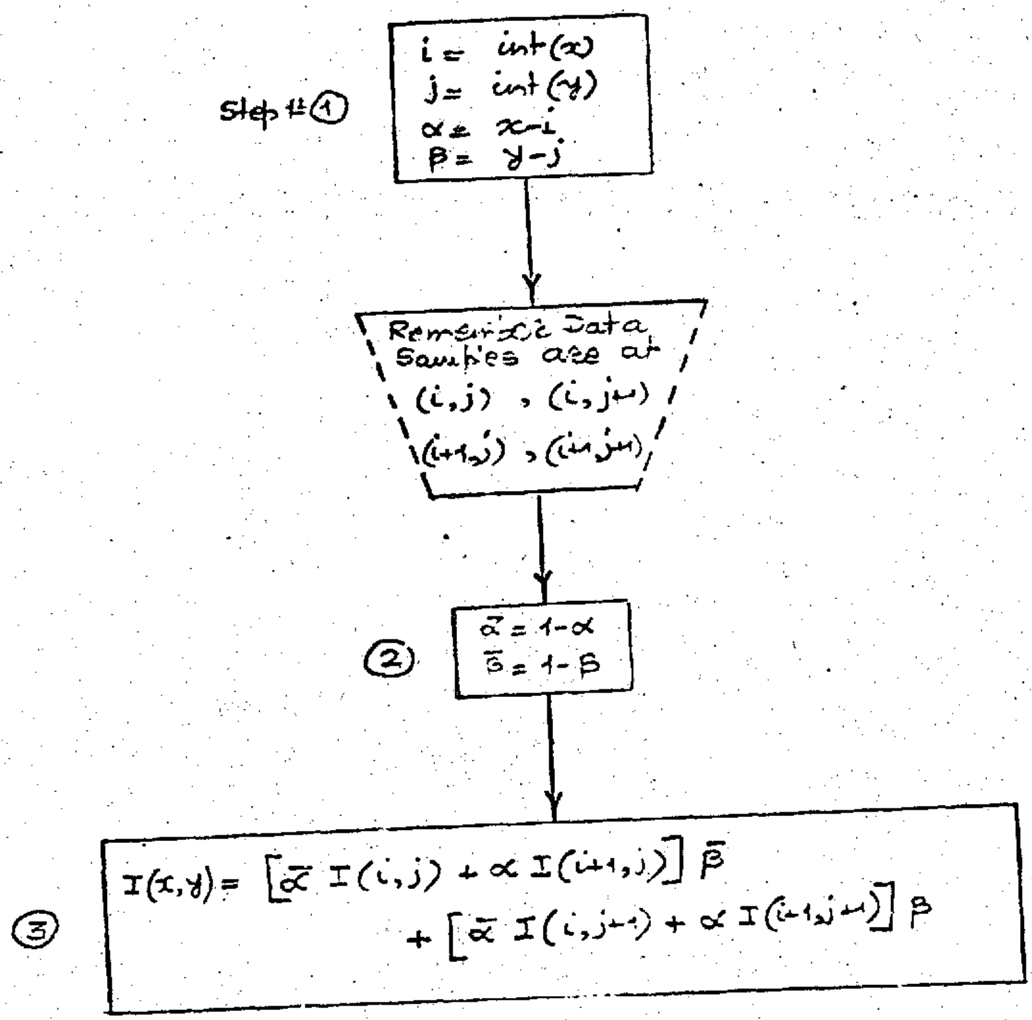

Figure D.2.3.1-17 Bilinear Interpolation Computations

Table D.2.3.3.4-2 Computer Operations for Bilinear Interpolation

Interpolation Type	Step No.	Adds	Subs	Multis	Divs	Compare & Branch
Bilinear	1	0	2	0	0	0
	2	0	2	0	0	0
	3	3	0	6	0	0
	1-5	3	4	6	0	0

Table D.2.3.3.4-3 Computer Operations for Cubic Interpolation

Interpolation Type	Step No.	Adds	Subs	Multis	Divs	Compare & Branch
Cubic	1	0	2	0	0	0
	2	0	2	2	0	0
	3	12	4	24	0	0
	4	0	0	0	0	3
	5	3	1	6	0	0
	1-5	15	9	32	0	3

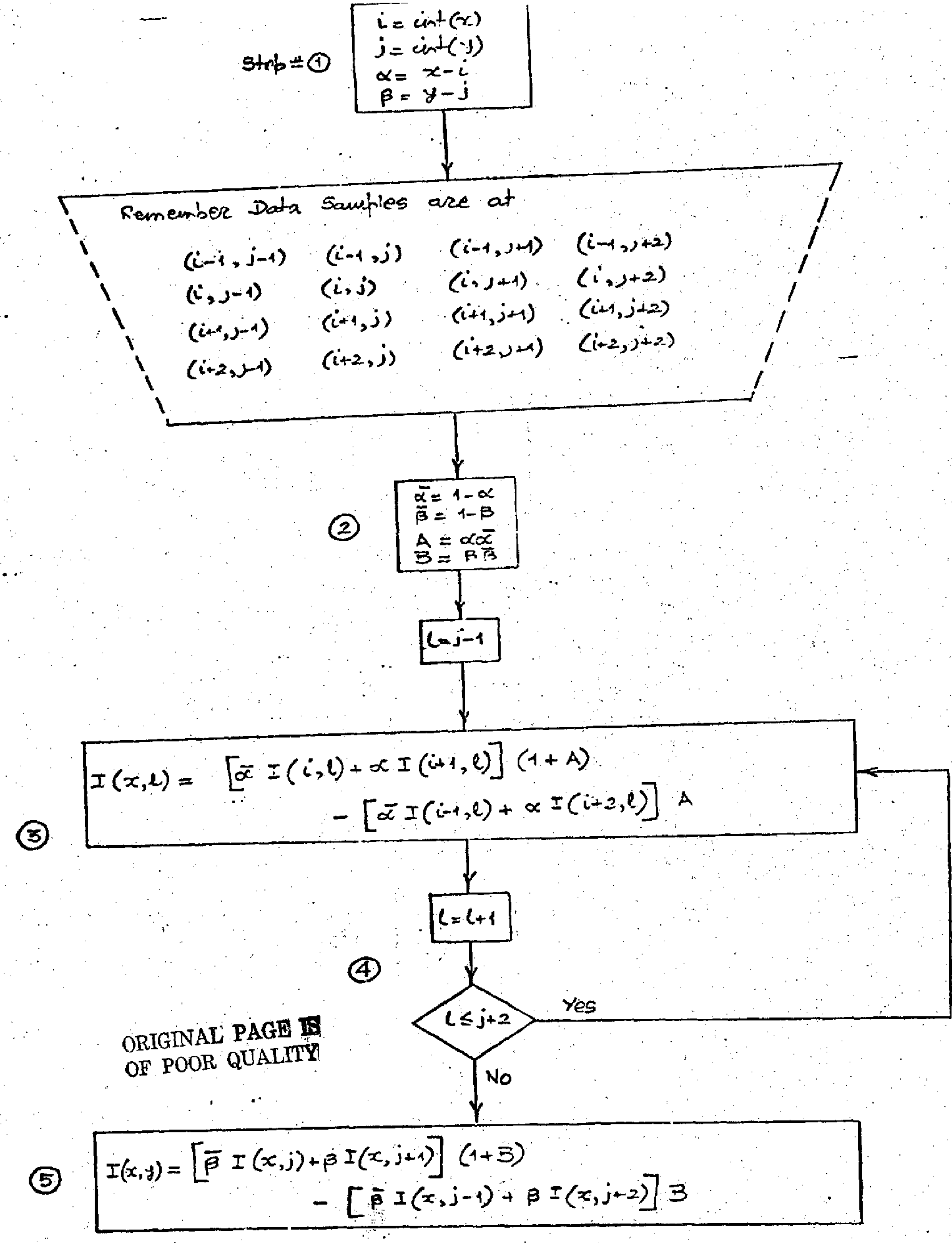

FIGURE D.2.3.1-18 Cubic Interpolation Computations

$$f(\Delta x) = 1 - 2|\Delta x|^2 + |\Delta x|^3 \text{ for } 0 < |\Delta x| < 1$$

$$= 4 - 8|\Delta x| + 5|\Delta x|^2 - |\Delta x|^3 \quad \text{for } 1 \le |\Delta x| < 2 \tag{4}$$

$$= 0 \quad \text{for} \quad |\Delta x| \ge 2$$

Using equation (4) and the appropriate light intensities we obtain using distances in Figure D.2.3.1-14.

$$I(x, \ell) = [1 + \alpha(1 - \alpha)] [(1 - \alpha) I(i, \ell) + \alpha I(i + 1, \ell)]$$
$$- [\alpha(1 - \alpha)] [(1 - \alpha) I(i - 1, \ell) + \alpha I(i + 2, \ell)] \tag{5}$$

for light intensities at positions (x, ℓ); $\ell = j - 1, j, j + 1, j + 2$.

A similar formula as given in equation 5 can be used with β to obtain $I(x, y)$ which is given by

$$I(x, y) = [1 + \beta(1 - \beta)] [(1 - \beta) I(x, j) + \beta I(x, j + 1)]$$
$$- [\beta(1 - \beta)] [(1 - \beta) I(x, j - 1) + \beta I(x, j + 2)] \tag{6}$$

Figure D.2.3.1-18 shows cubic interpolation computations and Table D.2.3.3.4-3 summarizes the computer operations required for this interpretation.

(4) Execution Time and MIPPS Estimates for PDP-11

Computer operations listed in Tables D.2.3.3.4-1, 2, -3, (without data transfers in/out of memory) can be used to compute the execution T_e. This execution time can then be expressed in terms of Machine Instruction per Pixel, MIPPs. We shall define a MI being made up of (LOAD, ADD, STORE) computer instructions.

Table D.2.3.3.4-4 lists the timings for PDP-11 computer using fixed point arithmetic. From there we have

$$\text{MI time} = \text{Machine Instruction time} = T_b = 7.6\ \mu s \tag{7}$$

These tables along with the timings given in Table D.2.3.3.4-4 are used to compute the execution times for interpolation computations. This data along with equation (7) can be used to compute MIPPs. The results, exectuion times and MIPPs, are listed in Table D.2.3.3.4-5.

TABLE D.2.3.3.4-4 PDP-11 Timings for Fixed Point Arithmetic

Processor Timings	μs	Instruction Timings	μs
b = a ± b	7.6	Add/Subtract	2.3
c = ab (EAE* option)	27.1	Multiply (EAE option)	4.3
c = a/b (EAE option)	27.6	Divide (EAE option)	4.8
		Compare (Register mode)	2.3
		Branch	2.6

*Extended Automatic Element (EAE) Option

Although conceptually the EAE option increases the processor's capability, it is an I/O device and operates independently of the processor. The processor controls EAE by supplying it with operands via the I/O device addresses dedicated to EAE. Addresses are reserved for the following EAE registers: AC (accumulator), MQ (multiply quotient), multiply, SC (step count), SR (status register), normalize, logical shift, and arithmetic shift.

TABLE D.2.3.3.4-5 Execution Time and MIPPs for Various Interpolations Using PDP-11 (Fixed Point Arithmetic)

Interpolation Type	Execution Time, T_E (s)	$MIPP = \frac{T_E}{T_b}$
Nearest Neighbor (I or II)	34.8	4.58
Bilinear	215.8	28.4
Cubic	1064.3	140.0

The following conclusions can now be drawn

1. Table D.2.3.3.4-5 gives an idea of the execution time, T_e, and machine instructions per pixel, MIPPs, required for different interpolations. MIPPs of the order of 5, 28, 140 are required for the nearest neighbor, bilinear and cubic interpolations respectively. It must be noted here that MIPPs are not only machine dependent but also T_b dependent (the way T_b is defined). Also these MIPPs do not include the time to transfer data in/out of memory.
2. Tables D.2.3.3.4-1,2,3, which summarize computer operations for various interpolation computations, can perhaps serve (along with the data transfer in/out memory) as a better and more meaningful way of comparison between different computers to be considered for use in EOS data processing.
3. Cubic interpolation involves only a weighted sum depending on the distances. There is no $\frac{\sin x}{x}$ function storage and table look up involved.
4. Some of the computer operations involved in interpolations can be removed from computations.
5. Computers with special capabilities and thumb rules like a predetermined nearest neighbor during the section(s) of a sense can also conceivably reduce the MIPPs.

D.2.3.4 TYPE III Processing

A third type of processing, Type III differs from the Type II processing only in the means that are used to precisely determine the resampling grid. In the Type III processing, ground control points (GCP's) are found in the scenes and these points are used to refine the resampling grid prior to resampling the data.

The purpose of this section is to describe the techniques that can be used for automatic GCP location. We will first try to describe the problem generally and then show that straightforward techniques can result in excessive computation times. Several alternative approaches are described which are reported to give significant reductions in the number of computer operations required to locate GCP's. The machine operations required by the four algorithms for several cases of GCP and search-area sizes are also compared.

D.2.3.4.1 The Basic Problem

The combined effects of earth rate, orbit inclination, S/C attitude and orbit errors, and scanner imperfections, will make it necessary to resample the data taken by the sensor according to a resampling grid that is only an estimate of the grid that was viewed by the sensor. If we retain the concept that the resampling grid consists of a mapping of hypothetical lines of latitude and longitude, which are painted on the earth, into the sensor's coordinate system (the pixels taken by the sensor) then the relationship between the two coordinate systems can be summarized as shown in Figure D.2.3.1-19. In this figure we show a rectangular array of data samples containing M rows and N columns. For the TM data, each line contains approximately 8000 pixels (picture elements) and there are approximately 6000 lines. Superimposed upon the rectangular data array is a set of grid lines representing lines of latitude and longitude which are an estimate of the way that these lines were "seen" by the scanner. We should emphasize that these are only estimates using the best available attitude and orbit data, and the assumption that scanner distortions have been removed to the extent possible.

To state the basic problem, we consider the intersection of grid lines U and V in Figure D.2.3.1-14 which is shown greatly expanded in Figure D.2.3.1-20. This intersection is shown with respect to the picture material in the immediate area. We assume that the picture

material can be recognized in the sense that some natural or man-made structure can be identified. In the example, this structure might be a bridge passing over a body of water. We select as a ground control point the southeast "corner" where the bridge ends. This corner may be easily identified (visually) in the photograph. We also assume that the coordinates of this corner, or point, are precisely known either by ground survey or from precise aerial photograph. If the intersection UV should coincide with the coordinates of the control point, we would conclude (in the example) that our estimated grid was in error (90 meters to the west and 60 meters to the south of its locations). The "control point" would then provide a fine correction for the grid. Without any additional information-- i.e., finding more control points -- one could do no more than shift the entire grid. Such a shift would attribute the disagreement between estimated and actual grid intersection to an orbit error, for example, and correct accordingly. If more GCP's are found in the images, more localized refinements could possibly be made to the grid to account for errors that are not constant over the entire scene.

Precise geometric correction of images during Type 3 processing will make use of a set of ground control points that are predetermined for a particular scene and for which accurate coordinates are known. For this treatment, we will neglect the question of how the coordinates are known. Given that the set of GCP's can be located in the image data, then the resampling grid would be refined further, and the Type 3 processing would then be identical to the Type 2 processing described in Reference 2.

In the remainder of this section we will be concerned with the automatic location of GCP's in an array of image data. We assume that a reference image (sometimes referred to as a "template") exists and our primary task is to find the precise point where this reference agrees with the data. This is basically a correlation problem, i.e., the template is moved around in the image until a point of maximum agreement or correlation is found. The same procedure would be used to "register" two images of the same scene; for example, data in different spectral bands from the Thematic Mapper. We will compare several techniques. First the straightforward correlation procedure is described. Next, an alternative procedure using the two-

dimensional FFT[4] (Fast Fourier Transform) is described that yields a reduction in processing time. A sequential search procedure, called the sequential similarity detection algorithm (SSDA)[5] is also described which is reported to reduce search time by orders of magnitude. A final procedure[6] determines contours or edges in the images, thresholds these, and produces a binary (1's and 0's) image which can then be correlated rapidly with a similar reference image.

[4] P. E. Anuta, "Spatial Registration of Multispectral and Multitemporal Digital Imagery Using Fast Fourier Transform Techniques", IEEE Transactions on Geoscience Electronics, Vol GE-8, No. 4, (October 1970), pp 353-368.

[5] D. I. Barnea and H. F. Silverman, "A Class of Algorithms for Fast Digital Image Registration", IEEE Transactions on Computers, Vol C-21, No. 2, (February 1972), pp 179-186.

6. Conversation with Dr. R. White, Computer Science Corporation.

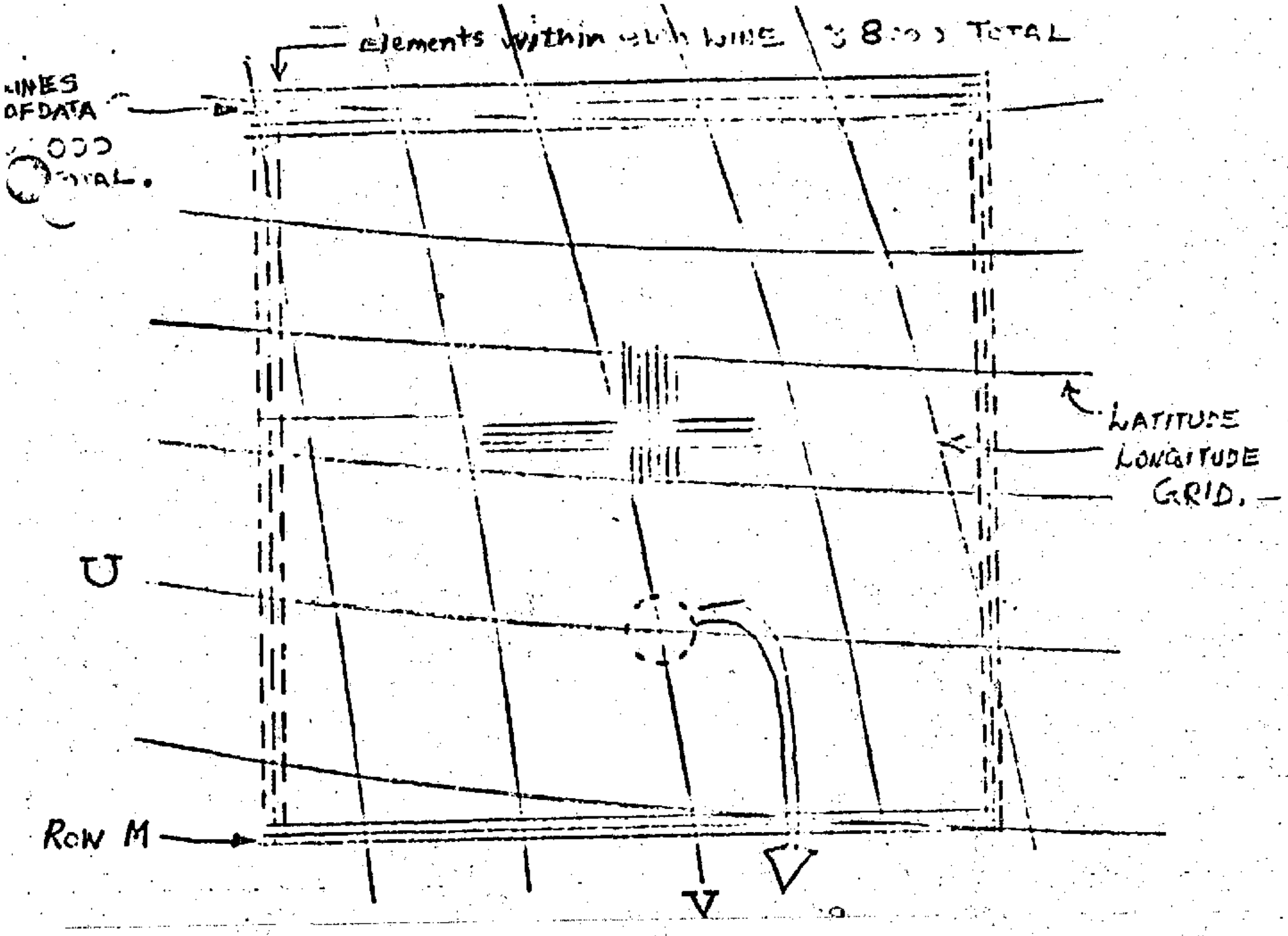

Fig. D.2.3.1-19 Relationship Between Sensor Data and the Resampling Grid

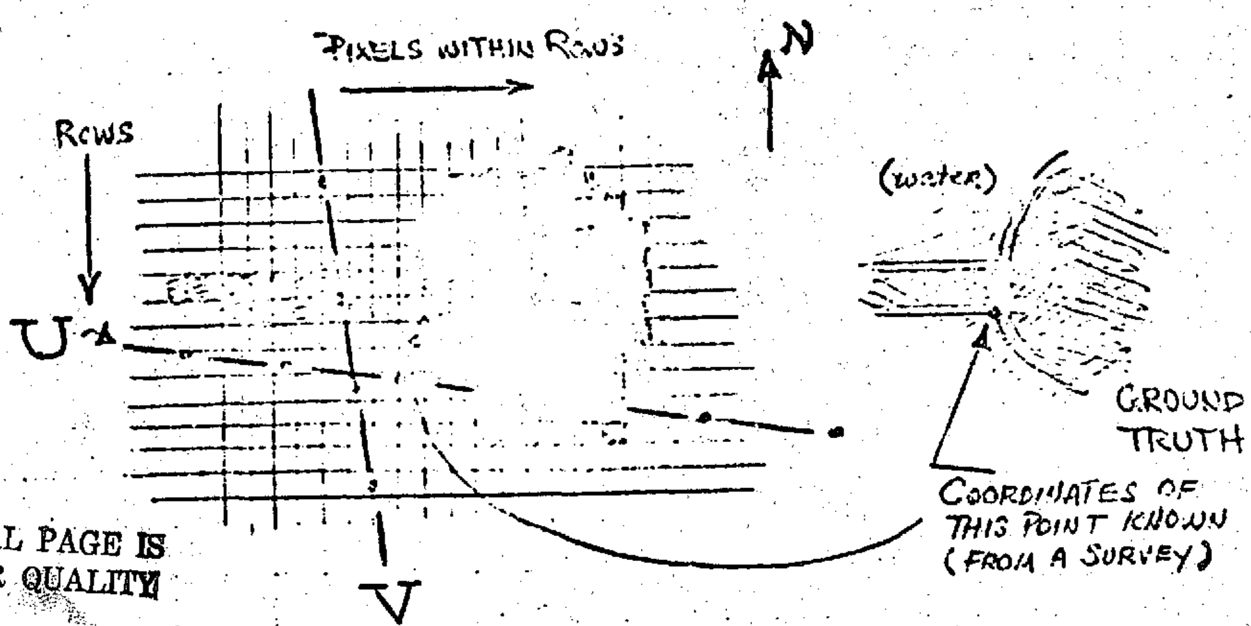

Fig. D.2.3.1-20 Interjection of Grid Lines UV Shown with Respect to the Local Picture Material

D.2.3.4.2 Alternatives for GCP Location

We will assume in the following comparisons that we are required to locate the point of registration of an M-by-M point template in an L-by-L point search area.

Furthermore, we will assume that no apriori information is available so that any of the $(L-M+1)^2$ locations within the area is equally likely to be the registration point. The image data within the search area will be denoted as $P(i,j)$; $1 \le i \le L$, $1 \le j \le L$; and the reference or template will be denoted as $R(k, \ell)$; $1 \le k \le M$, $1 \le \ell \le M$. The elements in both the image and the template are 7-bit picture values (numbers on the range 0 - 127). If we are concerned only with translation, then the upper left corner of the template, R (1,1), is first overlayed with P(1,1) and the two are compared, then R(1,1) is made to coincide with P(1,2) and a comparison is made, and so on for all possible displacements where the template is contained within the image data. There are $(L-M+1)^2$ such positions.

(1) SEARCH BY STRAIGHTFORWARD CORRELATION

To find the point of registration by straightforward correlation, one computes the correlation coefficient C(m,n) as (see Figure D.2.3.4.2-1)

$$C(m,n) = \frac{\sum_{k=1}^{M} \sum_{\ell=1}^{M} R(k,\ell)\; P(k+m, \ell+n)}{\left[\sum_{k=1}^{M} \sum_{\ell=1}^{M} R^2(k,\ell)\right]^{\frac{1}{2}} \left[\sum_{k=1}^{M} \sum_{\ell=1}^{M} P^2(k+m, \ell+n)\right]^{\frac{1}{2}}} \tag{1}$$

In Equation (1) it is assumed that the image has been reduced to zero mean (the mean over each area is computed and then subtracted from each data point) before the correlation is performed. With the normalization, C(m,n) should be between ± 1; also note that the shifts m and n, are restricted to be between 0 and (L-M). The template would be stored in properly normalized form for use in each correlation. Following a computation for the function C(m,n), a search must be performed to find the peak which is then taken as the point of registration. From Reference 5, the number of machine operations required for strightforward correlation would be:

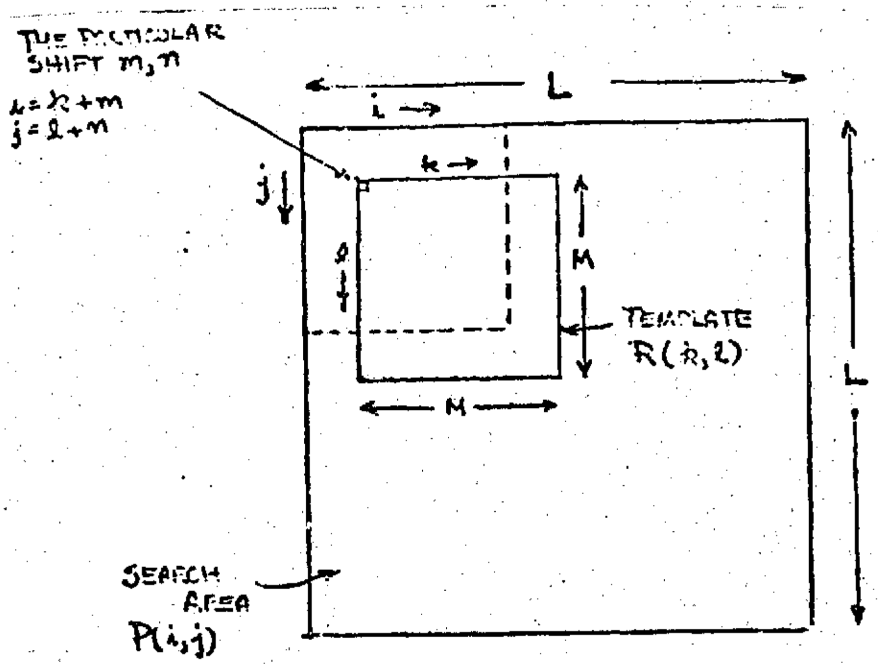

Fig. D.2.3.1-21 Relationship of Template to Search Area.

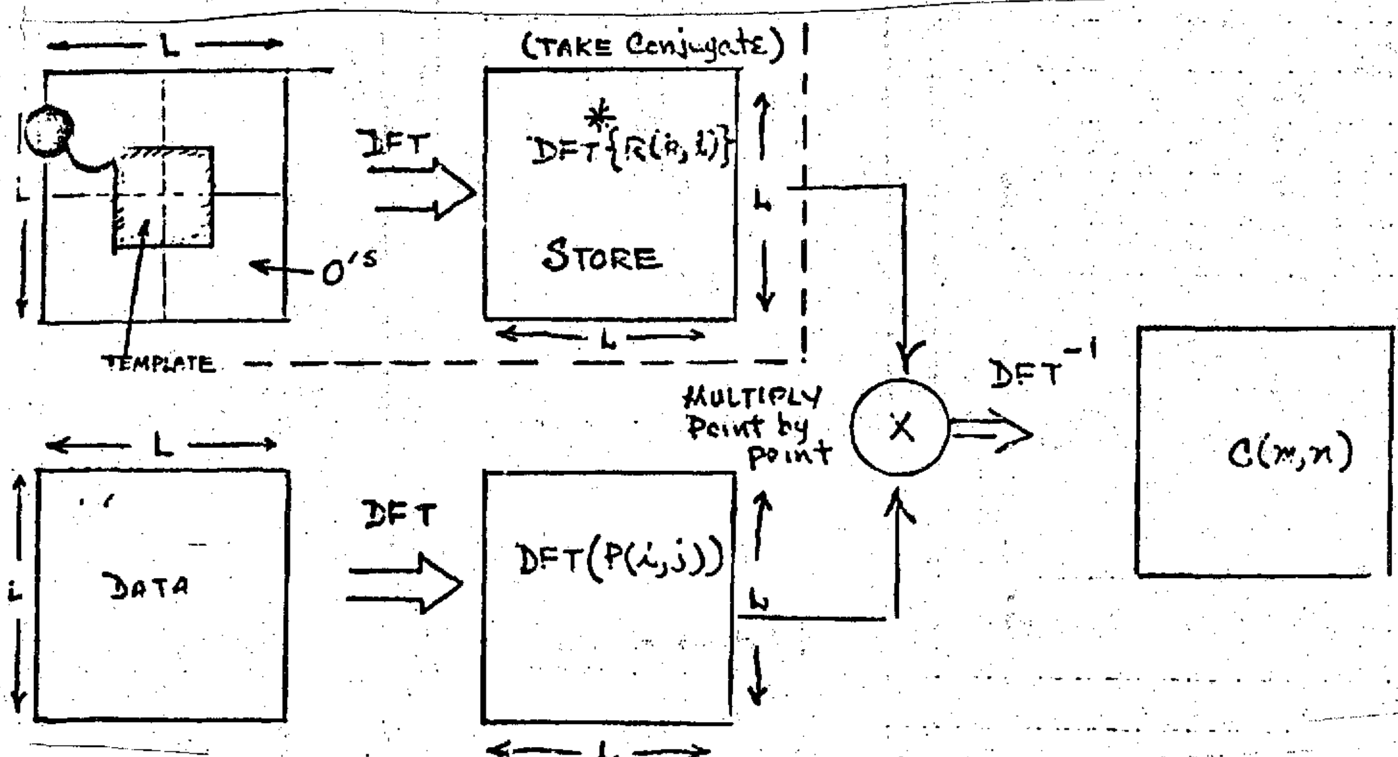

Fig. D.2.3.1-22 Correlation Using the Two Dimensional FFT

$$O_{corr} = 4.5\,M^2\,(L-M+1)^2 \text{ equivalent integer adds} \tag{2}$$

The operations in Equation (2) exclude normalization and the "peak-finding" procedure that must be performed on $C(m,n)$.

(2) CORRELATION BY USING THE TWO-DIMENSIONAL FAST FOURIER TRANSFORM (FFT)

The two-dimensional correlation function $C(m,n)$ can also be found by using the relationship:

$$C(m,n) = DFT^{-1}\left\{DFT\,[P(i,j)]\quad DFT^*\,[R(k,\ell)]\right\} \tag{3}$$

where DFT $\{\ \}$ indicates the discrete Fourier transform, $DFT^{-1}\{\ \}$ its inverse, and * denotes the complex conjugate.

The one-dimensional DFT of a L point block of data requires $L\log_2(L)$ complex real multiplies and an equivalent number of complex additions. The two-dimensional DFT of an LxL area therefore requires $L^2\log_2(L)$ complex multiplies and adds. If we adopt the following equivalent operational times from Reference 5 (relating everything to integer add times)

Integer Multiply Time	=	3.5 x Integer Add Time
Real Add Time	=	2 x Integer Add Time
Real Multiply Time	=	6 x Integer Add Time
Compare Time	=	Integer Add Time
Complex Real Add	=	4 x Integer Add Time
Complex Real Multiply	=	28 x Integer Add Time

Then the operations can be estimated with the help of Figure D.2.3.1-22, First, $L^2\,\mathrm{Log}_2\,(L)$ complex multiplies and adds must be performed to obtain DFT $\{P(i,j)\}$. Next, the stored value of DFT* $\{R(k,\ell)\}$ is multiplied point-by-point by DFT $\{P(i,j)\}$ requiring $28\,L^2$ equivalent integer adds. Finally, the inverse transform is taken of the product giving $C(m,n)$. Total operations, excluding normalization and "peak-finding" become

$$O_{FFT} = 32\,L^2 \log_2(L) + 28\,L^2 + 32\,L^2 \log_2(L)$$
$$= L^2 \left[64 \log_2(L) + 28\right] \text{ equivalent integer adds.} \tag{4}$$

Equation (4) gives at least an order of magnitude reduction in machine operations compared to Equation (2).

(3) SEQUENTIAL TESTS TO DETERMINE CORRELATION

A sequential procedure is proposed in Reference 5 that searches over the [L-M+1] by [L-M+1] area as with correlation but makes a decision at each registration point in far fewer than M^2 multiplications and additions. Rather than multiplying corresponding points, the absolute value of differences (or errors) between the corresponding points in the template and the image are accumulated. The time for these accumulated errors to exceed a threshold (T) are recorded and the larger values of time (or test length) correspond to points of similarity. In other words, the error values are smaller and accumulate more slowly when the image data is similar to the template. The time spent processing each possible registration point is now a random variable and in Reference 5 this average value is estimated as $10\,(M/32)^{\frac{1}{2}}$. The number of operations for this procedure (termed SSDA or sequential similarity detection algorithm, is estimated in Reference 5 as

$$O_{SSDA} = 4\left[1 + 10\,(M/32)^{\frac{1}{2}}\right] \left[L\text{-}M\text{+}1^{\;2}\right] \text{ equivalent integer adds} \tag{5}$$

(4) CORRELATION USING CONTOURS IN THE IMAGES

A final technique for GCP location makes use of contours or "shapes" in the image data and forms a binary image (1's and 0's) to perform correlation with. In addition to the simplicity of the binary correlation, the procedure may be much less sensitive to noise and variations in the image data. [Note that we are not performing correlation on noise-free data and, to make matters worse, ground control area may change their appearance with seasonal variations.]

The contouring technique is described conceptually in Figure D.2.3.1-23. As an example, we use the structure in Figure D.2.3.1-20; the template and the image data are processed to sense "edges"; i.e., lines where brightness values change rapidly along constant contours. These edges generally will be closed lines around objects although they may also follow shorelines. The result (after comparing these "gradients" to a threshold is a 1 or a 0 in each pixel location (the resultant image might contain only 10 or 15 percent 1's). Correlation is then performed with these binary images.

We can only estimate the operations required for this procedure in a very crude manner. This is accomplished as follows:

1. The original LxL points must be processed over possibly a 4x4 point surrounding area to determine gradients. We can estimate this as $32\,L^2$ equivalent integer adds.
2. L^2 compares must be made to compare each gradient to a threshold.
3. Binary correlation involving only 15 percent of the points in MxM areas are performed. Each point must, however, be tested so that M^2 compares are needed.

Total operations for the binary correlation become:

$$O_{bin} = 1.15M^2\,(L-M+1)^2 + 33\,L^2 \text{ equivalent integer adds} \tag{6}$$

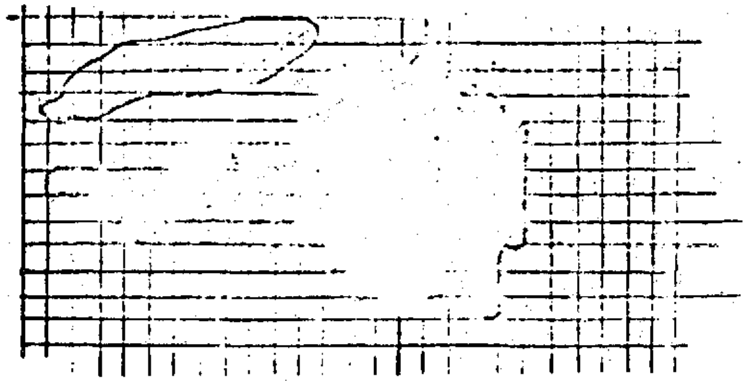

a) Original Data; Lines of Constant Brightness are "Connected"

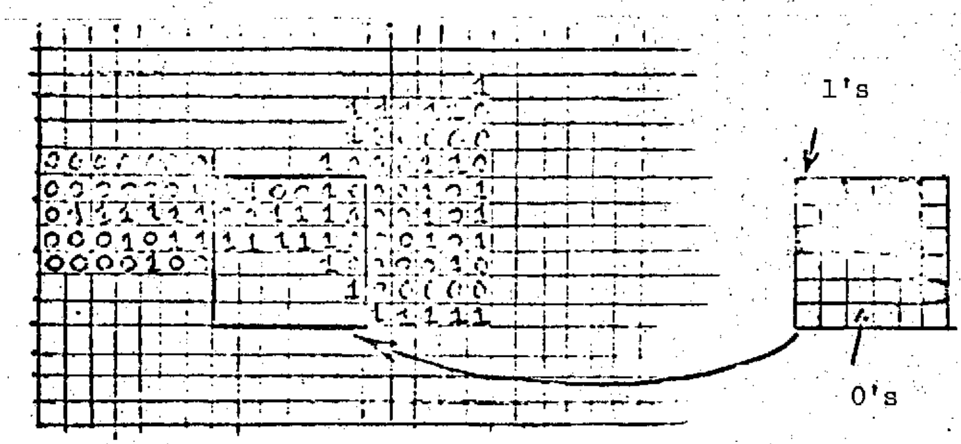

b) Contours Compared to Threshold; Those That Exceed Threshold Cause Corresponding Pixels to be Set to 1

Fig. D.2.3.1-23 Correlation Using Binary Image Which Represents Contours

ORIGINAL PAGE IS OF POOR QUALITY

D.2.3.4.3 COMPARISON OF THE ALGORITHMS

We can now compare the number of operations required to locate GCP's using the four algorithms previously described (briefly).

Comparison of Machine Operations (Integer Adds)
for GCP Location

Search Area L x L	GCP Size M x M	Correlation O_{corr}	FFT O_{FFT}	Sequential O_{SSDA}	Binary O_{bin}
128	32	4.3×10^7	7.8×10^6	4.1×10^5	1.15×10^7
256	32	2.3×10^8	3.5×10^7	2.2×10^6	6.0×10^7
512	32	1.06×10^9	1.6×10^8	1.0×10^7	2.8×10^8
1024	32	4.5×10^9	7.0×10^8	4.3×10^7	1.2×10^9
128	64	7.7×10^7	7.8×10^6	2.5×10^5	2.0×10^7
256	64	6.8×10^8	3.5×10^7	2.2×10^6	1.7×10^8
512	64	3.7×10^9	1.6×10^8	1.2×10^7	9.5×10^8
1024	64	1.7×10^{10}	7.0×10^8	5.5×10^7	4.3×10^9

A general conclusion is that the FFT approach yields approximately an order of magnitude reduction in the number of machine operations required for GCP location as compared to straightforward correlation. The binary correlation scheme appears to offer about the same reduction although, at present, not enough is known about this technique to make a detailed comparison. The SSDA yields reductions from 50 to 200 compared to correlation. Reductions of this magnitude are significant in that they reduce GCP location from an operation that is excessive in terms of processing time (dominates the processing) to an operation that is almost negligible when compared to the other processing that must be performed on the digital images.

Simulations of these four techniques must be performed, preferably on real image data, before any conclusions about the relative accuracy of the techniques can be made.

CONICAL SCANNERS

D.2.3.5 THE IMPACT OF THE CONICAL SCANNER ON THE COST OF PROCESSING THE THEMATIC MAPPER (TM) IMAGES

D.2.3.5.1 INTRODUCTION

One of the candidate approaches to the Thematic Mapper (TM) design is the image-plane scanner developed by Minneapolis Honeywell. Advantages of this alternative design include a rotating rather than an oscillating mirror, better scan linearity, and possibly lighter weight of the overall instrument. A disadvantage is that, in order to keep the optics as simple as possible, the image is scanned at an angle with the result that the earth is scanned with conical rather than linear scan lines. More precisely, the path of the scanner for any particular sweep of the earth can be envisioned as following a path along the rim of a cone. The cone has some thickness since each sweep produces 15 scan lines at a time, each 30 meters wide in the north-south direction. Although the rim of such a cone would intersect a flat surface with no overlap of the scan lines, the intersection with a sphere will result in an overlapping of the 15 scan stripes near the edge of the scan. This effect, and the shape of the scan lines on the curved earth, will be dependent on the angle with which the cone intersects the earth. Also, picture samples can be taken during the forward or backward looking portion of the scan. Generally, then, we are dealing with scan patterns that are sectors of circles which are concave forward with respect to the ground track for a scan at the rear of the nadir point, or convex forward when scanning ahead of the spacecraft. These two options have no clear advantages over one another. The cone orientation can also be selected to scan through the nadir point. Although this option may produce slightly less image distortion, it will not be considered in the following disucssion (scan lines become parabolas rather than circles and the mathematical complications could obscure the first-order effects which are the only effects to be included in the analysis).

Our goal here is to compare the conical-scan and linear-scan Thematic Mappers in terms of the processing that must be performed to achieve precise geometric correction of the resulting digital images. By geometric correction, we shall refer to

all of the digital processing steps that are necessary to produce a precise map in a UTM coordinate system. We will attempt to quantify the extra storage and the extra machine instructions (if any) required to correct the conical scan data compared to the linear scan data.

In Section D.2.3.5.2, the conical-scan geometry is described for a simple flat-earth case. This case should be adequate to reveal the major (first-order) geometric distortions. Complexity and costs are then estimated for the processing of these images and these are compared to the costs for the linear case. Since a definitive set of numbers for the conical scan parameters are not available at present, the necessary numbers have been assumed. The results should be adequate for the cost estimates which are shown here, however.

D.2.3.5.2 ASSUMED GEOMETRY OF THE CONICAL SCANNER

The relationship of the conical scan pattern with respect to the 185 km swath is shown in Figure D.2.3.1-24. We assume that six segments are used on the scan wheel and that the scan is to be 80 percent efficient. Active scanning therefore covers 0.8 x 360 = 288° and each segment covers 48°. In Figure D.2.3.1-25, we show the detailed geometry of the scan lines within the 185 km swath. For the case shown, the bow in the scan lines is given by the distance b which is

$$b = R - x = 227.418 \text{ km} \quad [1 - \cos \Theta/2] = 19.66 \text{ km} .$$

With a resolution of 30 meters, 655 resolution elements or 43 sweeps of the scanner are contained in the bowed region.

In Figure D.2.3.1-26, we show in more detail the relationship of the conical scan line to the resampling grid structure. This drawing is approximately to scale and we have assumed a 10 X 10 resampling grid. The large 185 X 185 Km rectangular area corresponds to the "scene" taken by the sensor. Within this scene, there are 6166 individual scan lines representing approximately 411 sweeps of the sets of 15 detectors in each band. Each sweep of the scanner traces out an arc of a circle with radius 227 km. The scanner produces pixels at equal-angle increments within the ± 24° sector with the individual elements representing angles of approximately 97 μ radians (this should not be confused with the 44 μ rad resolution of the TM from orbit altitude).

The scan pattern is normal to the S/C heading which is itself oriented by Θ_H^o with respect to south (Θ_H^o measured clockwise with respect to due south). This heading angle is given by

$$\Theta_H = \sin^{-1} \left[\frac{\sin \Theta_E}{\cos \lambda} \right] \tag{1}$$

where

Θ_E is the polar inclination (6° assumed)

λ is the latitude.

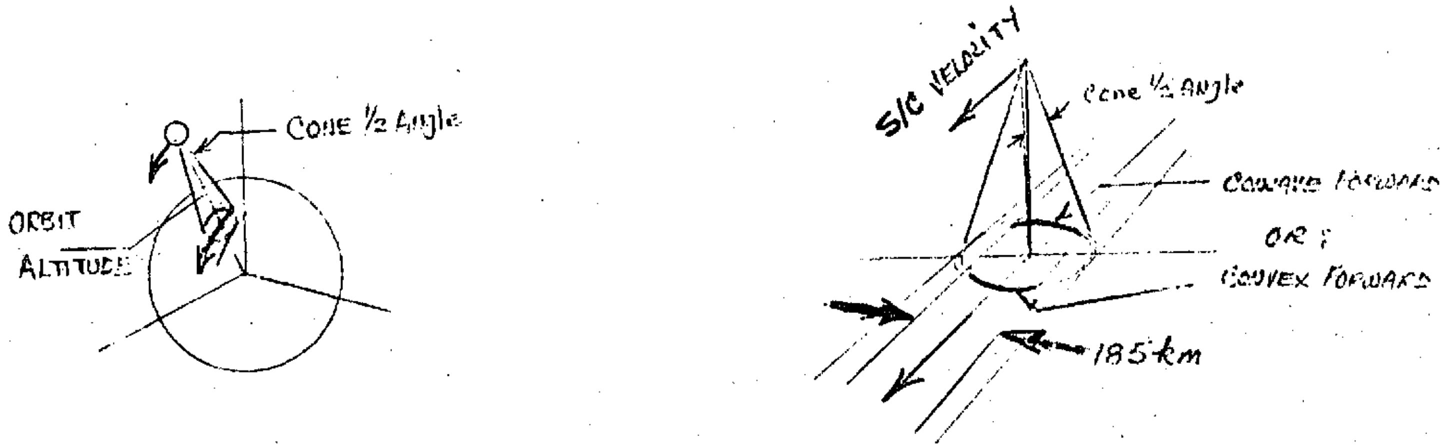

Fig. D.2.3.1-24 Basic Conical Scan Pattern & Flat-Earth Assumption

$\theta = 48°$

$\sin \frac{\theta}{2} = \frac{S/2}{R}$

$\therefore R = \frac{185\,km}{2} \times (\sin 24°)^{-1}$

$= 227.418\ km.$

For orbit alt of 680 km
½ cone angle ~ 18.5°

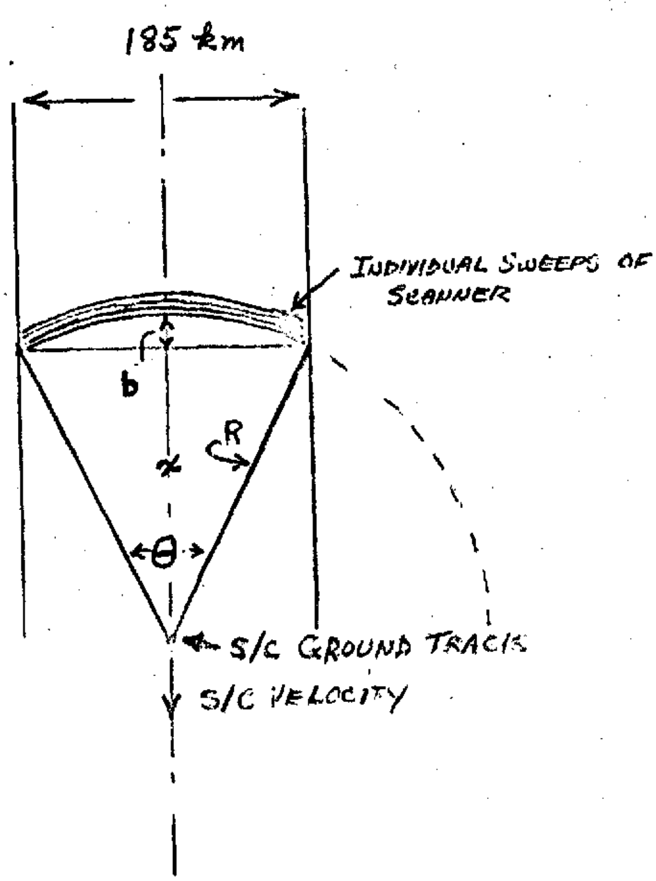

Fig. D.2.3.1-25 Geometry of Backward Conical Scan

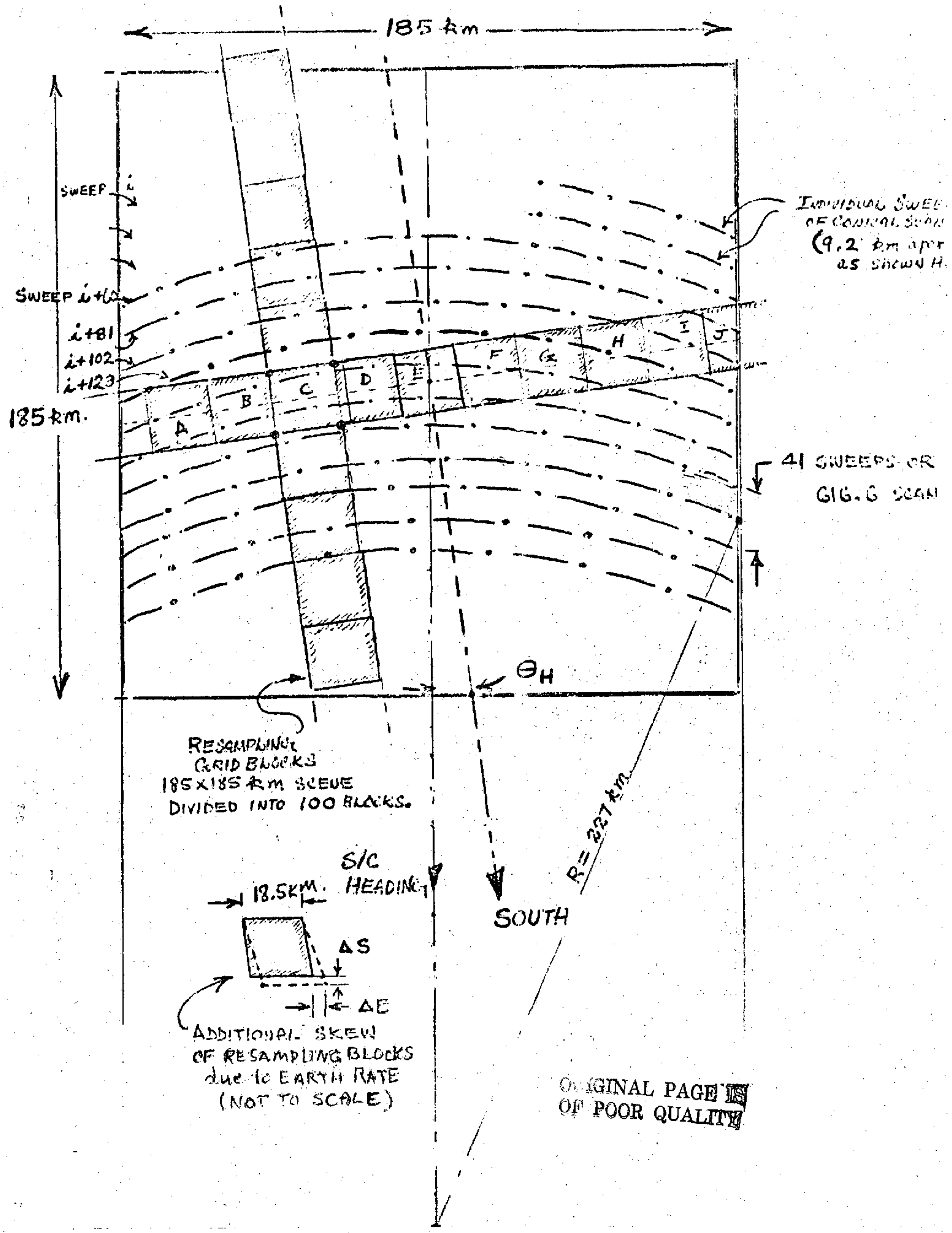

ORIGINAL PAGE IS
OF POOR QUALITY

Fig. D.2.3.1-26 Location of Resampling Grid Blocks Within the 185 X 185 km Scene

For a latitude of approximately 37°, the heading angle is 7.5°. Therefore, we show the orientation of the resampling grid blocks within the scene as oriented at an angle of nominally 7.5° with respect to the S/C ground track. There are approximately 100 of these blocks representing a 10 x 10 subdivision of the desired output grid. Each of these blocks is subjected to an additional skew due to the earth's rate of rotation. This skew can be estimated as

$$\Delta S = V_E \, \delta t \, \cos \Theta_H \cos \lambda \tag{2}$$

$$\Delta E = V_E \, \delta t \, \sin \Theta_H \cos \lambda \tag{3}$$

Where V_E is the velocity of the earth at the equator (463.38 m/s) and δt is the time for one sampling block to be scanned (approximately 1/10 of the scene time or 2.7 seconds). For a 6° inclination at 37° latitude, we obtain ΔS = 130 meters and ΔE = 990 meters. Compared to the skew due to ground - track heading (approximately 18.5 km x tan (7.5°) = 2423 meters) these additions are fairly small but they do add to the overall skew of the resampling blocks with respect to the image data.

Even for a linear scanner, the skew of the resampling grid relative to the scan pattern causes some complication in collecting together the data needed for the blocks. This complication is increased for the conical scan lines. For example, sweep (i + 123) in Figure D.2.3.1-26 contributes to block A but is not needed again until block G, H, and I. To reconstruct a single output scan line, say the top line in all blocks A through J, the number of scan lines that must be accessed (hence stored) is determined by the bow in the scan lines (d = 19.66 km corresponding to 655 scan lines) plus the tilt due to the heading angle (185 km x tan 7.5° corresponding to 24.2 km or 807 scan lines). The conical scanner, therefore, requires 1462 scan lines to produce one output line which is an increase of 80 percent over the linear scanner. An additional complexity concerns the algorithm that must be used to compute the coordinates of the desired output data points with respect to the conical scan data.

D.2.3.5.3 PROCESSING COMPLEXITY

(1) INTRODUCTION

Some of the processing which must be performed on the TM data is peculiar to the conical scan pattern and will, therefore, require more processing than for the linear case. A second factor that must be considered is the increase in storage required to process the conical scan data. Finally, the third factor that must be considered is the accessability of the resampling blocks from the intermediate storage device which we will assume to be a disk.

(2) CALCULATION OF COORDINATES OF THE CONICAL SCAN DATA IN THE OUTPUT COORDINATE SYSTEM

The main computational complication in resampling the conical scan data is the determination of the coordinates of the original data points (line number and pixel number within the line) for each desired point in the output grid blocks. In Figure D.2.3.1-27 we show a worst case situation where we are resampling the data in grid block "I" of Figure D.2.3.1-26. The cross-track distance to a general point (x,y) in this block is

$$d = \frac{S}{2} - \left[(G - y) \sin \beta + x \cos \beta\right] \tag{4}$$

where G is the dimension of the grid block (assumed square) and β is the total tilt angle. Given d, one can find Θ as

$$\Theta = \sin^{-1} \left\{d/R\right\} \tag{5}$$

and the distance D is then found as

$$D = R \cos \Theta + y \cos \beta \tag{6}$$

If the angle Θ is known, then the element (or nearest element) in a particular scan line is known. If D is known, we can find the nearest scan line to the desired output

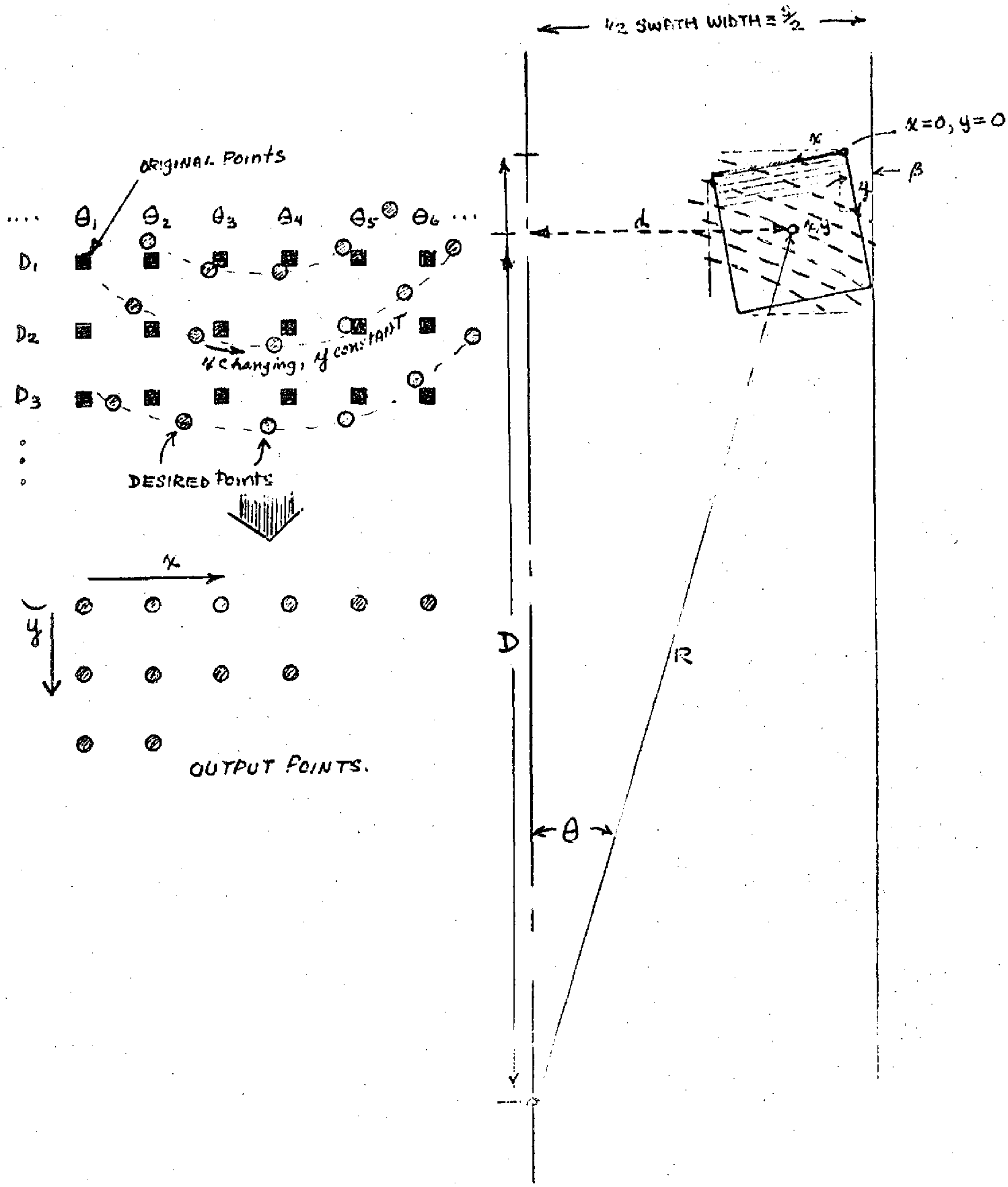

Fig. D.2.3.1-27 Resampling Geometry for One Grid Block

point. This situation is shown at the left of Figure D.2.3.1-27. Here we show the original array of sampling points as squares and these points define an array of data indexed by Θ and D (P (Θ, D)). The coordinates x and y define the coordinates of the points in the desired output array R(x, y). Given x and y, one can solve for d by using (3). Pixel number is then found by using (5) to obtain Θ. Finally, knowing Θ, one finds line number from D in (6).

It is clear that (4), (5) and (6) give a nonlinear set of equations for Θ and D as a function of x and y. Assume first, that we want a set of coordinates for a particular line in the output array where y remains constant at a value Y_o. To find Θ and D by straightforward techniques, one would solve (4), (5), and (6) as follows

Constants: S/2, $(G - Y_o)\sin\beta$, $\cos\beta$, R

		Floating Pt Mply.	Ft. Pt. Divide	Ft. Pt. Add	Trig. Function
Equation (4)	$x\cos\beta$	1			
	$[x\cos\beta + (G - Y_o)\sin\beta]$			1	
	$S/2 - [\quad] = d$			1	
Equation (5)	d/R		1		
	$\sin^{-1}[\quad] = \Theta$				1
Equation (6)	$\cos\Theta$				1
	$R\cos\Theta$	1			
	$R\cos\Theta + Y_o\cos\beta = D$			1	
	TOTAL	2	1	3	2

Using the equivalences:

Floating Point Multiply	=	5 integer add times
Floating Point Divide	=	11 integer add times
Trigonometric Function	=	22 integer add times
Floating Point Add	=	3 integer add times

we obtain a total of 74 machine instructions for the coordinate computation of each output point. This is an intolerable processing load (equivalent roughly to the operations required for "cubic convolution" interpolation) and a simple recursive implementation of (4) through (6) must be found.

To examine the complexity of such a recursive algorithm, we consider a further expansion of Figure D.2.3.1-27 and consider the changes in Θ and D as x and y move away from the origin in Figure D.2.3.1-28. Given that we start with x=0, y=0, we see that the starting value of d, θ and R are simply

$$d_o = S/2 - G \sin \beta$$

$$\Theta_o = \sin^{-1} \left[d_o / R_o \right]$$

$$D_o = R \cos \Theta_o$$

From the geometry, it should be possible to construct a simple recursive updating of x, assuming y is constant, of the form

$$\text{New } X = \text{Old } X + \Delta X$$

$$\text{New } \Delta X = \text{Old } \Delta X + \ddot{X} k_1$$

$$\text{New } \ddot{X} = \text{Old } \ddot{X} + \dddot{X} k_2$$

At the end of one resampling line, the coordinate y would be updated in a similar fashion. Also, there may be a dependence between x and y so that x initial conditions the x increments are related to the y increments. Simulations will be required to verify the accuracy of recursive equations of various degrees but it does appear that these techniques could reduce the number of instructions by 4 or 5 to 1 giving 15 to 20 instructions/pixel for coordinate computation.

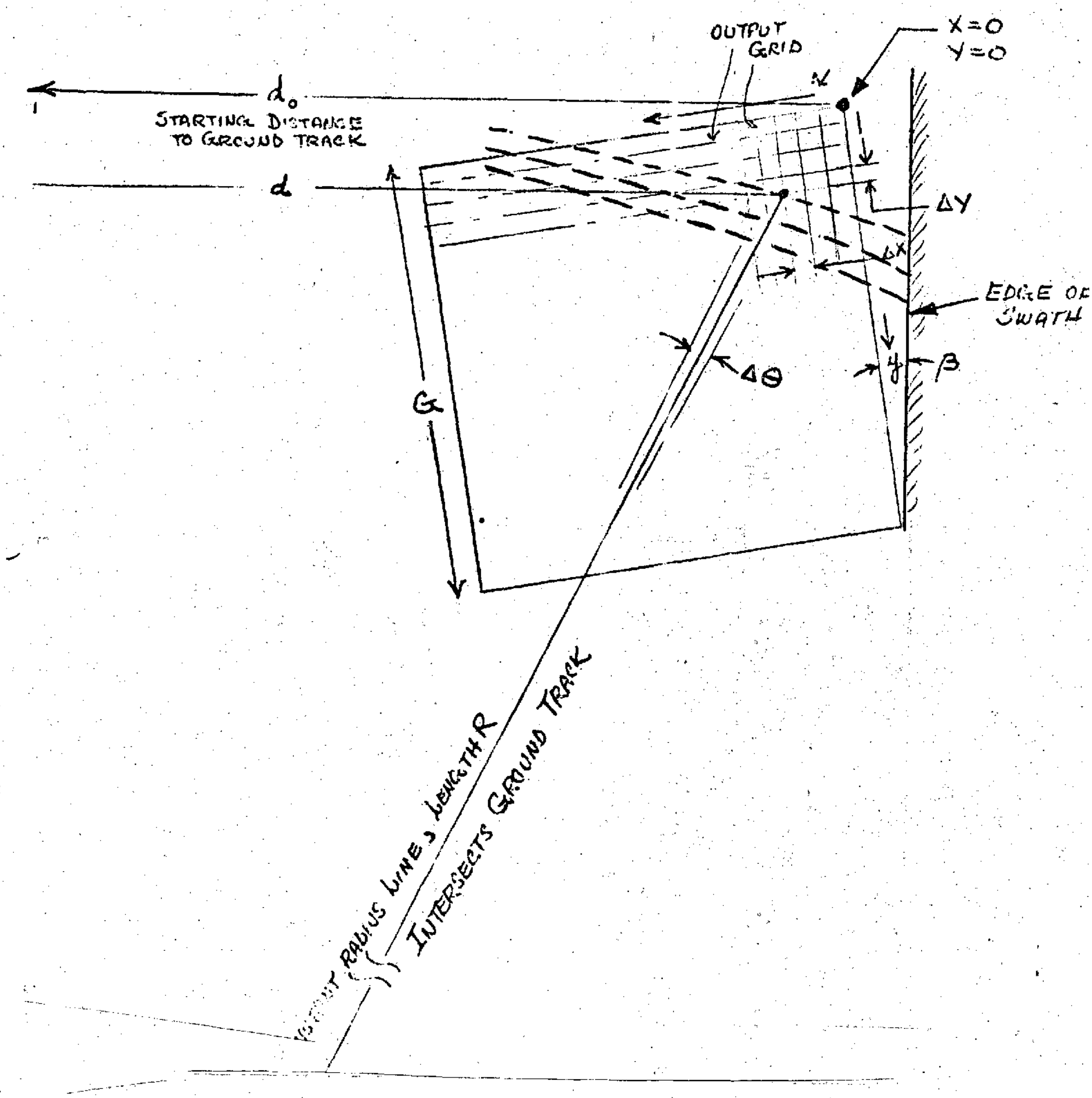

Fig. D.2.3.1-28 Detail of the Resampling Within One Grid Block

For the purposes here, we will use the conservative estimate of 74 instructions/pixel for the conical scan coordinate computation. The major contributors to processing load are summarized as:

	Instructions/Pixel Linear		Conical		Excess for Conical Scan
Radiometric Corr.	2		2		
Line Stretching	0.64*		0.64*		
Resampling Grid	Negligible for 100-point grid				
Coordinate Computation for Resampling	0.48*		11.8*		
Interpolation		Totals		Totals	
Nearest Neighbor (NN)	8.0	11.1	8.0	22.4	+100%
Bilinear (BI)	25.0	28.1	25.0	39.4	+ 40%
Cubic Convolution (CC)	60.0	63.1	60.0	74.4	+ 18%
GCP Location	Negligible for 4 per scene/baseline ACS.				

* Divided by 6.25 since one computation serves for all bands.

(3) ADDITIONAL STORAGE REQUIRED TO HOLD THE DATA REQUIRED TO PRODUCE A SINGLE OUTPUT GRID BLOCK

A second factor in processing the conical scan data is the storage required to hold the individual blocks. If we consider a block as 1 percent of a scene, then the number of pixels in a block are approximately

$$N_{PB} = 616 \frac{\text{lines}}{\text{block}} \times 866 \text{ pixels/line} \times 6.0625 \text{ bands} = 3.23 \times 10^6 \text{ pixels}$$

In Figure D.2.3.1-29 we plot the percentage extra points that must be stored to process a single block of data as a function of satellite inclination angle with several latitudes as the parameter (differences with orbit altitude in the range 640-775 km are negligible). ~~If~~ we express N_{PB} in terms of bits, and assign a cost of $0.05 per bit for high speed-storage, we can estimate the costs of this extra storage by the right hand scale on Figure D.2.3.1-29.

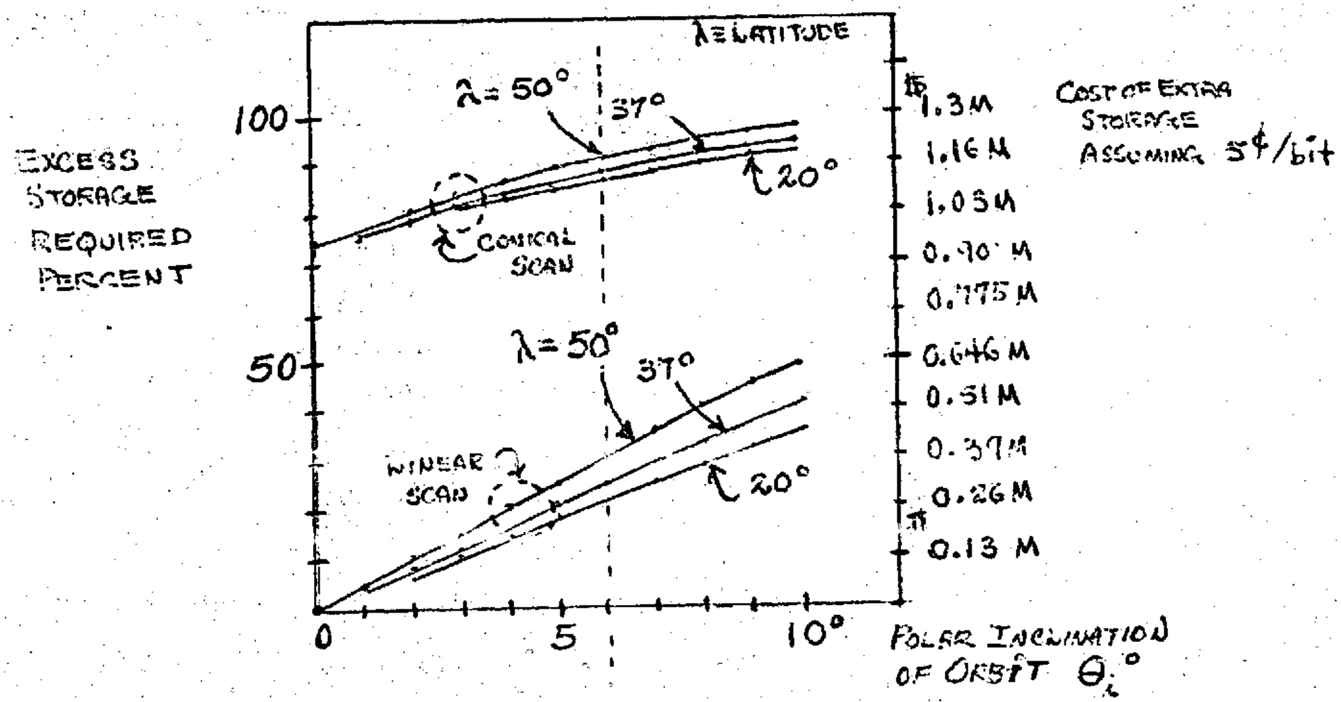

Fig. D.2.3.1-29 Extra Storage Required, Expressed as a Percentage of the Data in a Block, as a Function of Inclination Angle

In the comparison above, we are assuming that the individual blocks, each containing 3.23×10^6 eight-bit bytes of data (all bands), are processed individually in the computer. In the next section, we consider the increase in input/output time required to transfer the processing blocks from the intermediate storage device.

(4) DISK INPUT/OUTPUT TIME

The final factor that enters into the evaluation of the conical scanner is the input/output time required to access the data on an intermediate storage device and to load these data points into core storage. To make these estimates, we will assume the processing configuration shown in Fig. D.2.3.1-30. In this figure, we show a hypothetical* disk configuration which holds an entire scene. The individual scan lines for an entire west-to-east sweep occupy the individual records on a particular surface-each of these contain 325,000 bits. The 15 surfaces correspond to the 15 detectors in each band so that a "cylinder" (the same track on each of the 15 surfaces) holds a complete sweep of the sensor. Finally, the 412 tracks correspond to the 411^{+}_{-} sweeps that make up a complete north-to-south scene. With this configuration, an entire sweep is available for one positioning of the set of 15 read heads.

We will assume that 25 ms are required to position the read heads. Also, if we assume that the disk rotates at 200 revolutions/second, then a track is read in 50 milliseconds. We will assume two cases: 1) one track is read at a time giving a transfer rate to core of 6.5 Mbps and a total time of 750 milliseconds to read all tracks, or 2) all tracks are read simultaneously (in 50 ms) for a total transfer rate of 97.5 Mbps. The latter case obviously requires highly paralleled hardware to handle such a rate. To move the heads to a particular track and read the entire record will therefore take

$$T_2 = 75 \times 10^{-3} \text{ seconds or,}$$

$$T_1 = 775 \times 10^{-3} \text{ seconds.}$$

* If a single disk cannot hold all of the data and multiple disks must be used, it does not change these results appreciably.

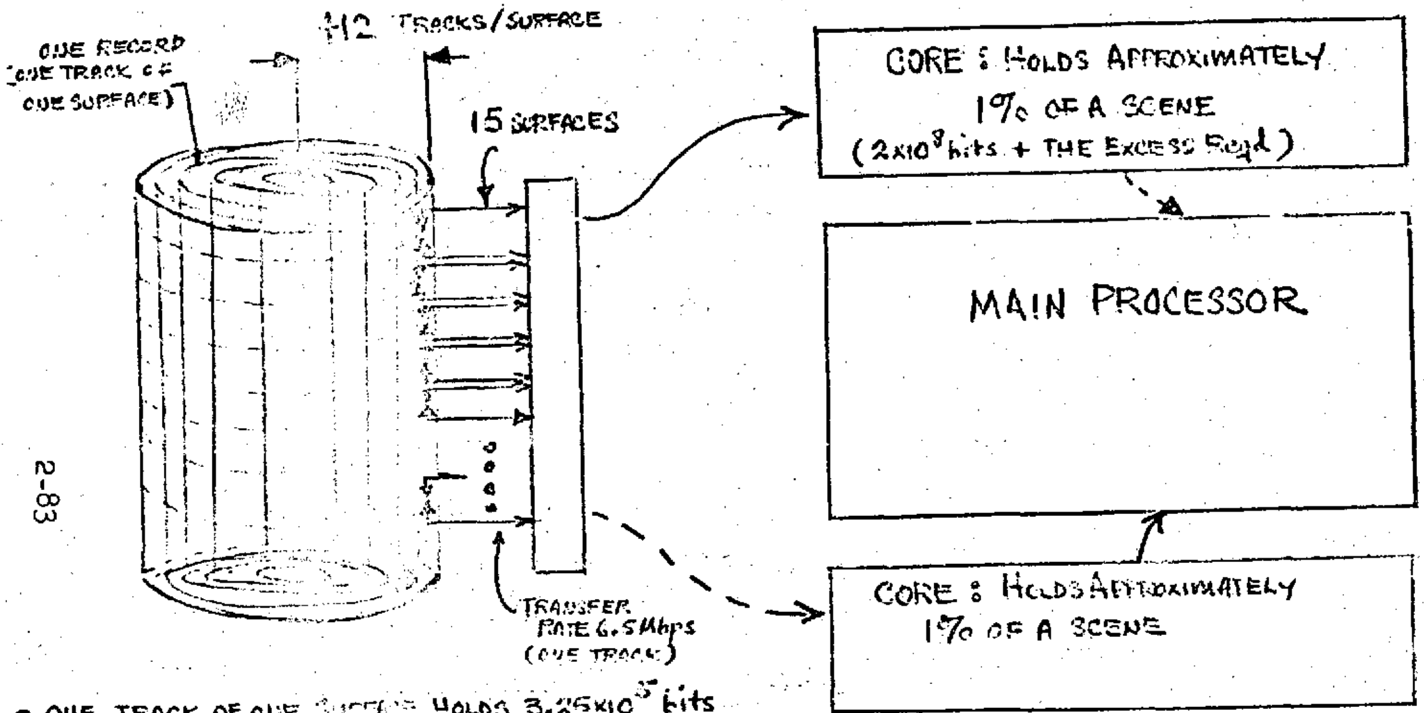

- ONE TRACK OF ONE SURFACE HOLDS 3.25×10^5 bits Corresponds to one 80m. line, all bands, 3667 PIXELS
- THE 15 SURFACES CORRESPOND TO THE 15 detectors Therefore ONE CYLINDER HOLDS ONE COMPLETE SWEEP $= 4.87 \times 10^6$ bits
- THE 412 TRACKS EACH CORRESPOND TO A DIFFERENT SWEEP WITHIN THE 185 KM SWATH. A TOTAL OF 411 SWEEPS GIVES 2×10^9 bits /SCENE

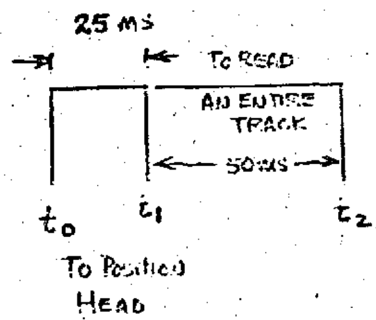

Fig. D.2.3.1-30 ASSUMED CONFIGURATION OF INTERMEDIATE / WORKING STORAGE AND MAIN PROCESSOR.

For the linear scanner, we must access extra lines of data to account for the fact that the resampling grid is tilted with respect to the original data. For the linear scanner, the extra lines are approximately

$$N_\ell = 2\ G \tan \beta$$

where G is the number of lines in the grid square (approximately 616). We will obtain our estimates of extra lines from Figure 6 by assuming that a square-root realtion - ship exists between extra lines stored and extra pixels. From this figure, for a 10 x 10 subdivision, and a nominal of 41 scans/block we obtain at 6^o inclination:

Nominal, No Tilt	Linear Scanner	Conical Scanner
41 scans	47 scans	56 scans
616 lines	701 lines	840 lines

These numbers give the following times required to read 100 augmented blocks of data from disk to core storage.

	Linear Scan	Conical Scan
Case I - 75 millisceonds to read an entire scan	352 seconds	420 seconds
Case II - 775 milliseconds to read an entire scan	3642 seconds	4340 seconds

There are a total of 3.3×10^8 pixels/scene so that a processor that is capable of 1 Mip (10^6 operations/second) requires 330 seconds to perform one operation on each pixel. Figure D.2.3.1-31 plots the number of seconds required to process one scene as a function of the number of operations performed on each pixel. We have added to these times the input transfer times above. When the processing time per block is less than the transfer time, the latter will determine the throughput rate. When the transfer times becomes negligible, throughput rate is determined by the number of operations per pixel.

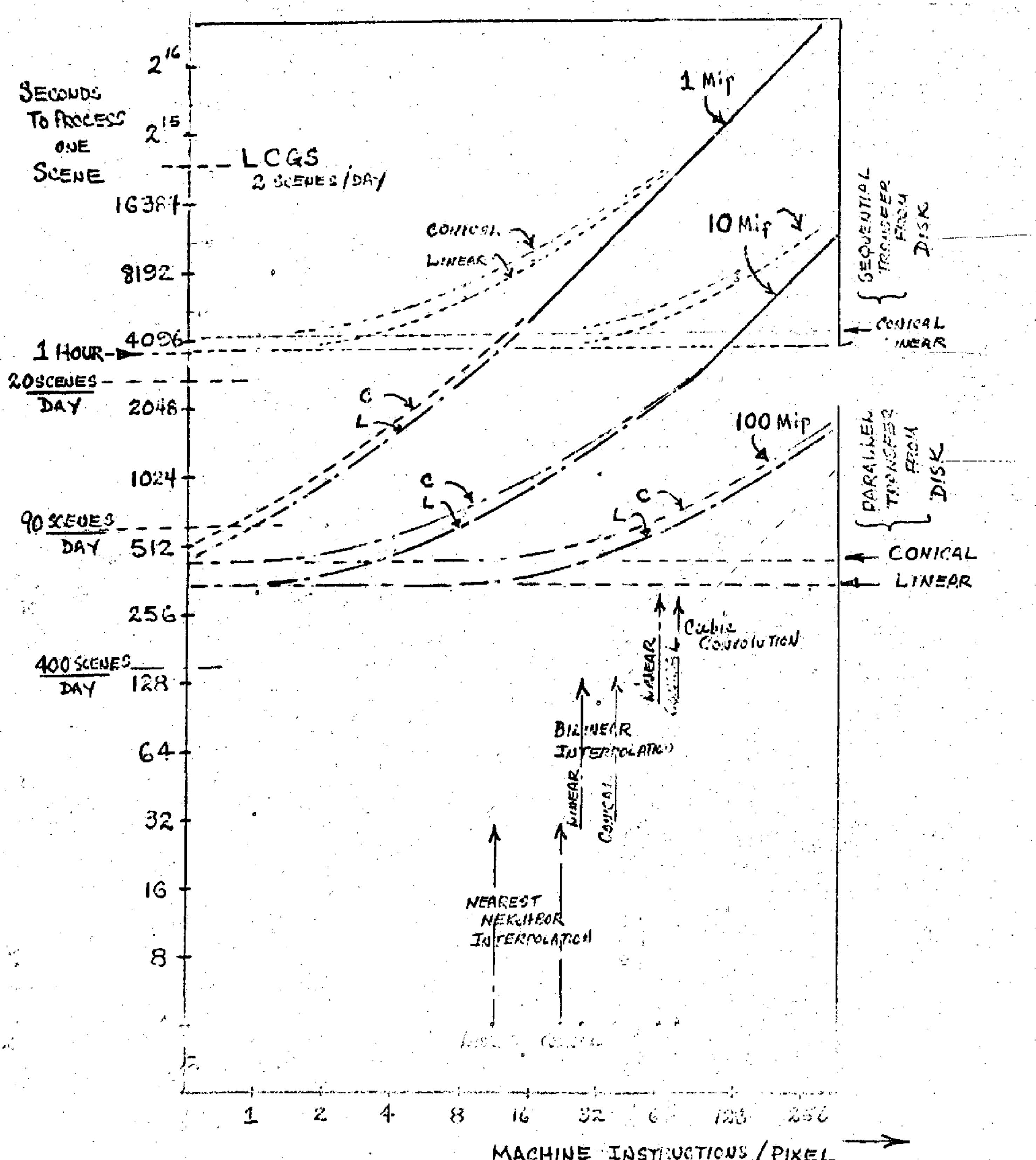

Fig. D.2.3.1-31 Time (Seconds) Required to Process One Scene vs the Number of Instructions Performed on Each Pixel

ORIGINAL PAGE IS OF POOR QUALITY

For sequential transfer of data from the disk, more than an hour is consumed in data transfer for each scene. The slow processor (1 Mip) becomes processing limited at approximately 16 instructions/pixel and the 10 Mip processor at about 100 instructions/pixel. Clearly, this type of data transfer results in a marginal through-put rate even at the lowest input load (20 scenes/day) and would be considered only for the lower cost processing configurations.

For the case where complete scans can be read simultaneously from the disk, the 1 Mip processor is always limited by the processing time, and the 10 Mip, processor becomes limited at only 8 instructions/pixel. Only for this case can the 100-Mip (hypothetical) processor be effectively utilized. Note that none of the configurations will handle 400 scenes/day.

A general conclusion from Fig. D.2.3.1-31 is that the conical scan has only modest impact on throughput (10 - 20 percent reduction) in the region where the processing is limited by the data transfer. When processor speed is the limitation, the conical scan has an impact only in the extra instructions/pixel required for coordinate computation. These increases amount to 100 percent, 40 percent and 18 percent, for nearest neighbor, bilinear, and cubic interpolation, respectively.

D.2.3.5.4 COMPARISON OF SCAN TECHNIQUES

We can now summarize the impact of the conical scanner, as compared to the linear scanner, in the three major areas:

1. Extra instructions required for coordinate computation - at 3.3×10^{8} pixels/scene and $\$10^{-8}$/operation, we have the following dollar costs per scene

	Linear	Conical	Increase	Increase
Nearest Neighbor	\$ 36.60	\$ 74.05	100%	\$ 36
Bilinear	\$ 92.73	\$ 130.00	40%	\$ 38
Cubic Convolution	\$ 208.00	\$ 245.52	18%	\$ 37

2. Additional storage required -

   From Fig. D.2.3.1-29 we estimate the additional storage costs to process the conical scan data as \$1.2M *. For a 5-year system that processes 20 scenes/day, this extra cost amounts to \$32.86 per scene. For the baseline system (90 scenes/day) this reduces to \$7.30 per scene, and for the expanded capability system (400 scenes/day) to \$1.64 per scene. These pro-rated costs are negligible compared to the above except for the low cost system.

3. Reduction in throughput due to input transfer time -
   By referring to Figure D.2.3.1-31 we can estimate the reduction in throughput (if any) due to data transfer.

Several cases can be identified in Fig. D.2.3.1-31 and these are summarized below Parallel data transfer is assumed. The table contains two entries; 1) approximate number of scenes/day and 2) the throughput <u>reduction</u> due to data transfer caused by the conical scan. Note that the extra instructions are not included in these estimates since these are accounted for in 1 above.

* \$600,000 per bank & two are required

Interpolation Algorithm	PROCESSOR SPEED 1 Mip	10 Mip	100 Mip
Nearest Neighbor			
Scenes/day	~10	90	150
Reduction in throughput	~ 5% ($2.50)	~10% ($6.00)	20% ($80.00)
Bilinear Interpolation			
Scenes/day	~ 5	45	100
Reduction in throughput	-	5% ($6.00)	10% ($45.00)
Cubic Convolution			
Scenes/day	~ 2	25	90
Reduction in throughput	-	-	5% ($30.00)

The third entry in the table assigns a dollar cost to throughput reduction by simply converting the seconds of extra processing cost for each scene to dollars using $\$10^{-8}$ per operation. An obvious conclusion from these costs is that the penalty in requiring the extremely fast processor to wait for input data is severe. Using the 10 Mip processor as more representative, cost penalties are small compared to 1.

As an overall conclusion, the coordinate computation is the main contributor to cost increases in processing the conical scan data. The percent increase in cost of processing a single scene ranges from 100% (N.N) to 18% (cubic convolution). The prorated cost of extra storage is significant (equivalent to the cost of extra operations) for the minimum 20 scene/day system but is reduced to a negligible amount when the system processes 400 scenes/day. Throughput reduction due to data transfer is only a moderate factor as long as data - transfer and processing loads are reasonably balanced.

Clearly, the impact of the conical scan is dominated by the complexity of the resampling coordinate algorithm. The estimates above are based upon a straight forward algorithm and may, therefore, be somewhat pessimistic. With a more efficient algorithm, it is likely that the increase in processing cost could be halved; for example, the 40% increase for bilinear interpolation could be reduced to 20%. If this can be done, the cost of extra storage would become more significant for the systems that process only moderate input loads (up to 90 scenes/day).

PROCESSOR OPTIONS

D.2.3.6 PROCESSOR OPTIONS - DIGITAL TO PHOTO

Salient characteristics of electron beam and laser beam image recorders are tabulated herein and compared with the corresponding EOS requirements. To briefly summarize the available information, it appears that laser beam recording is preferred to electron beam recording. This conclusion is based upon the ease with which LB techniques can be applied to the required format of about 9" x 9" whereas EB recorders appear limited, or at least most suited, to a considerably smaller image format. In addition, experience with EB recorders in ERTS has not been encouraging as a down time of about 27 percent has been reported.

With respect to the EOS requirements, the image size of 229 mm square corresponds to a 9 inch square image on a 9-1/2 inch film. This appears to be the standard size image for this size film. The required scan density of 27 lines/mm is based upon 6180 lines over a 9 inch length of film. The spot dimensions of 27 M x 37 M (horizontal x vertical) are based upon pointing lines contiguously (to avoid banding) and contiguously pointing 8640 pixels per line. It is noted that it is standard practice to "oversample" in the direction of scan in order to provide comparable image quality in the horizontal and vertical dimensions of the scene. A modulation transfer function (MFT) requirement of 95 percent at 38 lines/mm was taken. This appears to be an unrealistic goal; it is too stringent. The registration of ± 3 M represents ± 0.1 pixel diameter. This can be met with LR72 which has been measured to provide an rms registration error of about 2 M in the direction of scan and about 1 M in the direction of film transport. However, film deformation is typically 0.05 percent which represents 115 M registration error over a 9 inch span. This represents about four pixel widths.

Based upon the EOS requirements, it appears that the RCA LR72 is more than adequate. Table D.2.3.6-1 compares various LBR and EBR units.

2-90A

Table D.2.3.6-1; LBR/EBR Comparisons

Characteristics	EBR Type 70C (CBS)	EBIR Type 70f (CBS)	LBIR 2nd gen. (RCA)	LBIR LR 72 (RCA)	DRGS Recorder (III)	EOS Requiremen
Raster Size (mm)	55 x 55	55 x 55	229 x 229	229 x 229	533 x 533	229 x 229
Scan Density (lines/mm)	85	85	26	80	27	27
Spot Dia. (μM)	5	5	20 x 38	5	39 x 75	27 x 37 (h x
MTF	50% at 145 1/mm	50% at 145 1/mm	80% at 26 1/mm	50% at 80 1/mm	70% at 25 1/mm	95% at 38 1/r
Registration (μM)	± 5	± 5	± 30	± 2	± 11	± 3
Time to Record Frame	<20 sec.	>0.2 sec.	5 sec.	20 sec.	15 min.	30 sec. *
Cost	$ 350K	$ 200K	$ 450K	$ 250K	$ 500K	

* 16 hours/day; 1600 frames/day

D.2.3.7 Archives

D.2.3.7.1 General

The data volume stated in the EOS RFP is from 10^{10} to 10^{12} bits/day. This volume corresponds to both TM (Thematic Mapper) and HRPI (High Resolution Pointable Imager) sensors. Because this volume critically affects the size, complexity and cost of an archiving system, it is reasonable to attempt some refinement to this volume. There are basically two independent methods of calculating the expected EOS data volume for archiving.

<u>Method 1</u>

This method assumes a downlink data rate from satellite to the primary ground station (PGS) at 240 Mb/sec. A continuous acquisition time of 15 minutes (900 sec.) is assumed for each revolution.

$$\therefore \text{Data collected per revolution} = 240 \times 10^{6} \times 900$$

$$= 2.16 \times 10^{11} \text{ bits}$$

If a 90 minute period of revolution for a sun synchronous satellite at 400 to 900 kilometers is assumed, the

$$\text{Number of revolutions per day} = \frac{24 \times 60}{90}$$

$$= 16$$

Also, assuming that a contact is made every revolution with the satellite for collecting data, the

$$\text{Total data collected per day} = 2.16 \times 10^{11} \times 16 \text{ bits}$$

$$= 3.456 \times 10^{12} \text{ bits}$$

$$\simeq 3.5 \times 10^{12} \text{ bits}$$

Method 2

This method is based on the number of possible scenes collected per day. A scene corresponds to 7 bands of TM sensor and 4 bands of HRPI sensor.

TM

The following assumptions are made in calculating the total number of bits per seven bands of TM sensor:

Number of pixels per line = 6167

Number of bits per pixel = 6

Number of lines per band = 6167

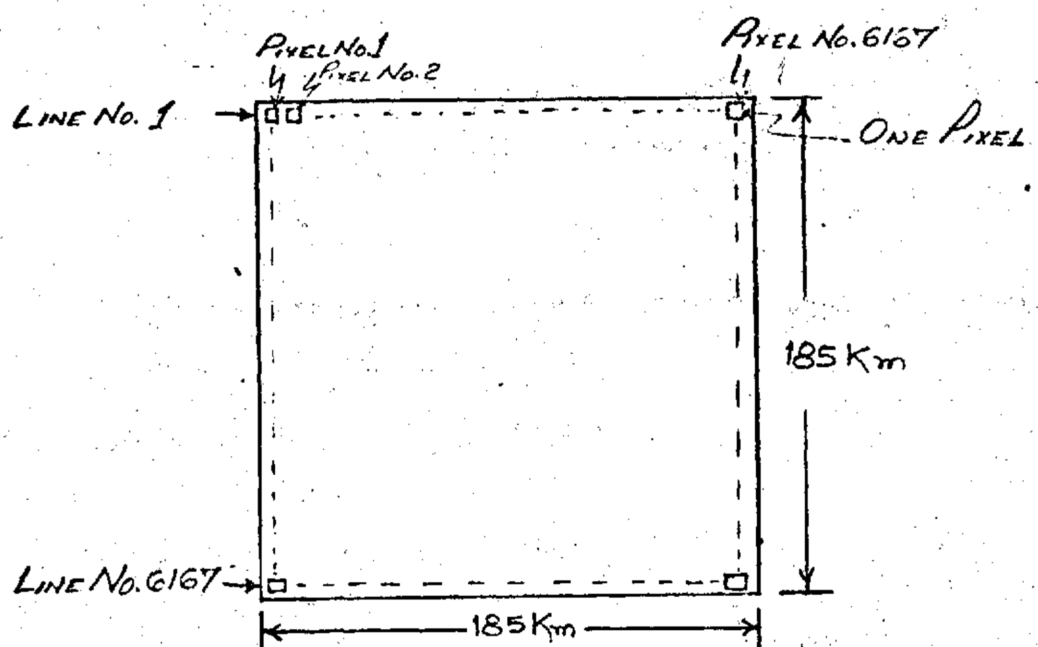

ONE TM BAND

The 7th band is at 1/16th resolution of any other band of TM.

∴ Total number of bits per band = 6167 x 6167 x 6

= 228,191,334

∴ Total number of bits for first 6 bands = 228,191,334 x 6

= 1,369,148,004

$$\text{Number of bits for 7th band} = \frac{228,191,334}{16}$$

$$= 14,261,958$$

$\therefore$ Total number of bits for all seven bands corresponding to

$$\begin{aligned} TM &= 1,369,148,004 + 14,261,958 \\ &= 1383409962 \\ &= 1.3834 \times 10^9 \\ &\simeq 1.4 \times 10^9 \end{aligned}$$

HRPI

For calculating total number of bits corresponding to the four bands of HRPI sensor, the following assumptions are made:

Number of pixels per line = 3600

Number of bits per pixel = 6

Number of lines per band = 18500

$$\begin{aligned} \therefore \text{Total number of bits for 4 bands} &= 3600 \times 6 \times 18500 \times 4 \\ &= 1598400000 \\ &= 1.598 \times 10^9 \\ &\simeq 1.6 \times 10^9 \end{aligned}$$

$$\begin{aligned} \therefore \text{Total number of bits per scene} &= 1.4 \times 10^9 + 1.6 \times 10^9 \\ &= 3.0 \times 10^9 \end{aligned}$$

Assuming that 20-300 scenes are archived per day, we have

$$\text{Total number of bits per day for 20 scenes} = 3.0 \times 10^9 \times 20 = 6 \times 10^{10}$$

and

$$\begin{aligned} \text{Total number of bits per day for 300 scenes} &= 3.0 \times 10^9 \times 300 = 9 \times 10^{11} \\ &= 9 \times 10^{11} \end{aligned}$$

The data collected by Method 1 seem to be unreasonable and lies outside the range of specified in EOS RFP. The actual data archived will, therefore, correspond to somewhere between 20-300 scenes, as calculated in Method 2 which seems to be much more realistic. Therefore, the data calculated by Method 2 will be used in all calculations for estimating the archiving cost on-line and off-line. In the calculations the EOS requirements are rounded up (high) and the storage capacity is rounded down (low).

D.2.3.7.2 Digital Archiving Systems

Several digital archiving systems were investigated for a possible use in EOS program. A summary of characteristics of such systems along with their size, cost and the availability is shown in Table D.2.3.7.2-1 The Ampex TBM system was chosen at this time for a detail study. The reasons for selecting this system are its minimum cost for initial system and the easiness in expansion of the system to meet the increased demand. A minimum system configuration of Ampex TBM system for possible use in EOS is shown in Figure D.2.3.7-1. The other possible systems in the table must be studied in detail before final recommendations can be made.

The minimum system shown consists of a Storage Control Processor (SCP), a Transport Driver (TD), a Dual Transport Module (DTM), a Data Channel (DC), a Channel Interface Unit (CIU) and a Data Channel Processor (DCP). This system has no built in hardware redundancy. The system could record or reproduce continuously a data stream of 5.6×10^6 bits/sec or approximately 4.8×10^{11} bits/day. This corresponds to about 160 scenes per day.

The TD is used to control and position TBMTAPE on the DTM. The TD is program controlled and can switch to either reel of TBMTAPE on the DTM. The DC can read or write either TBMTAPE through the CIU at a rate of 5.6×10^6 bits/sec. An external clock signal is supplied by the DC through the CIU to the primary input source for synchronization.

Table D.2.3.7.2-1 **Digital Archiving Systems**

	Ampex	RCA	Grumman	CDC	Precision Instruments	CDC	XYTEC	Texas Instruments	Philco/Ford
Type	Terabit	Video Tape Carousel	Mass Tape	Scroll	Unicon	Tape Library	Tape Library	IVC Mass Memory	IVC Mass Memory
Storage Medium	Magnetic	Magnetic	Magnetic	Magnetic	Optical	Magnetic	Magnetic	Magnetic	Magnetic
Type of Storage	Video Tape	Video Tape Cart	Cassette	Very Wide Video Tape	Strip	4"x100" Tape Strip	Computer Tape	Video Tape	Video Tape
Useful Storage Density (Bits/inch^2)	7×10^5 (Dual Recording)	1×10^6	2×10^5	3×10^5	14×10^6	4.4×10^5	1.1×10^5	1×10^6	1×10^6
Useful Storage in G Bits	45/Reel	14/Tape	.5/Tape	120/Tape	2/Strip	.12/Strip	1.4/Reel	85/Reel	85/Reel
Tapes/Drive	1	22	44	1	60	1700	Up to 8000	1	1
Bits Accessable per Drive	4.5×10^{10}	31×10^{10}	1.4×10^{10}	12×10^{10}	13×10^{10}	20×10^{10}	Up to 800×10^{10}	8.5×10^{10}	8.5×10^{10}
Drives/Controller	64	N/A	8	1	8	8	8	1	1
Minimum Storage Element	45×10^9	14×10^9	$.32 \times 10^9$	120×10^9	2.2×10^9	$.12 \times 10^9$	1.4×10^9	85×10^9	85×10^9
Maximum Bits/Controller	29×10^{11}	N/A	1.1×10^{11}	1.2×10^{11}	10×10^{11}	2×10^{11}	80×10^{11}	$.85 \times 10^{11}$	$.85 \times 10^{11}$
Worst Case Access Time for 10^{12} Bits (Sec)	45	20	12	60	10	5	60	216	216
Transfer Rate (Bits/Sec)	5.5×10^6	6.6×10^6	4×10^6	10^7	3.2×10^6	10^7	7.6×10^6	10^7	5.8×10^6
Uncorrectable Error Rate	1.6×10^{-11}	N/A	10^{10}	N/A	10^{-9}	10^{-10}	10^{-11}	10^{-7}	10^{-7}
MTBF (hrs.)	N/A	N/A	N/A	400	350	N/A	1300	500	500
MTTR (hrs.)	.58	N/A	N/A	4	N/A	N/A	.36	2	2
Temperature (°F)	65-75	N/A	50-90	N/A	50-70	N/A	60-90	N/A	N/A
Humidity Limits (%)	30-50	N/A	40-60	N/A	20-60	N/A	20-80	N/A	N/A
Mismounting of Tape	Easy	Hard	Hard	Hard	Hard	Hard	Hard	Easy	Easy
Floor Area Reqd. for 10^{12} Bits (Sq. Ft.)	181	80	125	N/A	N/A	200	175	N/A	N/A
Floor Area Reqd. for 24×10^{12} Bits (Sq. Ft.)	200	200	600	N/A		1000	1000	N/A	N/A

Table D.2.3.7.2-1 Digital Archiving Systems (Cont'd.)

	Ampex	RCA	Grumman	CDC	Precision Instruments	CDC	XYTEC	Texas Instruments	Philco/Ford
System Cost to Store 10^{12} Bits (a) $	1.2M	.8M	2.2M	N/A	.8M	.65M	.2M	1.26M	1.26M
Addition over (a) to Store 2nd 10^{12} Bits (b) $	.9M	.6M	2.0M	N/A	.74M	.6M	.15M	1.26M	1.26M
Addition over (b) to Store 10^{13} Bits $	7.2M	4.8M	16M	N/A	5.6M	5.2M	.40M	10M	10M
Optimum Cost per Bit (¢/Bit)	.0001	.00008	.0002	N/A	.00008	.00005	.000005	.0001	.0001
Cost of Smallest Archivable Storage Media ($)	150	130	20	N/A	180	10	10	300	300
Cost of Media for 10^{12} Bits ($)	3,400	9,300	63,000	-	82,000	84,000	7,200	3,600	3,600
Reusable	Yes	Yes	Yes	Yes	No	Yes	Yes	Yes	Yes
Minimum Sources of Storage Media Supply	3	1	N/A	N/A	1	N/A	24	6	6
No. of Reliable Reads from Media	1,000	N/A	5,000	N/A	N/A	> 20,000	> 20,000	500	500
Shelf Life in Controlled Environment	High	High	High	High	High	High	High	High	High
Media Standard?	Yes	?	Yes	Yes	?	Yes	Yes	?	?
Equipment Design	Few Produced	?	Few Produced	New	Few Produced	New	In Production	Reported Problems	Reported Problems
Remarks									

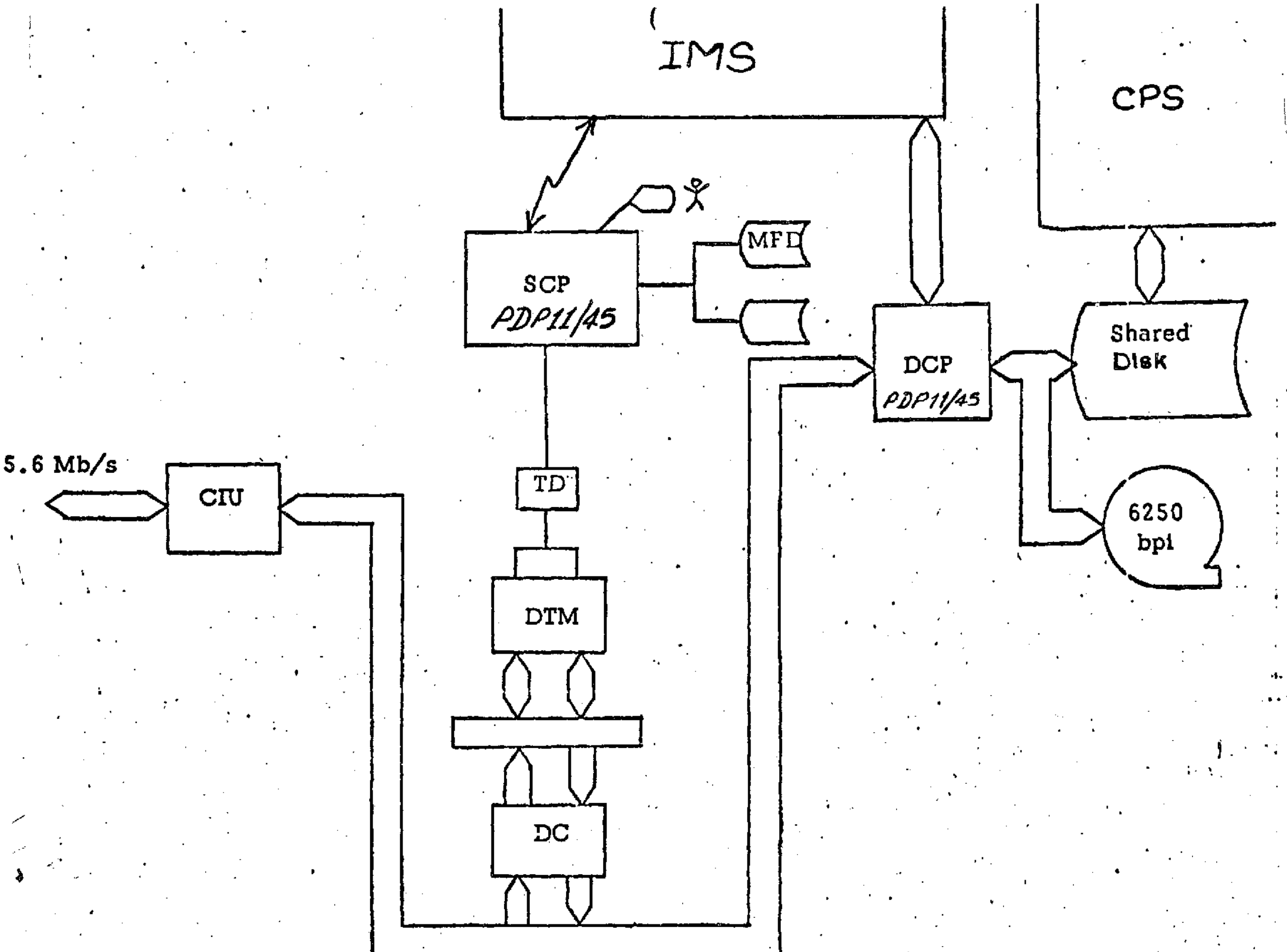

Fig. D.2.3.7-1 Minimum System

A TBMTAPE can store 45 x 10^9 bits of useful data (or about 15 scenes) thus requiring an operator to change TBMTAPE approximately every 2-¼ hours. Since the DTM contains two independent transport units (two reels of tape), the SCP will switch the input stream to the second tape when the first TBMTAPE is filled.

The DC contains a write channel and a read channel in one cabinet. The read channel and write channel are logically independent and can operate simultaneously. Thus, for example, the CIU could be writing on one tape at 5.6 Mbps and the DCP could be reading out from another tape simultaneously at the same rate, i.e., input/output rate of 11.2 x 10^6 bits/second.

The SCP has its own local disk for managing the master file directory (MFD) of all data files (scenes or images) stored in the archive and for managing its own internal work queues based on requests generated by the IMS CPU or other CPUs.

The DCP is capable of communicating data files (scenes or images) directly to the IMS CPU over a standard interface or indirectly to the IMS CPU or any other CPU through a shared disk or drum storage device. The shared disk interface is highly desirable for operational reasons.

The DCP also provides for generating off-line copies of scenes or images on standard 6250 bpi computer compatible tape (CCT) either for transmission to a remote facility or to an LBR for hard copy.

A more detailed discussion of Ampex TBM system and its capabilities is given in Section D.2.3.7.3.

The hardware cost of such a minimum system is approximately $600,000. This does not include any software package required to run the system. A non-recurring software cost would be required depending mainly upon the specifications of the IMS CPU and the type of requests to which the archive must be responsive. A total non-recurring software cost will be around $400-500K. This software will be capable of handling more units of the TBM system when expanded modularly.

Thus, a cost of about $1M will allow set up of the first unit (Prototype) for debugging the system before its expansion and use for archiving the EOS data.

D.2.3.7.3 THE TBM* MEMORY SYSTEM

(1) INTRODUCTION

The TBM Memory System was started in 1966 and reached the product stage some time ago. The TBM Memory System is the only mass storage system which is based on a field proven technology and a commercially available media (standard two-inch wide television tape supplied by several manufacturers).

A 1.8 trillion bit capacity TBM Memory System (reference Figure D.2.3.7-2 delivered to an agency of the U.S. Government in July of 1972 after passing the customer's acceptance test with outstanding results. The error recovery re-read rate was less than one error in 2.5×10^9 data bits, the unrecoverable error rate was less than one error in 6×10^{10} data bits, and the system up-time was better than 98 percent. Recent operational measurements on this same system have verified the better than 98 percent up-time figure. Based on these results, it is projected that the TBM Memory System configurations derived for the EOS Data Archive will amply satisfy the requirements.

The TBM Memory System utilizes standard two-inch wide magnetic viedo tape of the type used in commercial television. Data is recorded in a block format with each individual block identified by a unique address. Rapid random access to any record is achieved by performing block address searches at tape speeds of 1000 inches per second - both forward and backward.

The TBM Memory System specifications are listed in Table 2.3.7.3-1

The TBM Memory System architecture and technology reflect a significant departure from conventional approaches to the storage and retrieval of digital data. Data is stored on magnetic tape, but there the similarity to conventional computer tape devices ends. The TBM Memory System is a system; it is self-contained and capable of operation independent of, or in cooperation with, other processing units.

---

* Ampex Trademark

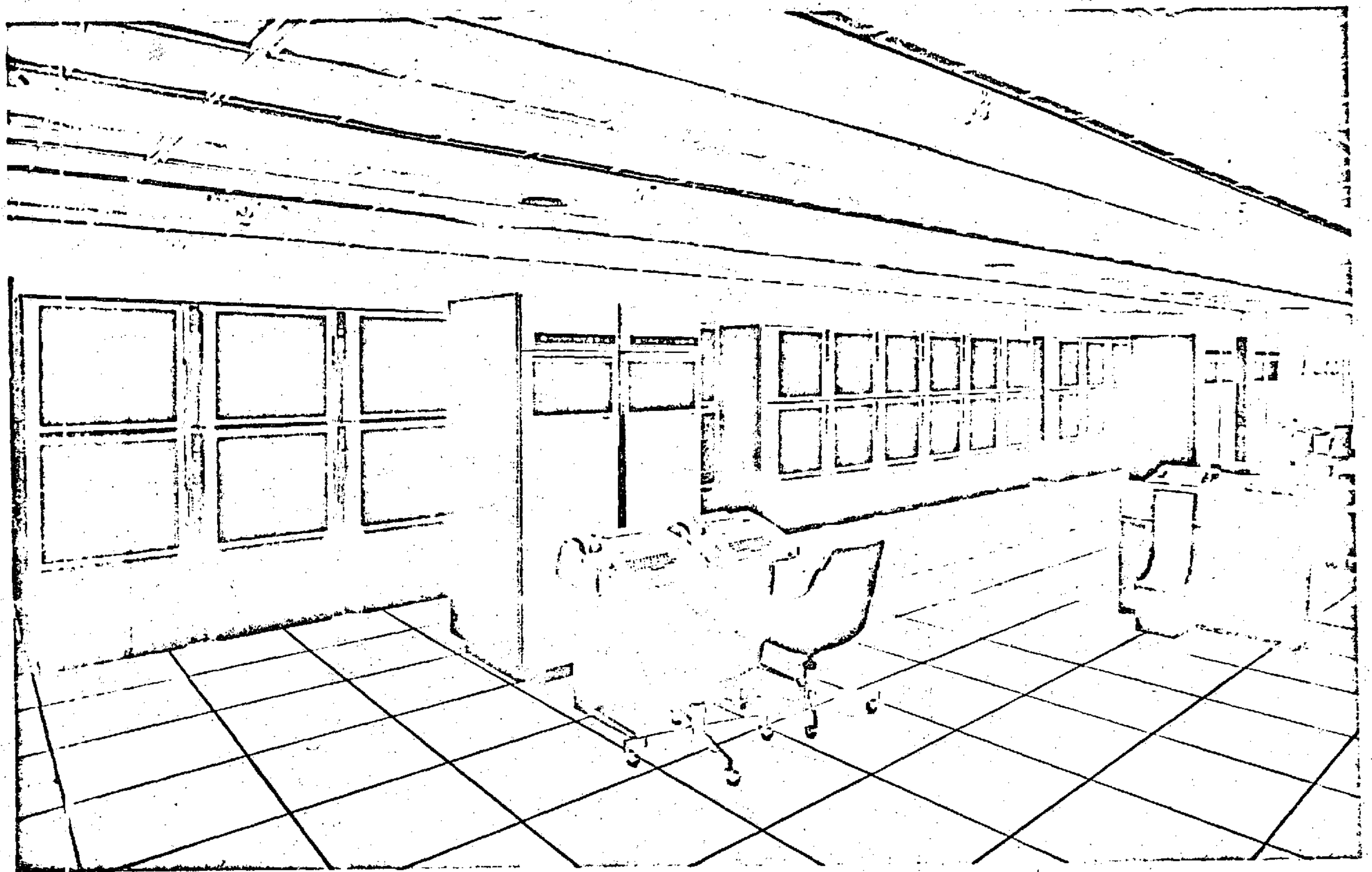

Figure D.2.3.7-2 1.8×10^{12} Bit Capacity TBM Memory System

Table D.2.3.7.3-1 TBM Memory System Specifications

Storage Capacity (bits)	
Max. System (32 Dual Transport Modules)	2,900,663,500,000
Per Dual Transport Module (2 transports	90,645,735,000
Per transport (1 TBMTAPE)	45,322,867,500
Per TBM Block	1,041,905
TBM Blocks per TBMTAPE	43,800
Sustained Data Rates (bits/sec)	
Per System (6 TBM R/W Channels)	33.6×10^6
Per TBM Data Channel module (R&W)	11.2×10^6
Per TBM Read Channel	5.6×10^6
Per TBM Write Channel	5.6×10^6
Concurrent Operations	
TBM Searches	6
TBM Channels	6

The TBM Memory System is highly modular in construction. System capabilities can be varied over a wide range by configuring the system to include different numbers of each of five basic building blocks: Dual Transport modules (storage capacity), Transport Driver modules (multiple seek/search), Data Channel modules (data thruput), Storage Control Processor (file management) and Data Channel Processor (data interface handling). Storage capacity is available over a range from 10^{11} bits to 3×10^{12} bits in approximately 10^{11} bit increments, while sustained thruput can be specified up to 33.6M bits per second in 5.6M bits per second increments.

Switching matrices interconnect the hardware modules. They are constructed to allow multi-path access to any of the modules. Systems configured with redundancy for the basic building blocks therefore offer highly desirable degradation characteristics since no single unit failure brings the entire system down.

(2) DATA RECORDING TECHNIQUE

The TBM Memory System utilizes standard two-inch wide magnetic tape (TBMTAPE) of the type used in commercial color television recorders as its basic storage medium. Such tapes are readily available from several vendor sources.

The frequency modulation recording technique adopted by the TBM Memory System is fundamentally the same as that of commercial television. Frequency modulation offers significant advantages over the saturation recording techniques used in conventional computer peripherals because of the absence of magnetic print-through effects. Print-through effects between adjacent layers of tape on a reel can destroy the integrity of a recording if tapes are left inactive for sustained periods of time. Elimination of print-through effects greatly enhances tape shelf life expectancy and, thus, the archival quality of the recording.

The commercial television recorder added a new dimension to the mechanics of magnetic recording. Data recording is across the tape (transverse), Figure D.2.3.7-2 as distinct from the technique applied in conventional computer tape recorders where

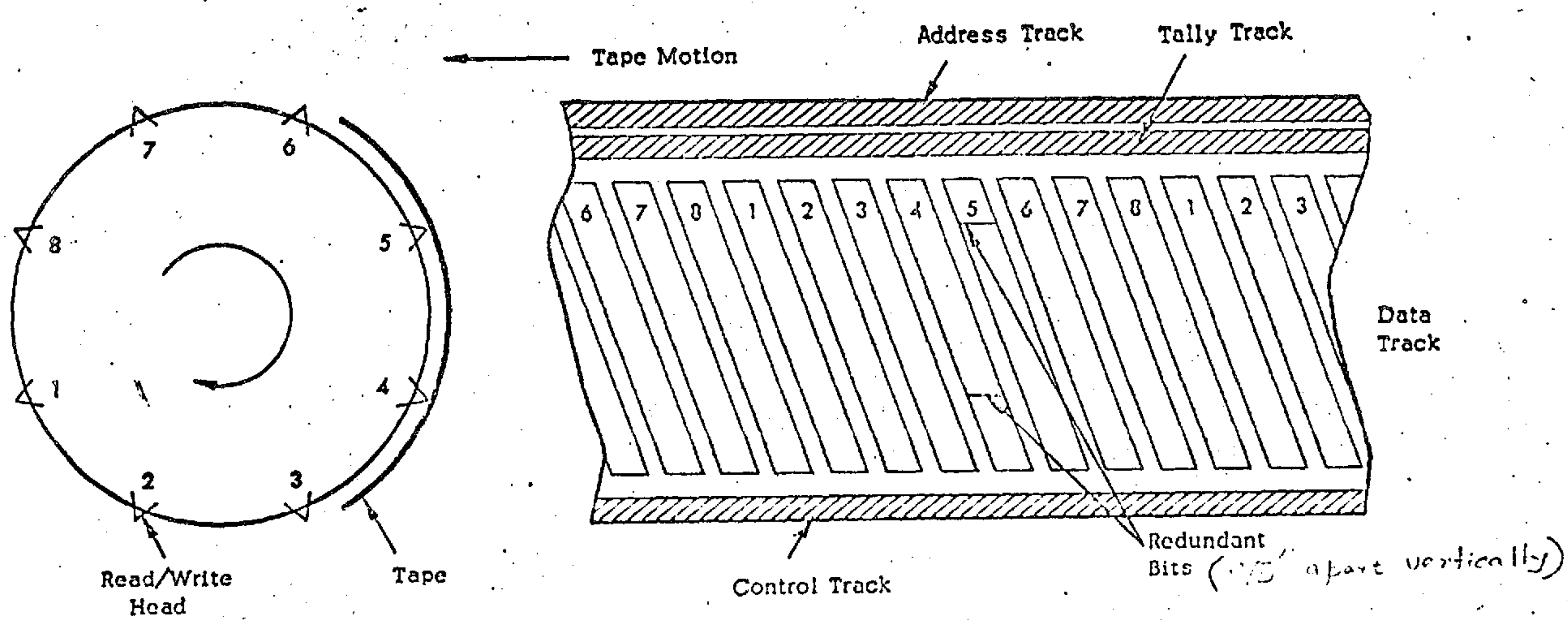

Figure D.2.3.7-2 **Transverse Redundant Recording**

data is recorded along the tape (longitudinal). The transverse recording technique allows the data to be recorded bit serially (as opposed to byte parallel) while retaining high channel rates. The serial bit recording approach, coupled with the time base correction technique applied to the bit stream, renders TBMTAPE insensitive to the type of physical distortions which normally result from sustained periods of tape inactivity, e.g., shelf storage. The excellent playback quality of commerical television tapes recorded more than a decade ago clearly demonstrates the excellent archival quality of this recording technique.

System storage capacity in the vicinity of 10^{12} bits is implicit in today's Mass Storage System concept. The need to provide a reasonably graceful system architecture dictates that data be stored at high bit area packing density. Even at one million bits per square inch, a 10^{12} bit capacity system must contain one million square square inches of media. Because each individual bit occupies an extremely small area, data accuracy is highly sensitive to media quality. Although it is possible to initially achieve high data accuracy by using carefully selected magnetic tapes together with powerful error correction codes, it is unlikely that such an approach will provide a sufficient margin to yield acceptable long term data integrity. The TBM Memory System provides outstanding data accuracy performance partially because of the superior recording technique, but primarily because of the redundant recording scheme which is used in addition to a hardware implemented error correction and detection technique. Every pair of redundantly recorded data bits is physically separated by .75 inches on a TBMTAPE. The error correction and detection code fields are intermixed with the actual user data.

The space diversity redundant recording approach renders insensitively to the adverse effects normally associated with tape wear, handling, environmental contamination, and time-dependent physical deformation effects.

Data is recorded on TBMTAPE in a fixed length block format with each individual block identified by a unique address. Each data block represents a physical record (one or more logical records) with a user data capacity approximately

that of ten full 3330 tracks (130,238 bytes or 1,041,905 bits). A TBMTAPE contains 43,800 user data blocks in addition to blocks reserved for maintenance and diagnostic functions.

In addition to the transverse data tracks, three longitudinal tracks are recorded on each tape. Two of these, the Address Track and the Tally Track, are of interest to the user. The third track, the Control Track, is used for internal servo purposes and is not discussed here.

Associated with each data block is a segment of each longitudinal track. The Address Track field associated with each data block contains both the tape number and the block address number. User tape block addresses are numbered sequentially from 1 through 43,800. Records or files may be accessed by physical addresses, i.e., tape number and block number. The user does not need to know on which transport a tape is mounted. The Storage Control Processor maintains a table which relates tapes to transports.

The Tally Track is a user-oriented facility. The Tally Track field associated with each data block may contain user security codes and search keys, data of last activity, Read-Only interlocks, and more.

The Tally Track is read prior to performing a block read, write or erase, and is updated after the process has been completed. The security code words read from the Tally Track can be compared to code words (passwords) supplied by a host CPU. Read, write and erase processes can be performed only if the Tally Track code words match.

(3) SYSTEM ARCHITECTURE

Functionally, the TBM Memory System can be viewed in two parts: the Data Storage Section (DSS) and the Communication and Control Section (CCS). The DSS is the repository of all data stored within the TBM Memory System while the CCS provides message and data interfaces for subscribing host CPU's.

The DSS contains some number of each of three basic building blocks: Dual Transport modules, Transport Drivers and Data Channels. A system must contain at least one each of the basic building blocks as shown in Figure D.2.3.7-3. Additional units are added to provide desired system capacity. (Dual Transport modules), multiple seek/search capability (Transport Drivers), and data thruput (Data Channels) for each application, as illustrated in Figure D.2.3.7-4.

The CCS, in addition to providing message and data interfaces for subscribing host CPUs, contains the mechanism for system file management and overall control of system hardware resources. The CCS may consist of some number of each of two basic building blocks: the Storage Control Processor (SCP) and the Data Channel Processor (DCP). The SCP complex performs overall management of the TBM Memory System, while the DCP controls data exchange with subscribing host CPUs.

The TBM Memory System throughput capability is determined by the number of Transport Drivers, Dual Transport modules, and Data Channels configured within the system. Furthermore, throughput is affected by the method of interfacing the TBM Memory System to the host CPU and other factors such as data file organization and access methods. The TBM Memory System is capable of delivering a sustained data rate of 33.6 x 10^6 bits per second. A single Data Channel module is capable of transferring 10^{12} bits within a 24-hour period.

The Communication and Control (CCS) consists of one or more data processors acting as an interface between the subscribing host CPU's and the Data Storage Section (DSS). The CCS provides message and data interfaces to the host CPU's as well as the overall control of the TBM Memory System.

The composition of the CCS is quite application and implementation approach dependent. The possible configurations range from no CCS at all up to a completely user-transparent interface. The CCS is constructed from some number of each of two basic building blocks: the Storage Control Processor (SCP) and the Data Channel Processor (DCP).

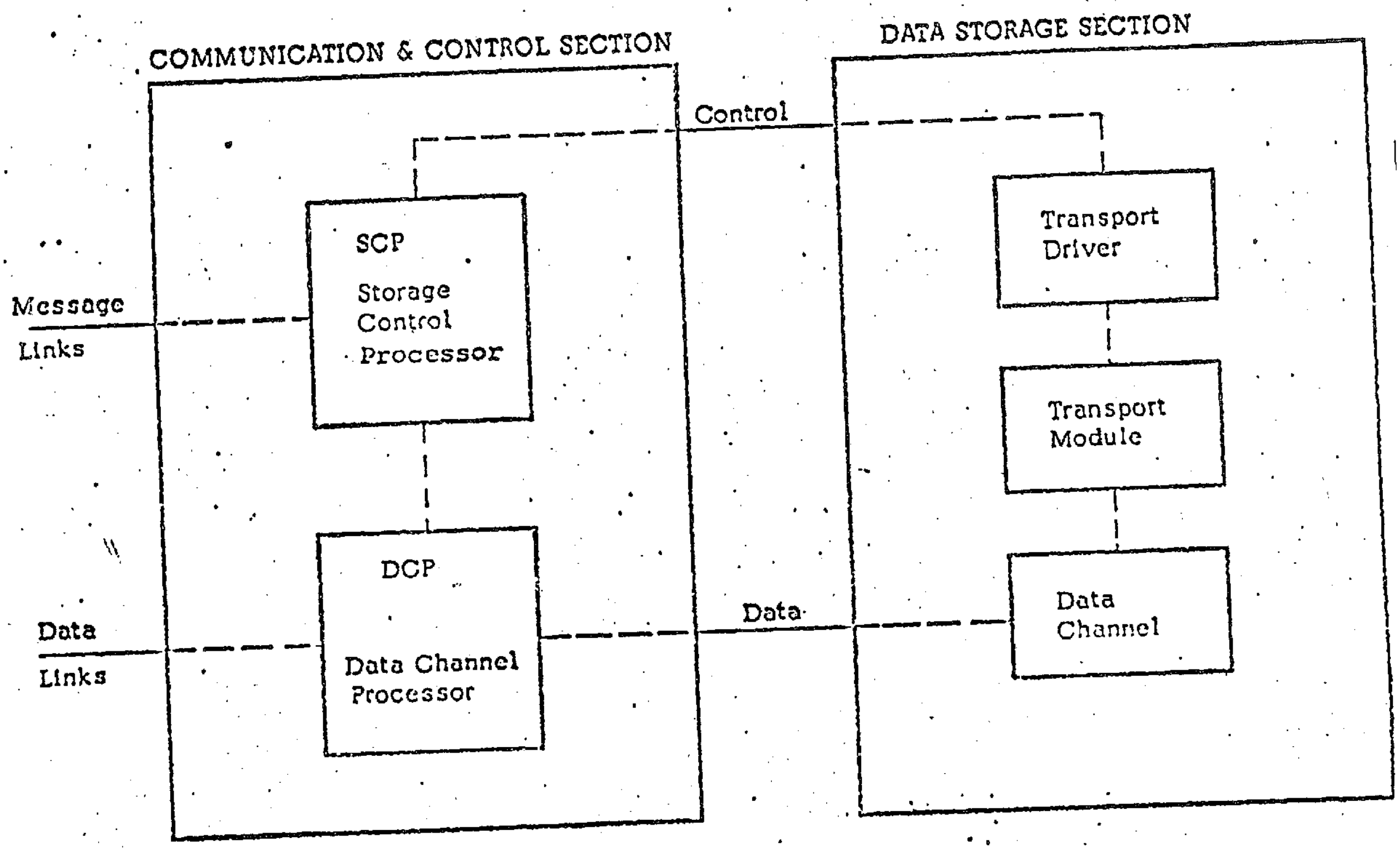

Figure D.2.3.7-3 Minimum TBM Memory System Configuration

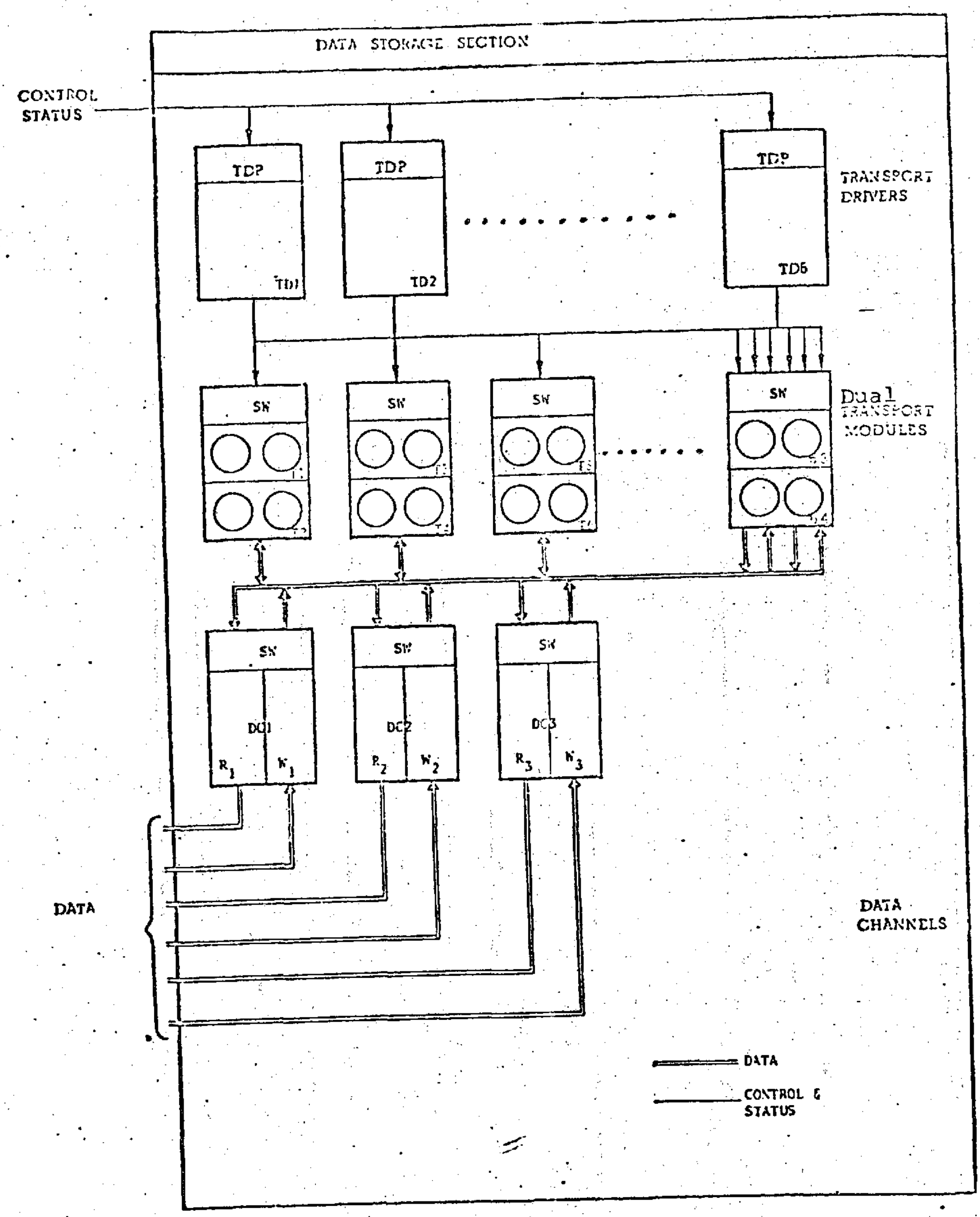

Fig. D.2.3.7-4 Expanded DSS Configuration

The SCP complex provides three capabilities: a host CPU message interface, a file management system, and an overall TBM Memory System control system.

The DCP complex controls and facilitates data transfers between the host CPU's and the DSS, as well as providing data manipulation capability.

The SCP is the controlling mechanism for the TBM Memory System. It provides a full array of executive functions including: command interface to the host computer(s), TBM Memory System file management (including space allocation, file access control, directory maintenance, history log recording, and recovery processing) and data file transfer control for the DSS and the DCP's. In addition, a multi-tasking executive is utilized as the basic monitor for the SCP, providing a multi-level interrupt driven system supporting both background and foreground processing. This also enables easy installation of application dependent programs (as tasks) to perform functions such as statistical reporting, file archiving, diagnostics processing, etc.

The SCP can be implemented to serve many diverse functions. For example, one approach is to implement the SCP merely as a device controller where all data and resource management functions are handled by the host CPU's. However, where multiple host CPU's are utilized, one CPU must have overall control of the TBM Memory System.

Another implementation is to place TBM Memory System resource management within the SCP while keeping the data file management function within the host CPU's. Again, one host CPU must have overall control of data file management.

A third implementation approach is to let the TBM Memory System SCP handle both data file and resource management, thereby providing a central data control facility and allowing for the best utilization of system resources. This approach lends itself to a totally user-transparent interface via the shared disk interface.

The SCP software is designed such that either a single or dual SCP configuration may be used. In the dual SCP configuration, a master/slave type relationship is established enabling full use of the backup SCP for workload sharing.

Attached to each SCP are also conventional magnetic tape and disk facilities. Disk storage, such as IBM-compatible 330's, may be used for storage of large file directories. Transaction and activity log backups are usually dumped to conventional magnetic tape.

The SCP functions have been implemented to run on single or dual PDP 11/45's. A typical SCP configuration is shown in Figure D.2.3.7-5.

The DCP is a programmable controller for high-speed data transmission between TBMTAPE and IBM-compatible 3330 disk systems. The DCP provides all hardware and software facilities necessary to execute complete data transmissions. Files are transferred by the DCP at the request of the SCP.

Contained within the DCP is a PDP-11/45 processor (reference Figure D.2.3.7-6) MOS memory for program execution and 900-nanosecond core memory used as data transmission buffers for data rate matching. The PDP-11/45 Unibus interfaces to the internal TBM Memory System Read/Write data channels via the TBM Memory System Channel Interface Unit (TCIF). The Unibus is connected to IBM-compatible 3830 controllers via the Channel Simulator (CHSIM).

The TCIF is designed to effect interlocked burst-mode data exchanges with TBM Memory System Read/Write channels. Data so transferred is fetched from, or stored into, the core buffers through direct memory access by the TCIF. The TCIF includes switch logic circuits, through which it may connect to any TBM Memory System channel under DCP program direction.

The CHSIM, supported by a PDP-11 processor, has the characteristics of an IBM 360 or 370 channel controller, e. g., a 2880. Choice of 2314 or 3330 compatibility is a mode selection feature in the CHSIM. The CHSIM can also be easily modified to support other types of disks, such as the CDC 844.

Extensions to the basic CHSIM make it especially powerful for automatic mass transfers of data between 3330 disk and the TBM Memory System. The sustained transfer rate is approximately 700K bytes per second. Chief among these extensions

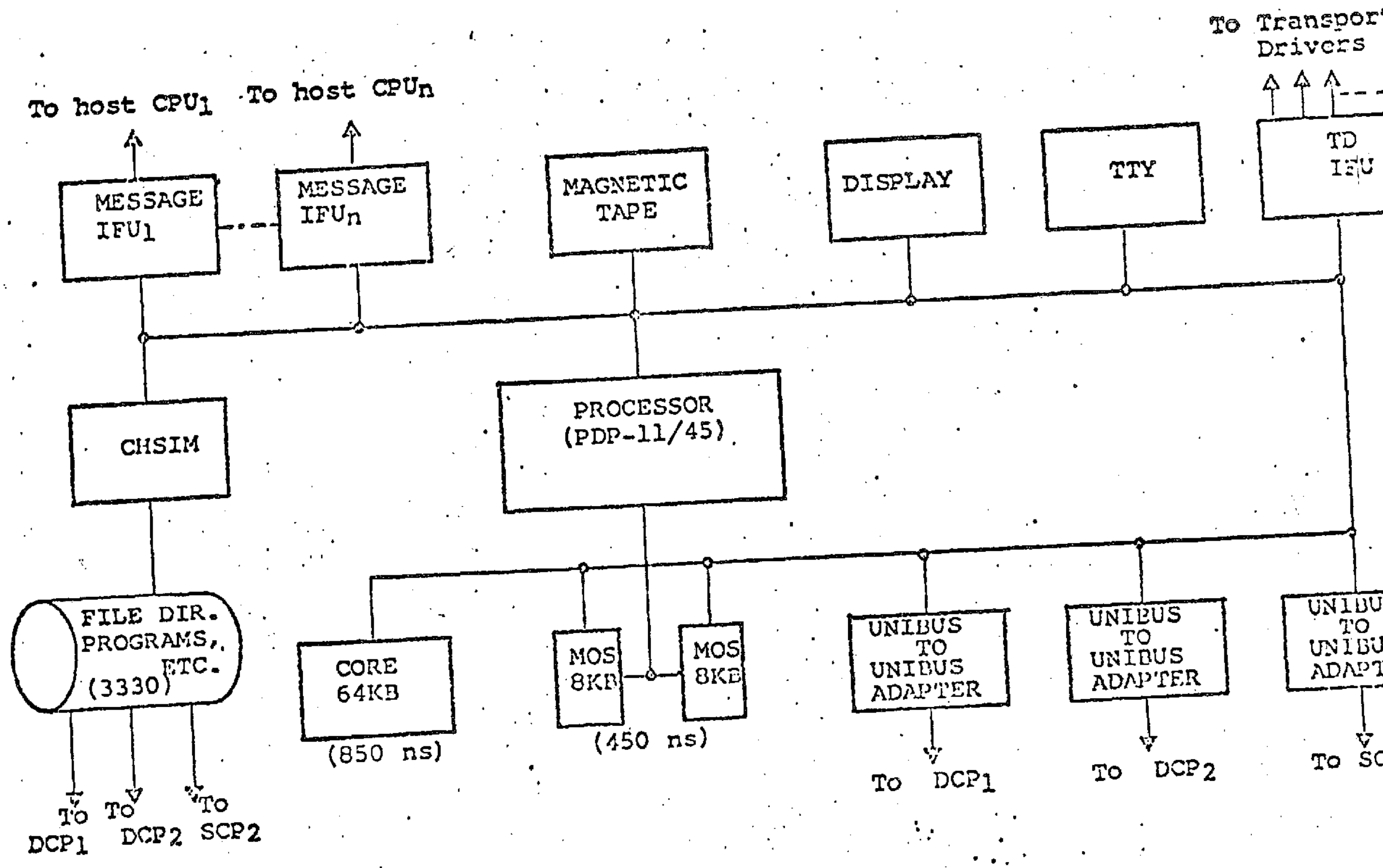

Figure D.2.3.7-5 Typical Storage Control Processor (SCP) Configuration

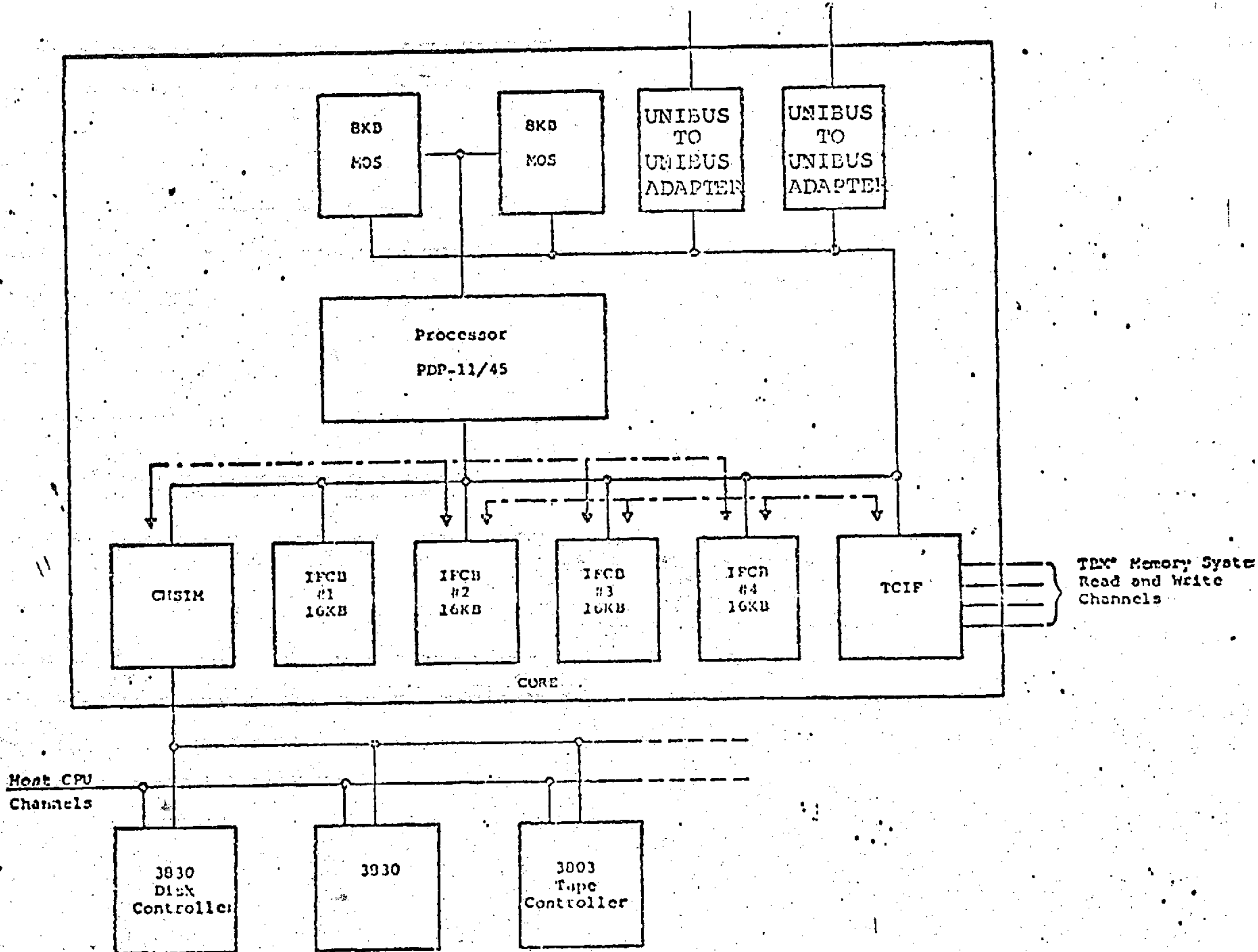

Figure D.2.3.7-6. DCP Block Diagram

is the provision for generation, by hardware lgoic, of Cylinder/Track fields to be inserted in record Count areas during multi-track/multi-cylinder data transfers. This feature eliminates the need for frequent DCP program intervention during disk Backfill or Copy-to-TBMTAPE operations.

The thoroughness of IBM 360 or 370 channel emulation by the CHSIM allows any type of IBM-compatible peripherals to be attached. A maximum of eight device controllers can be accommodated on each CHSIM. In addition to intermixing 3830 disk controllers with 3830 tape drive controllers, it is feasible to attach channel-to-channel adapters. This type of connection can be made to exhibit the same behavior as when used between host CPU's.

The hardware assortment comprising the DSS determines the storage capacity, access characteristics, and maximum data throughput rate of the TBM Memory System. The hardware modules and the interconnecting switching matrices are described below.

A TBMTAPE Transport is the basic TBM Memory System data storage unit and may store 5.6 billion bytes (4.6×10^{10} bits) of user data, the capacity of one TBMTAPE. In actuality more than twice that number of bits are contained within each transport, since all user and system utility data, together with error correction and detection code fields, are recorded redundantly on TBMTAPE.

A Dual Transport module contains two transports and has a storage capacity of 11.2 billion bytes (9.2×10^{10} bits). Although two transports are physically contained within each Dual Transport module rack, they are electrically and logically independent. Both transports can, therefore, be in operation simultaneously, or one can be taken offline for preventive maintenance while the other remains online.

The TBM Memory System architecture accommodates up to 32 Dual Transport modules (64 transports) for a maximum capacity of 358 billion bytes (3×10^{12} bits) of user data. If it is assumed that the average size of data sets stored on conventional computer tapes is 2.5 million bytes, then a single Dual Transport module can store

the equivalent of 4,500 computer tapes while the maximum TBM Memory System configuration can contain the equivalent of almost 150,000 conventional (1600 or 800 bpi) computer tapes.

Each transport contains all of the mechanical elements necessary to move a TBMTAPE, but only a fraction of the electronics normally associated with tape transports of this type. All of the electronics necessary to control a transport reside within the Transport Driver module while all of the electronics associated with the data signal conditioning and transmission are located within the Data Channel module. Transport Driver and Data Channel modules are shared between all transports in a system.

Also contained within each Dual Transport module rack are the switching elements which allow for any one of up to six Transport Drivers to connect to either of the two transports. Both transports can be connected to two different Transport Drivers concurrently. The switching elements are packed in easily replaceable switch drawers at the bottom of the Dual Transport module rack. Space constraints limit the size of the switch matrix in each Dual Transport module to six (Transport Drivers) by two (transports).

The Transport Driver contains all the electronics necessary to execute all TBMTAPE oriented functions with the exception of reading and writing data. A Transport Driver, when connected to a transport, can therefore accomplish random tape seek/searches, Address and Tally Track read/write processes, and data erase functions.

Each Transport Driver contains a NOVA minicomputer, the Transport Driver Processor (TDP), which is capable of controlling both the transport to which the Transport Driver is connected and a Read or Write channel connected to the same transport. The TDP operates in a real-time model. It executes commands received from the SCP and returns status information to the SCP as appropriate. The TDP performs extensive system diagnostic and maintenance services. Maintenance and diagnostic functions can be controlled either from the SCP or by a TTY attached to

the TDP I/O bus. The number of Transport Drivers contained within a TBM Memory System determines how many concurrent tape operations can be performed. The system architecture allows up to six Transport Drivers to have access to all of a maximum of 64 transports. A TBM Memory System can be configured with more than six Transport Drivers, but any one transport can only be accessed by six Transport Drivers.

The Data Channel module contains a Read Channel and a Write Channel. The channels are physically located within the same rack, but are functionally independent. A single Data Channel module therefore provides for two concurrent digital data transfers, each at a sustained rate of approximately 5.6M bits per second, for a total of 11.2M bits per second.

The switching matrix permits simultaneous Read Channel connection to one transport and Write Channel connection to another transport, and is located in the lower part of the Data Channel module rack. Switching elements connecting the Read and Write channels to DCP's or other types of interfaces are also provided in the module.

User data which is to be copied from an external source to TBMTAPE may enter the Write Channel. The data enters the Write Channel via small transmission synchronization buffers before being passed into the Error Detection and Correction Encoder (EDCE). Within the EDCE, segments of 955 bits of user data are formed into error detection/correction code words by the addition of 37 checkbits to the end of each segment. Checkbits are developed from the incoming data by hardwired logic. The data is then redundantly recorded in the frequency modulation mode on TBMTAPE in approximately one million bit physical records.

Transfer of user data from a TBMTAPE to an external destination involves the inverse process. The redundantly recorded bit streams are transferred from TBMTAPE to the Read Channel. Since dropouts within either bit stream are automatically compensated for by the presence of data in the other stream, excellent data accuracy is achieved. After combining the bit streams into one, the data enters the Error

Detection and Correction Decoder (EDCD). The correction and detection checksum bits are extracted and correctable errors in user data are automatically removed. Error-free data is transferred via the Read Channel to some external destination. Uncorrectable data errors detected in the EDCD are reported by the Transport Driver Processor to the SCP which may initiate error recovery by rereading. The reread rate which has been determined after nearly two years of TBM Memory System tests is extremely low; one TBMTAPE data block every 2500 blocks (2.5×10^9 bits) read.

The Data Channel module also contains bit generator and comparator facilities which serve maintenance and diagnostic purposes.

Single blocks, logical files, or whole TBMTAPE's may be copies from a TBMTAPE at any address to any other TBMTAPE at the same or a different address. This procedure does not utilize any interface or host CPU facilities, but utilizes internal read/write loop connection hardware found in the Data Channel modules. This optional facility provides the user an ideal method for file packing, file backup (off-line), and file organization optimization.

A.(4) SYSTEM AVAILABILITY AND MAINTAINABILITY

The up-time of a system like the TBM Memory System is a function of the MTBF and MTTR of each of the major system components as well as the method by which these major components are interconnected. The major TBM Memory System components are in parallel, with a complete connecting matrix between the TBMTAPE transports and Transport Driver modules as well as between the Read and Write Channels and the TBMTAPE transports. Thus, failure of any one of these major components does not result in total system failure. Failure criteria therefore have to be developed which describe how many of each of the major components can fail at any one time. The overall system failure rate can then be determined by calculating the probability of failure of the allowed number of major components based on the MTBF and MTTR of each component.

Mean time between failure calculations have been made by Ampex for each of the major TBM Memory System components. Such calculations, based on part counts and stress levels are, however, of questionable value, particularly for electro-mechanical components. It is strongly felt that MTBF determination based on actual test data is significantly more reliable than MTBF calculations based on part counts. According to Ampex, the MTBF and MTTR determinations were made during the successful acceptance tests conducted on the 1.8×10^{12} bit TBM Memory System delivered to an agency of the U. S. Government in 1972. The test results showed a total system up-time of 98.3 percent; a Level A/B Performance Summary is given in Table D.2.3.7-2.

To reduce facility downtime, the TBM Memory System can execute diagnostic tests on a failing component concurrent with normal operation of the system. This facility is provided by the VTO5 interface to the Storage Control Processor. This mode of operation (termed "inline") is effective only for tape transports which have been placed in an offline status; a failing online tape transport must be placed in offline status before the Customer Service Engineer can service it with inline diagnostics. During the inline mode, the SCP is time-shared between diagnostics and user operations.

The most basic step in fault isolation is to reconfigure the system and try the operation again. In this manner the faulty module can be isolated. The next step is to run test operations using maintenance programs and maintenance areas on the TBMTAPE. If special hardware sequences are required, a special diagnostic program, which allows the maintenance engineer to specify whatever hardware sequence he desires, is loaded into the TDP. Portions of the DSS can be placed either under local control at the SCP or under local control at the TDP.

The architecture and the modular structure of the TBM Memory System lends itself to a schedule for preventive maintenance which has minimal impact on system performance during maintenance. A large percentage of the total system preventive maintenance activity is devoted to the TBMTAPE transports partially because they are the most numerous, but primarily because tape drives need to be cleaned at

Table D.2.3.7-2. Level A/B Performance Summary

Calendar:
- Level A 3/22-4/28/72 (326 Hours)
- Level B 10/31-12/8/72 (600 Hours)

926 Hours

Activity:	ACTUAL	SPECIFICATION	MARGIN
Bits Written:			—
Multi-Blk	0.39×10^{12}		
Single-blk	0.41×10^{12}		
Total	0.80×10^{12}		
Bits Read:			
Multi-Blk	2.89×10^{12}		
Single-Blk	1.92×10^{12}		
Total	4.81×10^{12}		
R/W Total	5.61×10^{12}	0.77×10^{12}	7.3
Blk Updates-in-Place	55121		
Reread Rate (for error recovery)	0.4/1000 Blks	4.0/1000 Blks	10.0
Unrecoverable Error Rate	1 in 6.7×10^{10}	1 in 2×10^{10}	3.3
Block Demark Rate:			
Tape Pretest	0.009%	1%	111
After Pretest	0.0045%		222
Tape Life (Reads to Block Failure)	3020	1200	2.5
Up-time:			
Transports	98.1%	90%	5.2
Data Channels	99.4%	90%	16.6
Transport Drivers	96.9%	90%	3.2
System	98.3%	90%	5.9

regular intervals. Any transport can be removed from the system for maintenance with no impact on system capacity other than a proportionate loss in online memory capacity. Some transport maintenance functions require support of a Transport Driver, resulting in a proportionate reduction in seek/search capacity if the system is operating under an excessive load condition. There is only a nominal requirement for Data Channel support in connection with either transport or Transport Driver maintenance. This normally does not affect system throughput since Data Channel utilization is extremely low.

Scheduled preventive maintenance is normally performed during periods of low activity, on swing, or graveyard shifts. Because of the inherent redundancy of hardware modules, most corrective maintenance can be deferred to low activity periods while still maintaining more than adequate TBM Memory System capability. Therefore, one shift, five days per week preventive maintenance coverage, should more than suffice with on-call corrective maintenance coverage the rest of the time.

As per Ampex, based on the preventive maintenance schedules in current use with the 1.8 trillion bit capacity TBM Memory System in operation in the Washington, D. C. area, it is projected that less than 40 hours of preventive maintenance should suffice for a one trillion bit capacity TBM Memory System. A significant portion of this time is devoted to tape path cleaning.

For the most part, a normal complement of hand tools, test equipment and instruments will meet the needs of the maintenance operation. However, there are several types of special-purpose equipment which have been especially developed to facilitate checkout and adjustment of certain portions of the TBM Memory System equipment, particularly for checking key transport and Transport Driver functions. By using the special test equipment, it is possible to reduce the need for special test equipment, it is possible to reduce the need for using online system equipment in support of maintenance activities. This is particularly true of the Transport Driver Simulator which provides a substitute for an actual Transport Driver when performing a number of the checkout and adjustment functions which may be required

on transports. Also, a self-contained, computer-controlled, checkout fixture for logic modules with associated software has been developed for off-line isolation of defective elements in logic modules after removal from the TBM Memory System.

Most remedial maintenance on the TBM Memory System equipment is performed by isolating the defective subassembly and replacing it as a unit. The design of the equipment facilitates this repair approach. For example, any major subassembly, such a capstan, vacuum chamber, etc., on the transport top plate can be replaced by simply undoing three or four cap screws, removing the unit, inserting the replacement, and replacing the cap screws. Electrical, air, and vacuum connections are all completed as the replacement unit is positioned and secured in place. Most major subassemblies can be replaced in a few minutes without need for subsequent alignments or adjustments before restoring the equipment to operational status. Some assemblies, primarily rotary heads, do require alignment following replacement.

The electrical alignments include optimization of read/write signals levels and phasing, and certain servo trim adjustments required for optimum head/track registration. These alignments are executed by specially designed software modules, supported by measurement and adjustment circuits built into the hardware. The alignments may be initiated either at a TTY console local to a Transport Driver, or remotely at the SCP console. Human intervention and judgment in the actual alignment is not required. Mechanical checking and adjustment to ensure proper tape handling is facilitated also by special support programs, which do require human participation.

Preventive maintenance schedules for the three major TBM Memory System components: the Dual Transport module, the Transport Driver module, and the Data Channel module, are summarized in Table D.2.3.7-3.

A(5) GENERAL FACILITY REQUIREMENTS

In general, the facility requirements for a TBM Memory System closely match those required of a standard computer room. Room size and configuration is

Table D.2.3.7-3 Preventive Maintenance Schedules for the Major TBM Memory System Components

MAINTENANCE INTERVAL	TAPE TRANSPORT	TRANSPORT DRIVER	DATA CHANNEL
Daily	5 minutes		15 minutes
Twice Weekly	5 minutes		—
Weekly		35 minutes	
Bi-Weekly	15 minutes		60 minutes
Monthly	86 minutes	15 minutes	
Quarterly	2 minutes	50 minutes	5 minutes
Semi-Annually	60 minutes	15 minutes	
	1.1 hr/wk	.7 hr/wk	1.8 hr/wk
	4.8 hr/mo	3.0 hr/mo	7.8 hr/mo

obviously variable, and can be closely approximated through use of module floor space requirements indicated on the attached tables of physical specifications, making adequate allowance for aisle and maintenance provisions. Outline specifications of the Transport Module, Transport Driver and Data Channel are also included to aid in this review. Like modules of the system should be located adjacent to each other to the degree required for optimum room configuration, to minimize the complexity of module inter-cabling. Tables D.2.3.7-4 & 5 indicate electrical and physical data. Figures D.2.3.7-7,8,9 indicate ov + lme dimensions.

Table D.2.3.7-4. Power Requirements & Heat Dissipation

ITEM	ELECTRICAL SPECIFICATIONS VOLTAGE	FREQUENCY	CURRENT (Rating)	STEADY STATE POWER (KW)	HEAT DISSIPATIO (BTU/Hr.)
Transport Module	115VAC ± 5V Single Ø, 3 Wire	60 ± 2 Hz	3A	0.3	1,000
Transport Driver	115VAC ± 5V 3 Phase, 4 Wire	60 ± 2 Hz	ØA - 40A ØB - 100A ØC - 100A	7.5	25,000
Data Channel	115VAC ± 5V Single Ø 3 Wire	60 ± 2 Hz	10A	1.0	4,000
SCP	115VAC ± 5V Single Ø, 3 Wire	60 ± 2 Hz	20A	2.0	7,000
DCP	115VAC ± 5V Single Ø, 3 Wire	60 ± 2 Hz	15A	1.5	5,000

Table D.2.3.7-5 **Physical Specifications**

ITEM	HT.	DEPTH	WIDTH	WEIGHT	FLOOR SPACE
	(-----------	inches-----------	---------)	#'s	(Without Aisles) $ft.^2$
Transport Module	78.4	32.9	32.5	1200	7.5
Transport Driver	78.4	36.5	24.3	1100	6.3
Data Channel	78.4	36.5	24.3	900	6.3
SCP	78.4	36.5	48.6	1000	17.8
DCP	78.4	36.5	24.3	400	6.3

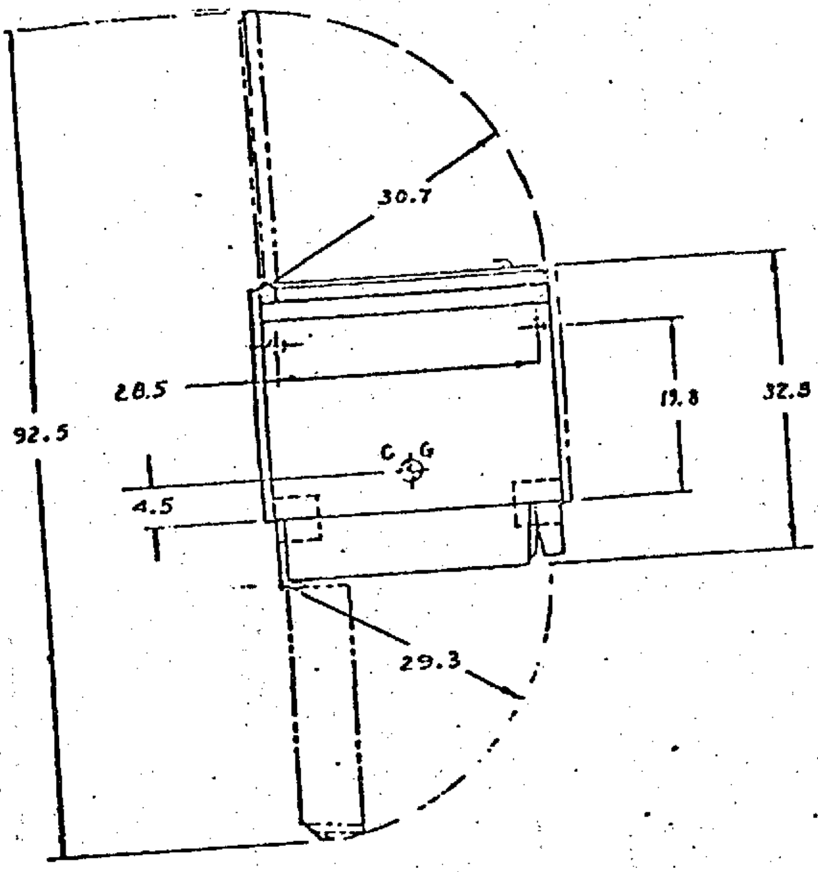

DUAL TRANSPORT MODULE	
WEIGHT	1200 LBS
FLOOR AREA	7.5 SQ FT
POWER REQ.	115V AC,1%
HEAT DISSIPATION	1000 BTU/HR
AIR PRESSURE	90 PSIG
VACUUM	50" WATER

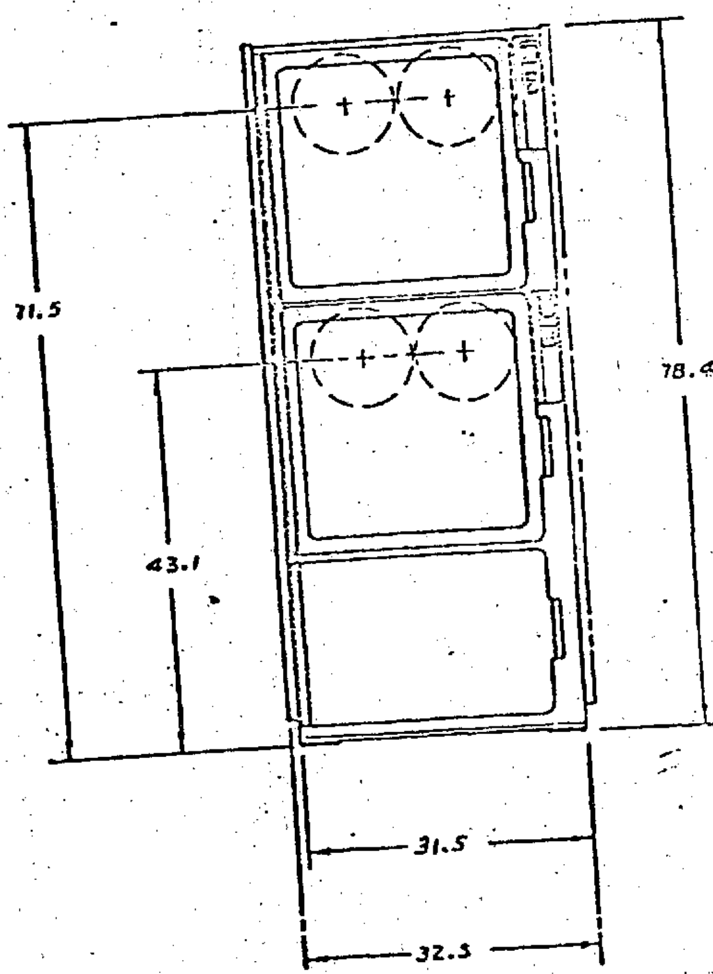

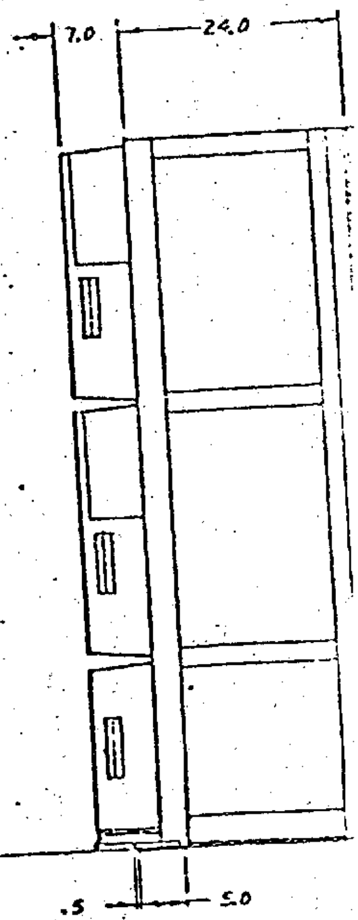

Fig. D.2.3.7-7 Outline Specification

TRANSPORT DRIVER

WEIGHT	1100 LBS
FLOOR AREA	6.3 SQ FT
POWER REQ.	115V AC, 3%
HEAT DISSIPATION	25000 BTU/HR

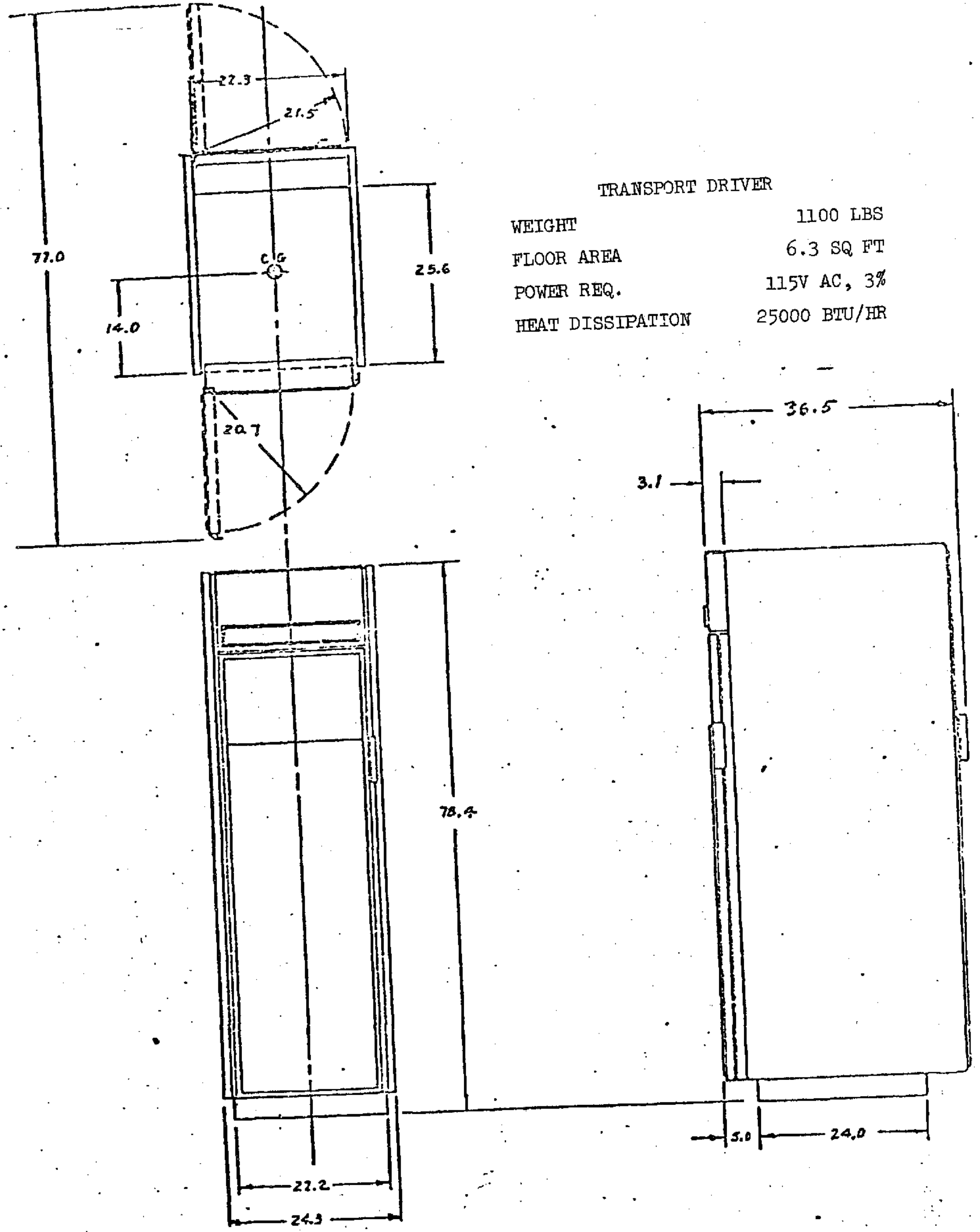

Fig. D.2.3.7-8 Outline Specification

DATA CHANNEL	
WEIGHT	900 LBS
FLOOR AREA	6.3 SQ FT
POWER REQ.	115V AC, 1Ø
HEAT DISSIPATION	4000 BTU/HR

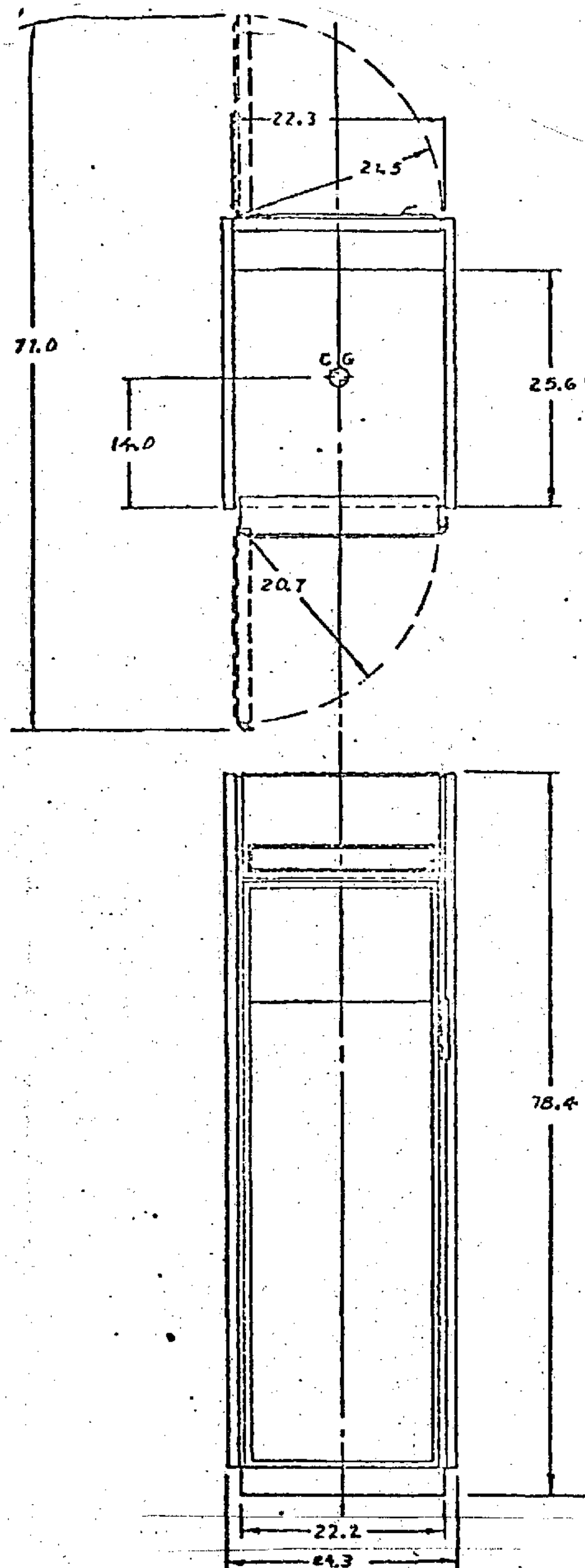

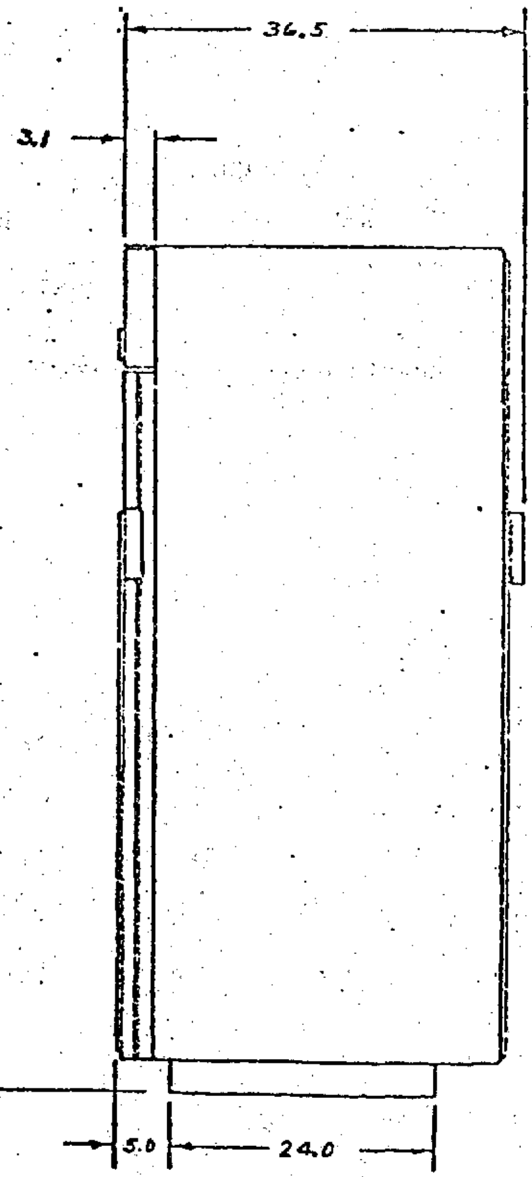

Fig. D.2.3.7-9 Outline Specification

INFORMATION MANAGEMENT
SYSTEM

D.2.3.8 Information Management System

This section describes the functions and principal characteristics of the EOS Information Management System (IMS). The IMS is the principal interface with the users for selection and ordering of data products as well as for requesting of programmable sensor observations. Three IMS system options are provided, representing three levels of system cost and capability. Table D.2.3.8-1 provides a summary of basic system functions and Table D.2.3.8-2 represents an overview of the characteristics of the three system options. Figure D.2.3.8-1 shows a block diagram of the major IMS system elements. The following paragraphs discuss the system functions and options in further detail.

D.2.3.8.1 Image Catalog and Data Inventory

The image catalog and data inventory function includes all activities involving the maintenance of directories for various purposes within the IMS. The system operates in two major roles: an internal role and an external role. In the external role the function provides the user with a catalog of acquired images based on information provided by the project control center. This catalog is further augmented by image descriptors entered by the investigators making use of the various images. In its internal role the function includes the maintenance of a comprehensive inventory of image originals and data products, possibly including detailed location tracking for purposes of system control.

The variation of this function with system option is largely a matter of the extent to which data are included in the catalogs and the degree of flexibility with which data can be retrieved using the query language. In addition the variable characteristics include the up-date cycle of the catalogue system and the question of real-time data entry.

D.2.3.8.2 Orders for Observations and Products

The user ordering function includes a number of activities in the areas of data acquisition and processing. In the data acquisition area the system provides the users

TABLE D.2.3.8-1

SUMMARY OF IMS FUNCTIONS

FUNCTION	ACTIVITIES
o IMAGE CATALOG AND DATA INVENTROY	o IMAGE CATALOG/DIRECTORY o IMAGE DESCRIPTOR INDEX o IMAGE ORIGINAL AND DATA PRODUCT INVENTORY/LOCATOR
o ORDERING FOR OBSERVATIONS AND DATA PRODUCTS	o STANDING ORDERS o DATA REQUESTS o OBSERVATION REQUESTS o ORDER STATUS INQUIRIES
o SCHEDULING AND CONTROL	o SCHEDULES o WORK ORDERS o OPERATOR INTERFACE o PRODUCT QUALITY CONTROL
o ACCOUNTING, REPORTING, AND HISTORICAL DATA	o SYSTEM UTILIZATION REPORTS o USER ACCOUNTING o USER/PRODUCT CROSS TABULATION
o PRODUCT ROUTINE AND DELIVERY	o MAILING LABELS o DIRECT TRANSMISSION

TABLE D.2.3.8-2
SUMMARY OF IMS OPTIONS

	1 LIMITED	2 EXTENDED	3 UNLIMITED
STANDING ORDER PRODUCT LIMITATION	3 MONTHS	1 YEAR	5 YEARS
SENSOR OBSERVATION REQUEST TIME FRAME			
USER ACCESS TO SYSTEM (ON-LINE)	LOCAL OPERATOR TERMINAL	REMOTE USER TERMINAL	REMOTE USER TERMINAL
TRANSACTIONS ALLOWED ON-LINE:			
CATALOG QUERY	SIMPLE	EXTENDED	EXTENDED
PRODUCT REQUEST	YES	YES	YES
ORDER STATUS REQUEST	SIMPLE	SIMPLE	EXTENDED
IMAGE DESCRIPTOR ENTRY	NO	NO	YES
ORDER PRIORITY	FIFO	FIFO AND SPECIAL	PRIORITY LEVELS
ACCOUNTING DATA REQUEST	NO	NO	YES
LIMITED DIGITAL PRODUCT DELIVERY	NO	NO	YES
PRODUCT/USER CROSS-TABULATION	NO	YES	YES
ACCOUNTING/REPORTING CYCLE	MONTHLY	MONTHLY	ON-LINE;DAILY SUMMAR
CDP SYSTEM CONTROL	PRINT DAILY ORDER LIST.	ORDER LISTING ON OPERATOR REQUEST	DETAILED SCHEDULE OPTIMIZED FOR CURREN LOCATION OF DATA
CATALOG LEVEL OF DETAIL	SIMPLE	SIMPLE	CURRENT DATA LOCATION
SENSOR REQUEST LEAD TIME REQUIRED	HIGH	MEDIUM	LOW

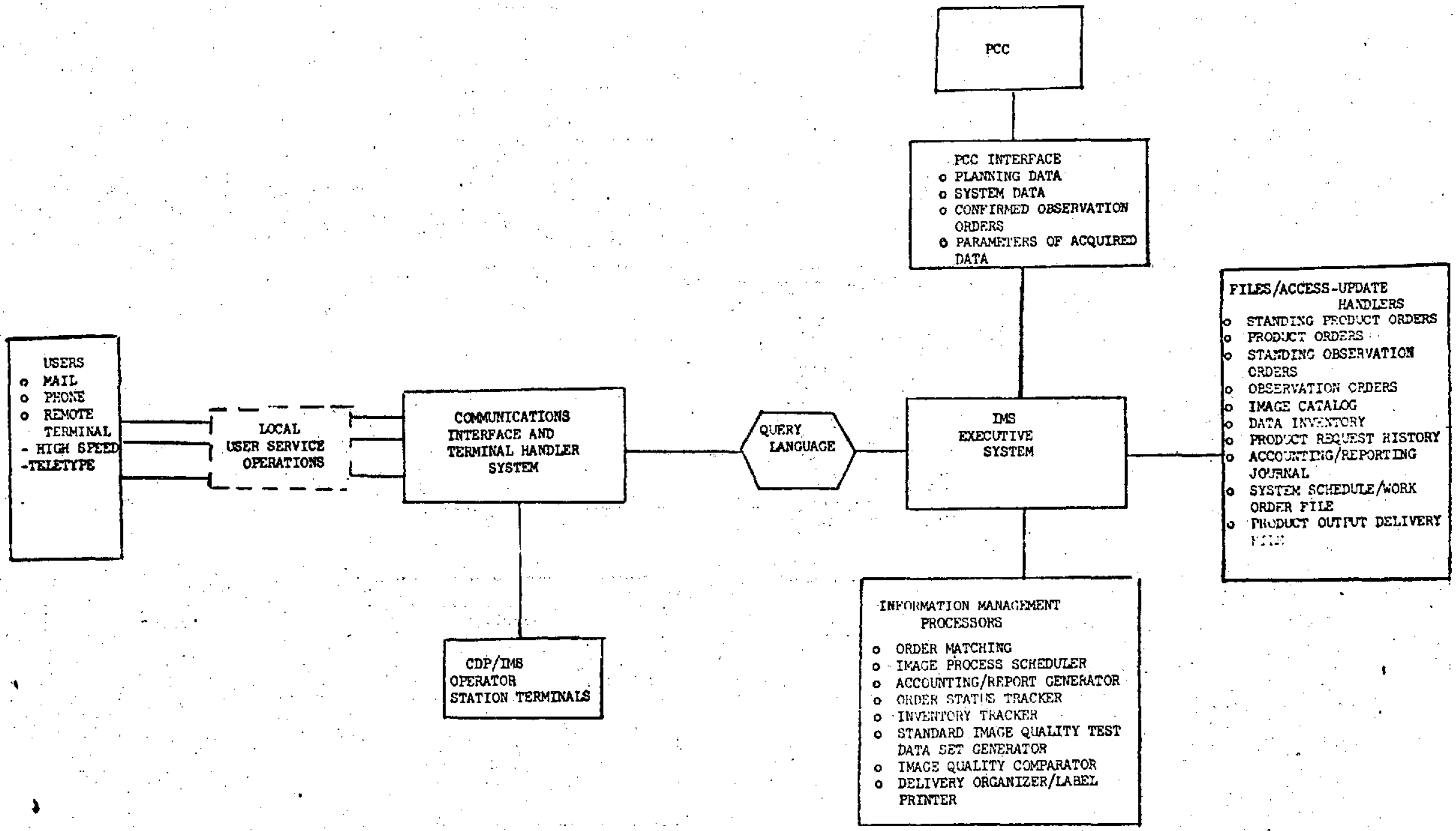

FIGURE D.2.3.8-1; MAJOR IMS FUNCTIONS

with the capability of requesting that specific sensors be turned on or that they be pointed at specific areas on the ground. In the processing area the user ordering system represents the basic medium through which requests for specific data products are received by the system. There are three basic classes of transactions taking place in the user ordering system. The first is a basic request for data previously acquired by the system or for observations specifically defined by the user and known to be within the orbital capability of the satellite. These requests are known as data or observation requests. A second category of transaction is standing orders. In the case of data products these represent generalized requests for classes of material by geographic area and quality that are placed prior to data acquisition and without specific knowledge of the specific identification of the data products requested. In the case of observations these are generalized requests made either too far in advance of availability of specific orbital and coverage parameters or alternatively they are requests for imagery known to be within the coverage capability of the satellite but where the user is willing to make the request with sufficient generality and flexibility to permit the system to choose among the various possible alternative means of satisfying the request. A third category of transaction is a request for order status information.

There are several types of transactions for which options are available in the alternative system concepts. These options are described in the paragraphs below.

(1) Standing Order Product Limitation

In the present ERTS system there are limitations on the formats of standing product orders. In the low capability EOS system these limitations will be retained. In the higher capability EOS options these limitations will be relaxed and finally eliminated.

(2) Sensor Requests

The three capability options in the sensor request area will have gradation according to the allowable request time frames and the extent to which the system will accept responsibility for choosing among alternative means of implementation.

(3) Order Status Requests and Order Service Priorities

The gradation with respect to the order status request transaction will range from a very simple acknowledgement of order existence in the low capability system to an extended tracking and tracing of the order in the higher capability system. Also there will be a variation with respect to the ability of the user to define or modify priorities. In the low capability system the order system will be strictly first-in-first-out (FIFO). In the mid level system the order priority will be FIFO with the addition of a special category for expedited service. In the high capability system a set of priority levels will be established which give the user the capability of expressing on a more detailed level the turnaround time required for product requests or the relative importance of an observation request.

D.2.3.8.3 Scheduling and Control

The scheduling and control function includes two activities. The major activity under this function is the organization of the product load for the various segments of the IMS, and the generation of appropriate instructions and work orders to efficiently accomplish the processing. The gradations of system capabilities in performing this function are principally related to the frequency with which the product load is reorganized and the rate at which the work orders or other instructions are transmitted to the system. In the simplest system the product load is scheduled and organized on a daily basis and the output of the scheduling process consists of a set of printouts and tapes that provide in a sequential format the relevant information required for the day's operations. In the higher capability systems the frequency of scheduling is increased and the linkage to the operator made more immediate to the extent that in the highest capability system the scheduling is performed on line at the time of the user request and is immediately available for operator or system action. The rapid degree of system control is required in order to permit reaction to user orders bearing the high priority capability associated with that system option.

The second activity of the scheduling and control system is the monitoring of product quality. This activity is effectively performed through the use of standard data and work orders generated by the IMS. The standard data includes both an input data set and output comparison set for use in testing various stages of processing. The comparison can be made either manually or automatically as appropriate to the nature of the process and the capability level of the IMS.

D.2.3.8.4 Accounting, Reporting, and Historical Data

The accounting, reporting, and historical data system performs two functions. The accounting/reporting activity accumulates and summarizes detailed data on system utilization both for individual users and on an overall basis. Because of the flexibility and capability of the system it is assumed that the accounting system must serve as the basic means of system control for resource allocation. Overall control of the system is exercised by the project manager by assigning each user some form of budget. The budget may be an actual dollar amount or it may involve the use of some kind of point system. The accounting system then functions in a manner substantially to the accounting system used with a computer batch processing or time sharing system involving a large number of users. By establishing a budget charge for each capability the project manager will be able to force the users to set priorities on their utilization of system resources in a manner consistent with the cost or complexity of the service requested. The variation in the accounting/reporting activity with system option is essentially a function of the reporting cycle. In the lower capability options each user transaction is journalled and a monthly summary produced. Neither the users nor the project manager are provided with access to the accounting records on an interim basis between report generation points. In the higher capability system the accounting data is kept on line and a daily summary provided to the project manager. The users can request summaries of their own status and activity on the same basis as any other system transaction.

In the higher capability systems an additional activity of the accounting system is the maintenance of a cross tabulation of data products by the users requesting them. This cross tabulation is maintained in conjunction with the system directories previously discussed, and permits the individual user on request to determine the identity of all other users requesting imagery in a specific category (primarily geographic area). Software provisions will be included to permit any user to exclude transactions from being included in the cross tabulation. The purpose of this activity is to permit users interested in specific imagery to obtain information by means beyond those provided by the image descriptor index.

D.2.3.8.5 Product Routing and Delivery

The IMS will include the product routing and delivery functions of the CDP system. In the lower capability options product routing is limited to mail delivery only. Under these conditions the function of the IMS will be to print appropriate labels in conjunction with the work order and scheduling process. In the higher capability IMS options, there will be provisions for limited delivery of small, high priority digital data orders directly to remote user terminals. This function will be performed in a manner completely analogous to the delivery of output files in a remote batch system.

D.2.4 Local User Systems

A systems viewpoint is taken with respect to a wide family of conceptual EOS Local User Systems (LUSs) which includes the Low Cost Ground Station (LCGS) concept. Centralized as well as local operations are necessary to assure systems' viability, and these operations are considered to the degree currently possible.

The basic approah for considering LUS hardware and software configurations was to develop a range of user capabilities for the display, hard-copy, processing, and analyses of EOS payload data. Further, a variety of data delivery methods were considered, but we have concentrated on the direct delivery method*.

Several methods of EOS payload data delivery are possible, but they are cost-effective only with respect to particular EOS system configurations as yet undefined. For example, dial-up 50 to 56 kb/s wideband common carrier lines should be available throughout CONUS during the EOS time frame. Computer-to-computer telecommunications could be efficiently used for delivery of selected data to the LUS. Additionally, CONUS DOMSAT communications could enable central to LUS data channels at 50 to 80 Mb/s rates depending on the selected EOS configuration.

However, for current study purposes, EOS to user communications at data rates of about 20 Mb/s were assumed as well as a CONUS LUS population of 50 to 150 units. The system concept could easily be expanded to include LUSs in foreign lands or contracted to just a few CONUS LUSs.

The systems concept is to provide modular hardware and software capabilities for the LUSs that would be complemented by centralized support capabilities. The centralized support elements are assumed to be located within the GSFC complex, and are collocated with (and within) the Information Management System (IMS), the Project Control Center (PCC), and the Central Processing System (CPS).

The two centralized support elements are the Applications Program Development Laboratory (APDL) and the LUS Diagnostic and Equipment Laboratory (LDEL). The

*"Specifications for EOS System Definition Study," EOS-410-02, page 2-6.

APDL provides a computerized capability for the development of LUS Applications Programs and the conversion of previously developed programs for use with the LUSs. Additionally, scientific consultation services would be available from the APDL personnel. Remote LUS processing and analysis equipment testing is provided by the LDEL via low-speed digital data dial-up telephone lines. The LDEL operators would be experts with the operational LUS hardware and software and would be able to exercise the local computerized equipment via low-speed digital communications from their central location.

Note that a basic assumption for the centralized/local system concept is that the LUS operators are primarily applications oriented (i.e., the operators are not necessarily computer programmers or computer operator experts). Therefore, the applications and diagnostic support which is necessary to maintain operational LUSs is provided by the shared centralized system elements. This concept would only be cost-effective if there were many LUSs. If only a few LUSs were deployed, the APDL and LDEL would not be economical. The breakpoint for the cost-effectiveness has not been determined, but because our cost breakout is detailed the costs for the two elements can easily be subtracted from the total estimated DMS cost.

Adding or eliminating the APDL and LRDC elements does not affect the acquisition, display, and processing capabilities of the LUS. However, one centralized element that is necessary for LUS operation is the IMS. The LUS operators communicate with the IMS via dial-up voice or digital low-speed telephone lines to receive precision EOS orbit and attitude data as well as make known their requests for CPS processed computer compatible tapes (CCTs) and picture products. Additionally, the operators would receive EOS orbit predictions and coverage time information from the IMS to point and acquire the direct EOS to LUS data transmissions.

The following paragraphs provide the purposes and preliminary descriptions of the LUS data receiving, handling, processing and display equipments and their capabilities. Estimated costs are also provided.

D.2.4.1 Purposes for the LUS

There are several purposes for the LUSs. They provide users such as federal, state, or county government agencies with the capability to view their local areas with high resolution (10, 30, 90 meter resolution possible) from an altitude of 600 to 900 km. Visual areas covered are in north-to-south strips from a few miles to a few hundred miles wide.

Commercial and private organizations can be provided with the same observation capabilities. For example, universities can establish practical cost Earth Survey Data Laboratories at reasonable investments for purposes of scientific investigation and student training. Oil, costal fishing, and mining companies can use EOS payload data for private purposes without revealing their particular interests to others.

Because EOS data are delivered directly to the LUS operators they can view their local areas within seconds to several minutes depending on their LUS capabilitie Precision EOS orbit and attitude data can be delivered via the low-speed IMS telephone lines that would enable precision film and computer products generation potentially within several hours rather than days or weeks as is now experienced for some ERTS system products.

In summary the purposes of the LUS are to:

- Display EOS image data in black and white or color visual images
- Produce copies of the visual images
- Format and selectively edit the image data
- Radiometerically and geometrically correct the image data
- Provide an analysis capability to support a multiplicity of applications

D.2.4.2 Functional LUS Description

A minimum set of equipment is required for the minimum capability direct data delivery LUS. This is an antenna system, an RF receiver, a data demodulator, and a visual display device. Proper formatting of the digital data is required within the display device to correct the baseband data for human observation. After display, the image can be photographed to provide a record of the information.

Manual antenna steering and a hand held camera complete the minimum capability LUS. However, it is expected that most LUS users would require a greater capability system.

Therefore, a basic system capability has been assumed where a data recorder, a data processor, and an LUS equipment operator interface are added to the minimum equipment set. These fundamental LUS elements are shown in Figure D.2.4-1.

An operational scenario for the Basic LUS envirions that the operator uses the predicted acquisition of signal (AOS) and loss of signal (LOS) parameters from the IMS for his particular location, enters the parameters into the processor via a teletype or CRT/Keyboard equipment interface, and at the predicted AOS time initiates the system operation. The data recorder would be started, and when the EOS transmission signal strength is observed from a reciever meter, the operator would maximize the signal strength indication by adjusting the antenna programmed track and receiver tuning.

At LOS, from 2 to 12 minutes after AOS, the data acquisition phase is completed and the data recorder would be manually controlled to enter data either directly or through the processor to the display. Assuming that the data were not displayed during the acquisition phase a visual image using EOS sensor calibrated data could be displayed within 5 to 20 minutes. The displayed image would cover an area of 1024 by 1024 pixels representing a geographical span of 10.2, 30.7 or 92.2 km in the north-to-south and east-to-west directions, depending on a 10, 30 or 90 meter pixel field of view.

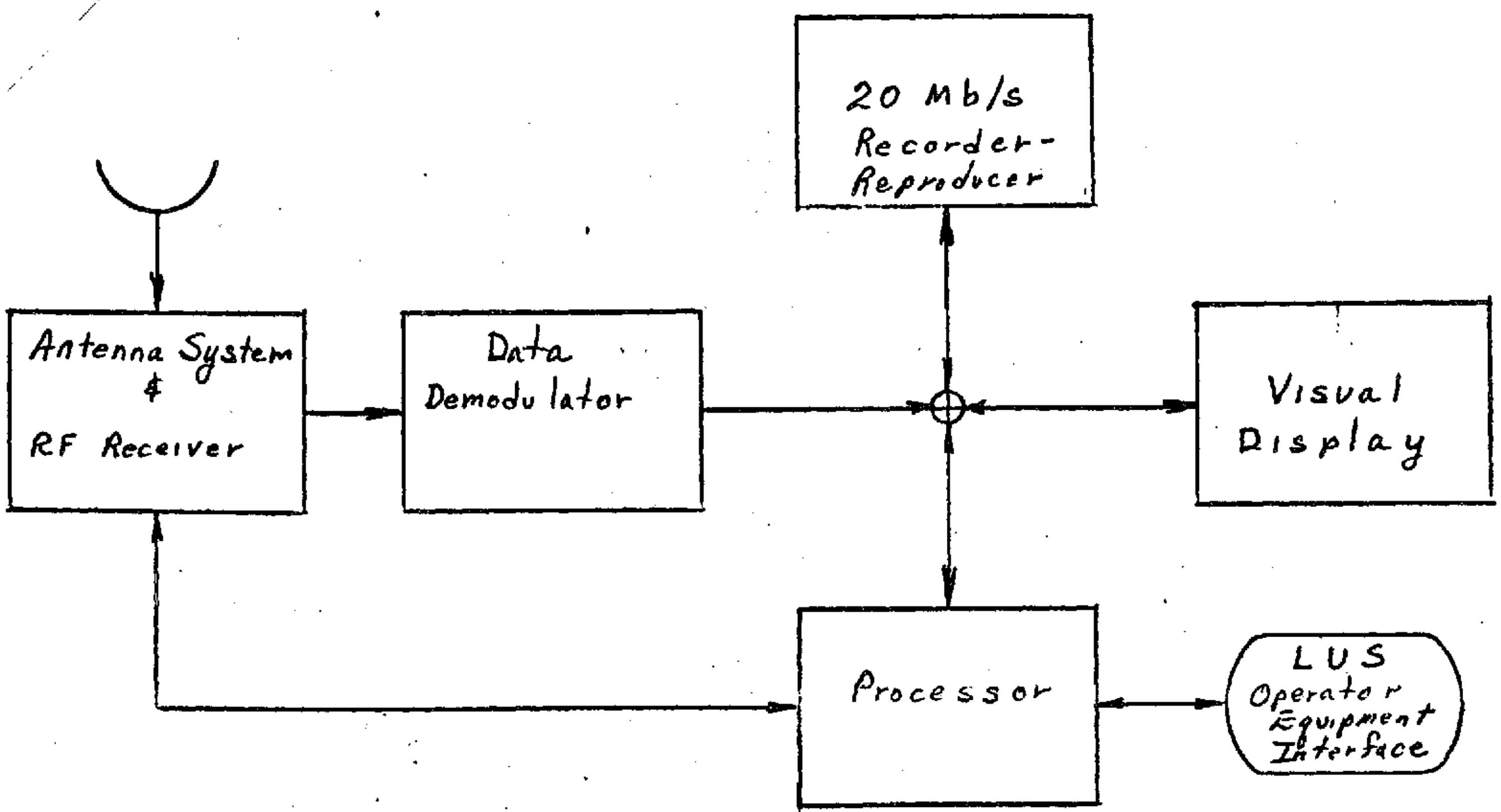

Fig. D.2.4-1 LUS Fundamental Elements

The intensity of any pixel would be represented by 64 possible levels corresponding to a 6-bit pixel intensity range, and the image area would be 11 by 11 cm. Predicted EOS ephemeris would provide geographical latitude (λ) and longitude (L) indications on the image. A Polaroid film holder or hand held camera could be used to produce second generation photo products.

Additional capabilities that can be added to the Basic LUS provide operator convenience for the data acquisition and image display, larger image displays, color images, data processing, image analysis and precision image products. A further capabilities increase enhances operator convenience through computer automation and provides the ability to perform data analysis, image analysis and product generation interactively and more quickly than with a lesser capability system although at an increased equipment and operator cost.

Because of the possible large range of potential LUS capabilities we selected three LUS equipment cost targets of $100K, $200K and $300K for study purposes. An assumption was that from 10 to 100 LUSs would be required and that the equipment costs would represent recurring costs only. The Basic LUS cost has been set at 100K. Therefore, the two higher cost targets represent enhanced capability systems.

D.2.4.3 Preliminary Designs for the LUS.

Pixel format that can be reasonably implemented on board the EOS and easily handled on the ground during the LUS data acquisition phase is an important design driver. The current assumption is that any one band of TM or HRPI sensor data can be transmitted at full resolution, and that any three TM bands at 1/3 reduced resoltuion can also be transmitted. It is further assumed that necessary sensor calibration data, predicted EOS subsatellite point ephemeris, S/C attitude and attitude rate data, as well as sensor housekeeping data will be transmitted with the sensor pixels.

An effective 185 km TM swath width and 35 km HRPI swath width ~~with 10 percent overlay~~ are assumed. The intensity levels for each sensor will be quantized by

6-bits. Further, 15 scan lines per earth swath are assumed for both sensors when operating at full pixel intensity range.

Based on the preceding assumptions a scan format would appear at the LUS demodulator output connection as follows:

FILL, LS ---, LSP, Multiplexed Pixel Data, LEP, LS ---, DSP, OD, FILL

where
- FILL - unused bit intervals (not necessary and to be avoided if possible)
- LS - Line Synchronization
- LSP - Line Start Pattern
- LEP - Line End Pattern
- DSP - Data Start Pattern
- OD - Overhead Data (Ephemeris, calibration, housekeeping, etc.)

Figure D.2.4-2 pictorially displays TM data definitions that are used in this report. These terms are scene, image, band, line, swath, and pixel.

Assuming now that the EOS subsatellite point velocity is 6.9 km/s, an 85 percent efficient scanner, retrace overlap, a seven band TM, and a four band HRPI, where the TM pixel field of view (FOV) is 30 meters, and the HRPI is 10 meters, a 1:1 sampling rate with respect to the FOV, then one TM scan line contains 6165 pixels and one HRPI scan line contains 3500 pixels.

A TM scan swath cover (15 x 30) 450 meters in 65.2 ms of subsatellite point time. At 85 percent scan efficiency, a line of pixels is generated in (65.2 x 0.85) 55.4 ms, that results in a line pixel rate of (6165/0.0554) 111,282 pixels/second. A composite TM band transmission rate is (111282 x 6 x 15) 10,015,380 b/s. The pixels require 8,513,073 b/s per band allowing 1,502,307 avaiable for synchronization and overhead data purposes.

The HRPI scan swath covers (15 x 10) 150 meters in 21.7 ms ground time and thus, the scan time at 85 percent efficiency is 18.5 ms. With 3500 pixels per line, the line pixel rate is (3500/0.0185) 189,189 pixels/second; that requires a transmission rate of (189189 x 6 x 15) 17,027,010 b/s. At 85 percent efficency there are 14,472,958 b/s for pixels and 2,554,052 b/s for overhead data.

Considering a TM three-band compaction, only (6165/3) 2055 pixels per line are required. This indicates a line pixel rate of (2055/0.0554) 37,094 pixels/second. A transmission rate for these data is (37,094 x 6 x 15) 3,338,460 b/s. Thus 2,937,691 pixel bits and 500,769 overhead bits per second would be transmitted depending on the particular overhead data format selected. A greater transmission rate may be necessary to keep the overhead data format the same for the compacted data as for the one-band TM data transmissions.

Figure D.2.4-3 shows the LUS direct data acquisition equipment. The data format from the demodulator was previously identified. The pixel decommutator would synchronze the incoming scan swath multiplexed bit stream and demultiplex it into 15 streams. These lower rate streams contain their own line synchronization patterns and form data blocks or Pacts (i.e. scan lines pacts) that become independent from each other. The image

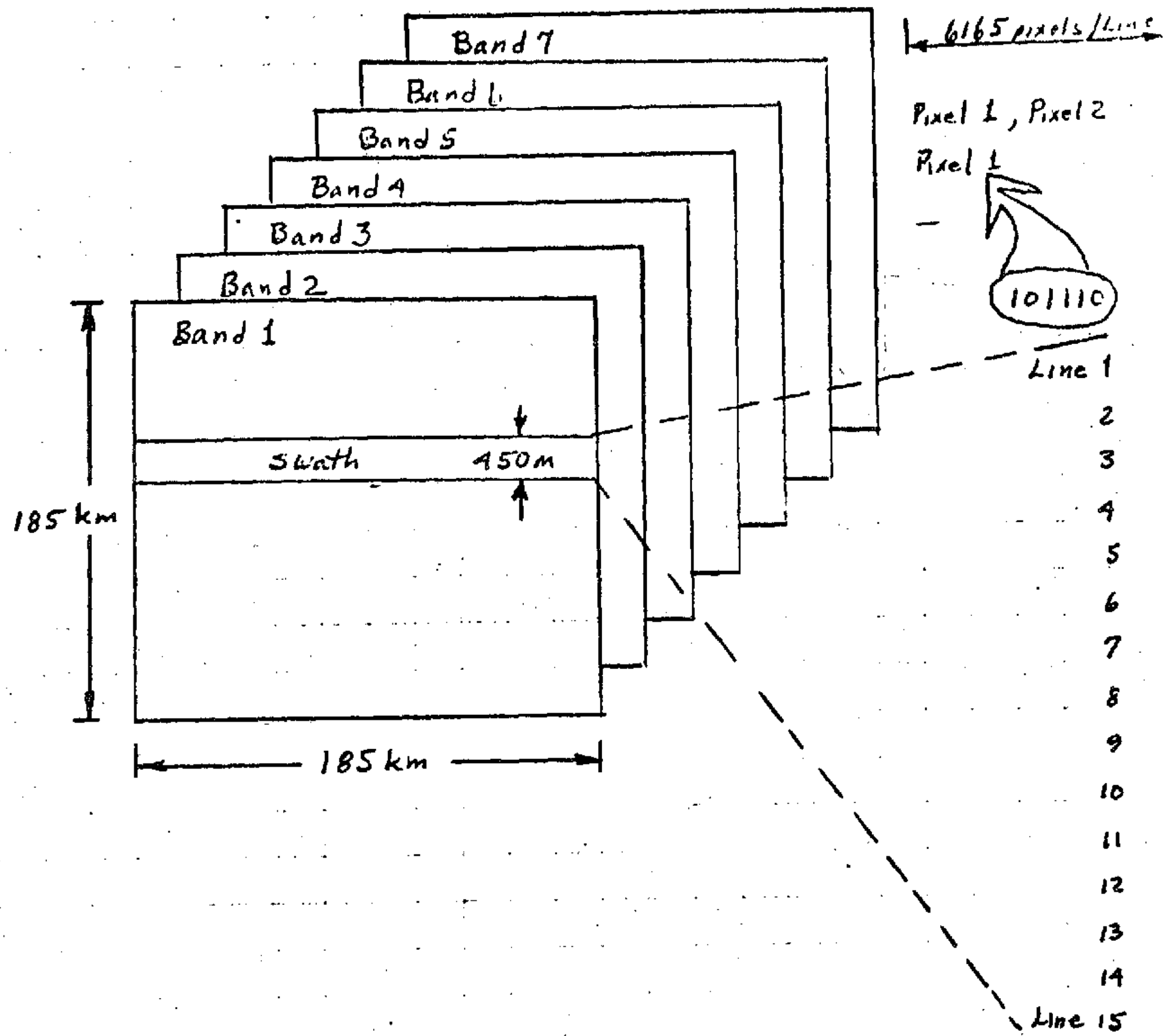

A scene is the collection of 7 TM Images covering a 185 X 185 km area. Each Image is composed of 1 Spectral Band Data covering the 185 x 185 km area. A swath is swept across a Scene or Image and is composed of 15 Lines of Sensors for each Band. Pixels result from sampling the sensor signals and converting an analog voltage to a 6-Bit Digital sample.

Fig. D.2.4-2 TM Data Definitions

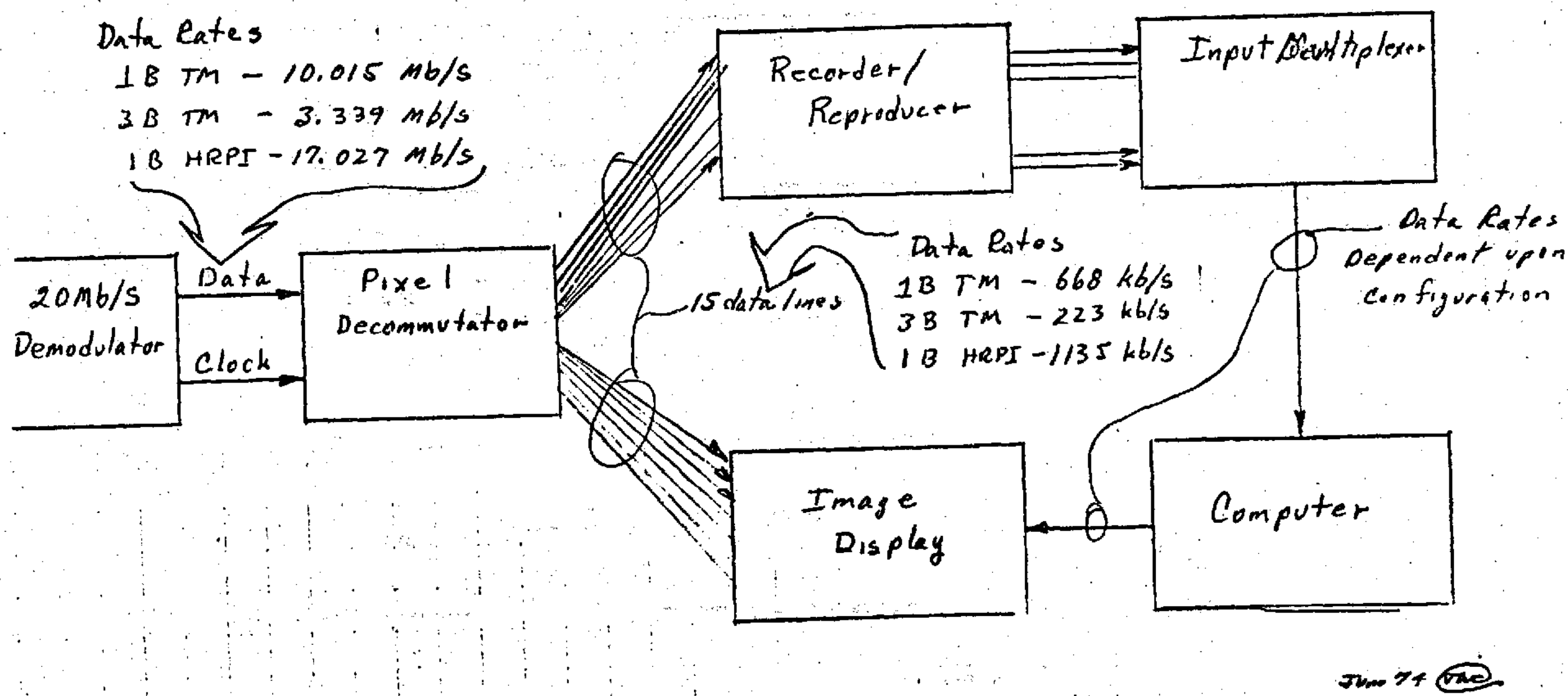

Fig. D.2.4-3 Detail for Acquisition Equipment Connections

may be displayed or recorded, depending upon the selected configuration.

The demultiplexed 1 Band TM data format is shown in Figure D.2.4-4. Each line of pixels is preceeded with a line pattern used later for line synchronization. Note that a tradeoff here was to use a recorder that would handle the LUS direct data as a single stream or the more conventional instrumentation type recorder. The latter was chosen as being less costly in the system context.

Blocks of data follow the pixel packs that contain housekeeping and calibration data. These overhead packs are multiplexed on board the EOS during the 15 percent scan retrace interval. These packs are synchronizeable and independent as are the pixel pacts.

The pixel decommutator demultiplexes the TM and HRPI LUS data with the same algorithm,minimzing the demultiplex cost. Figure D.2.4-5 shows the three band pixel pack. The multiplex detail is shown in Figure D.2.4-6. . The decommutator as well as the input multiplexer are development items. The recording unit is not.

Current practical data recording can be done to 35kb/inch on available recording units. Considering accuracy of data recovery and maintenance we have decided to use a packing density between 15 and 25 kb/inch at present. Table D.2.4-1 shows the data rates then available per track on an instrumentation tape recorder. It is seen that the highest line rate (1135 kb/s for HRPI data) can be captured at the 60 inch/second speed.

Table D.2.4-1 Density vs Data Rate vs Tape Speed

Tape Speed (LPS)	Density Range (kb/s)		Data Rate Range (kb/s)	
120	15	25	1800	3000
60	1	1	900	1500
30	1	1	450	750
15	1	1	225	375
7.5	1	1	112.5	187.5
3.75	1	1	5617	93.7

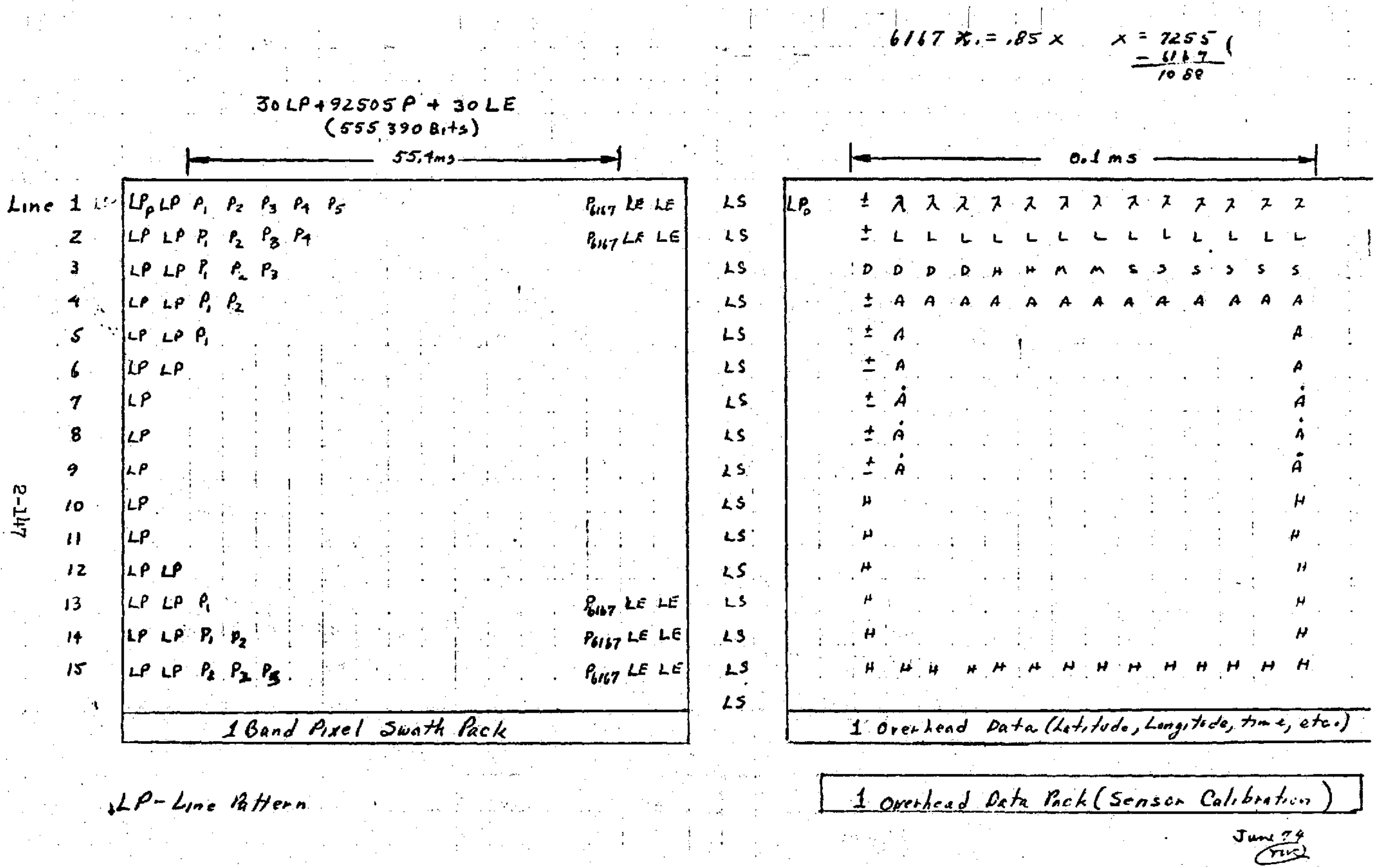

Fig. D.2.4-4 Demultiplexed TM 1 Band Data (1 Pixel Pack and 2 Overhead Packs)

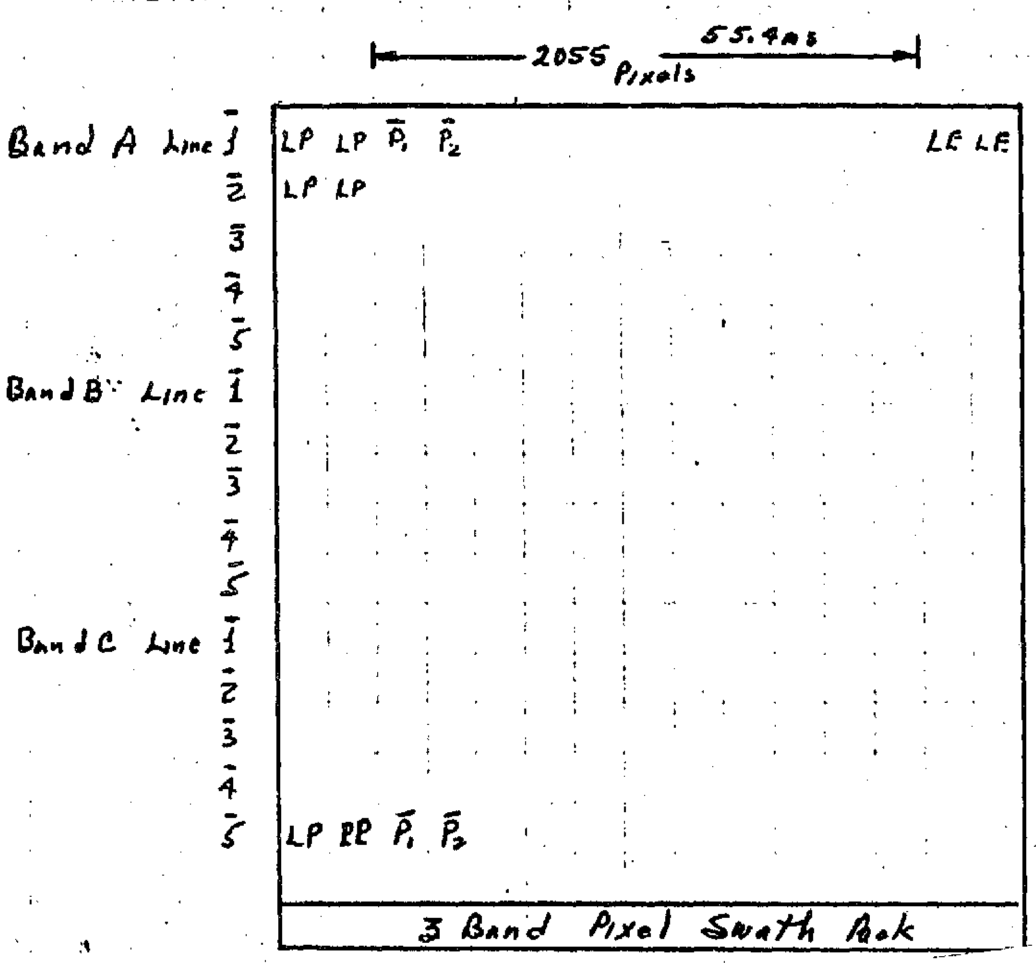

Fig. D.2.4-5 Demultiplexed TM 3 Band Data (1 Pixel Pack and 2 overhead Packs)

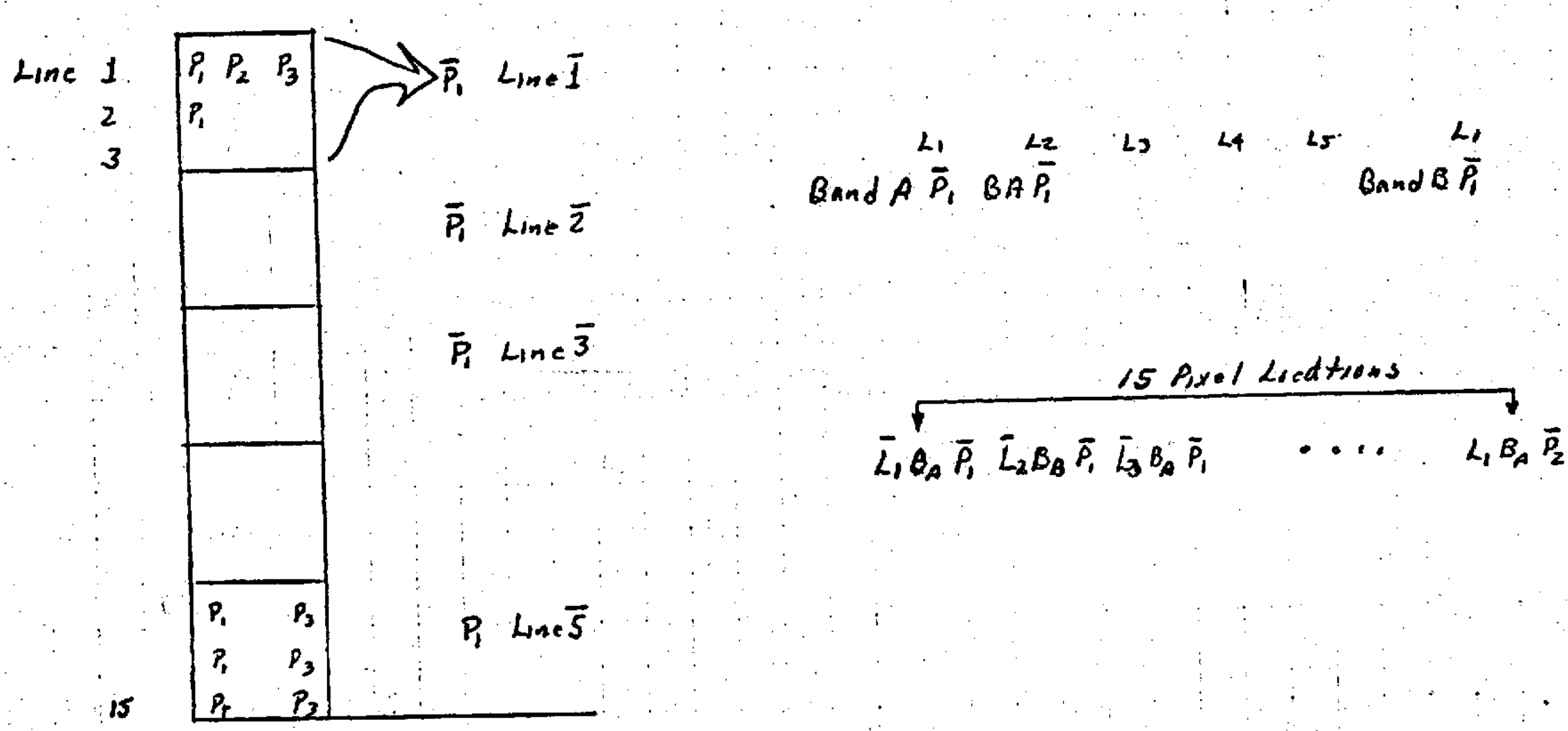

Fig. D.2.4-6 Reduced Resolution Pixel Packing

The recorder replay speed is compatible with the particular computer throughput rate. It would be between 1 and 6 Mb/s (composite of 15 data tracks).

Bit reshaping is accomplished in the input multiplexer for each data track. This is done with a signal conditioner costing about $240 in quanity, one unit for each of the 15 data streams. Line synchronization is accomplished in the multiplexer or the computer. Hardware synchronization provides greater computer throughout but is more costly that software synchronization. In either event the data are multiplexed into the computer in 8-bit or 16-bit bytes for ease of software format control. (Pixel per byte synchronization is performed when the line synchronization is implemented by hardware).

Assuming a direct visual image generation is required, then the 15 pixel streams would go to the visual display. This display would reformat the data depending upon the particular technique and transfer rate display capability. Full image display and resloution at the received rates is more expensive than reduce resolution displays, such as a television set.

For practical purposes a LUS real-time display, if required, would be composed of a "frame grabber", cheap disk, and a commercially available TV set. Even this system could cost between $6K to $10K, however, and has been ruled out for the present as too expensive. A more reasonably priced display system may be possible for the real-time data and will be investigated as the study continues.

A full resolution visual display is required , and it appears that even by eliminating the real-time display requirement at least $14K is required for a full resolution display. (Less costly versions may be possible, but will require further investigation).

Two additional items of equipment are functionally required to complete the Basic LUS. These are a disk data storage unit, and a magnetic tape unit. The disk storage serves as a temporary area for the volume of data bits that compose an image and as an online computer program library. Tape units necessary to hold the potential data volume received during one EOS overflight (i.e. the disk unit would be prohibitively expensive to hold the data).
hold the data).

The preliminary LUS designs should be further refined as a function of the particular user application developed during the study.

D.2.4.4 LUS Processor and Display Hardware

Processor and display hardware for the Basic LUS is shown in Figure D.2.4-7. The current "quantity 1" cost for the Disk Unit is $14, the Tape Unit is $20K, the Computer is $10K, the operator interface (Teletype Display) is $1.4K, and the small precision (Storage tube B & W) display is $15K. These costs include system interfacing for equipment operation with 60 H_z 115 Volt power. For 50 H_z or 230 Volt operation, add $1K. The composite Basic LUS processor, and display costs thus total to $61K or $62K.

The optional telephone interface runs $0.4K, plus rent of the digital modem and telephone of about $50 per month. Using a CRT/Keyboard to replace the Teletype operator interface adds $1K, and floating point options for computer throughput enhance, plus hardware multiply and divide, can increase the cost by $5K. The input multiplexer was priced in the data acquisition equipment.

The equipment costs for the processor were developed from manufacturers list prices and are subject to quantity discounts. A component discount schedule has been generated for estimating guidelines: 10 systems, 5%; 30 systems, 13%; 50 systems, 17%; 100 systems, 22%; and 150 systems, 25%.

A stripped system could be made less costly than the $61K by removing items such as the disk unit and one magnetic tape drive. The processor hardware cost is then about $26K. Table D.2.4-2 shows the stripped and Basic LUS processor (without options) and display costs as a function of quantity.

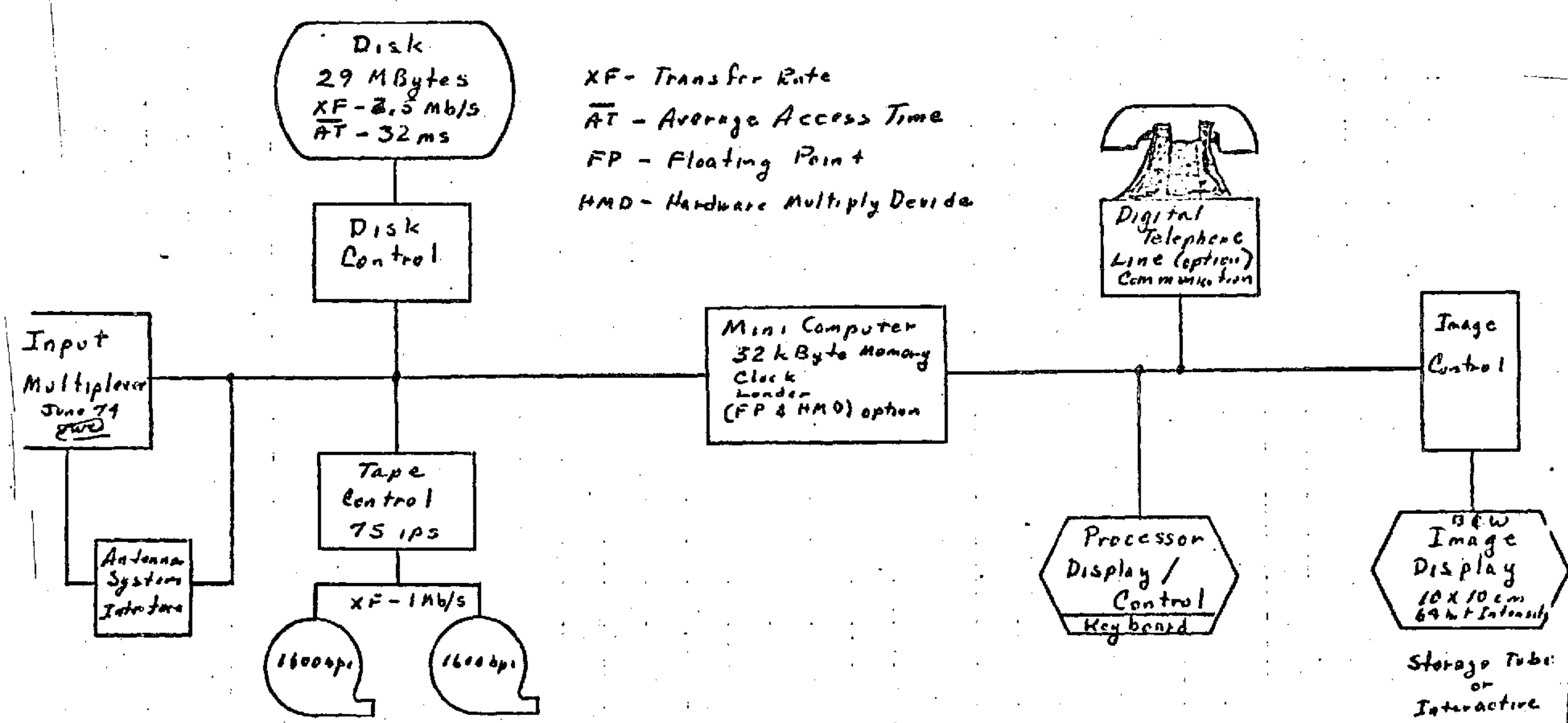

Fig. D.2.4-7 Basic LUS Processor and Display

Table D.2.4-2 Processor and Display Costs Vs. Quantity

Quantity	Discount (%)	Stripped	Basic ($K)
1	0	26	61
10	5	25	58
30	13	23	53
50	17	22	51
100	22	21	48
150	25	20	46

The optional telephone interface can be replaced with a 50 to 56 kb/s synchronous interface for about $800 increased cost, or an inter-computer digital communication interface for a large scale computer (such as an IBM 360/370 machine) for a further increase of $4K. Thus, the Basic LUS Processor and Display can be used as a relay data processor and analyiser either as a stand-alone unit or with support provided by a larger computer.

Note that the LUS does not include program development hardware such as computer card readers or printers. This is because the basic program development operations occur at the APDL. If the APDL is not implemented, a LUS would have to include the added program development equipment, increasing the system cost of the LUS by about $15K. Enhanced capability LUS Processor and Displays include throughput expansion, image display enhancement (image analysis) color display, photo copy convenience, and computer hardcopy (line printers).

Throughput enhancement can occur in several ways. Two methods under consideration are multiprocessing and computer expandability. Because our Data Operations Study indicates a minicomputers configuration cost less than large scale computor systems only minicomputors are considered for use in the LUS. For multiprocessing, additional minicomputers can be added to the one used in the Basic LUSs. Manufacturers have developed software and hardware for connecting several of their machines together. Thus minicomputers can be interconnected to supply increased throughput for data processing and image analysis.

Expandable minicomputer memories (adding 2,4,8, & 16 kilolyte core memory modules) increase the computer throughput for handling increased

image sizes. (The Basic LUS display is 1024 x 1024 pixels). This is currently practical up to memory sizes of 131K kilolytes (1.04 Mb). We have considered only a subset of the LUS processor and display options in line with the design cost targets. Although particular hardware elements were used to develop the LUS Processor and Display Configurations they should be considered as representative for the capabilities indicated.The preliminary hardware costs could be expected to vary plus or minus 10 percent as configuration optimization for various applications, throughput, and cost are performed.

All hardware currently considered is off-the-shelf and deliverable within 60 to 120 days after order. Quantity pricing is based on the total indicated number of units within a 12 to 18 month time period. There are no non-recurring hardware costs. System development costs do apply. These are estimated at $50K minimum and would be expected to increase as the LUS complexity increased. These costs include system documentation and initial unit checkout.

Data General, Interdata, Modcom, Varian, and Digital Equipment Corp. computer equipment, and Dicomed and Comtal Image Display equipment prices have been used in the costings.

D.2.4.5. LUS Processor Software

Table D.2.4-3 shows the software for a 32.768 K-bit word minicomputer memory. Smaller size memory can be used to reduce the LUS costs but the throughput will also decrease. The converse will occur if larger memories are used. The 32K word memory is a balance as to a reasonable minimum memory size.

Table D.2.4-3 MEMORY SIZE

Software Function	Memory Size (Words)
Real Time Operating System (Resident*)	4096
Data Processing & Image Analysis Executive (Resident)	4096
Processing & Analysis Packages (Resident)	4096 to 8192
I/O Buffer Areas	4096
Support & Applications	16384 to 20480
Data Working Space (Data & Cal. Tables,Etc)	16384 to 12288
Minimum Recommended Memory Size	32768

* Resident in computer memory during the particular processing or analysis Operations.

The data processing and analysis software packages are modular and are dependent upon the LUS operator's primary applications areas. Therefore, we have not specifically considered the applications packages but have concentrated on the data handling, management, processing, and general information abstraction areas. The hardware capability for the applications packages has been included, however.

Basic software for the LUS is modular and organized as indicated in Figure D.2.4-8.

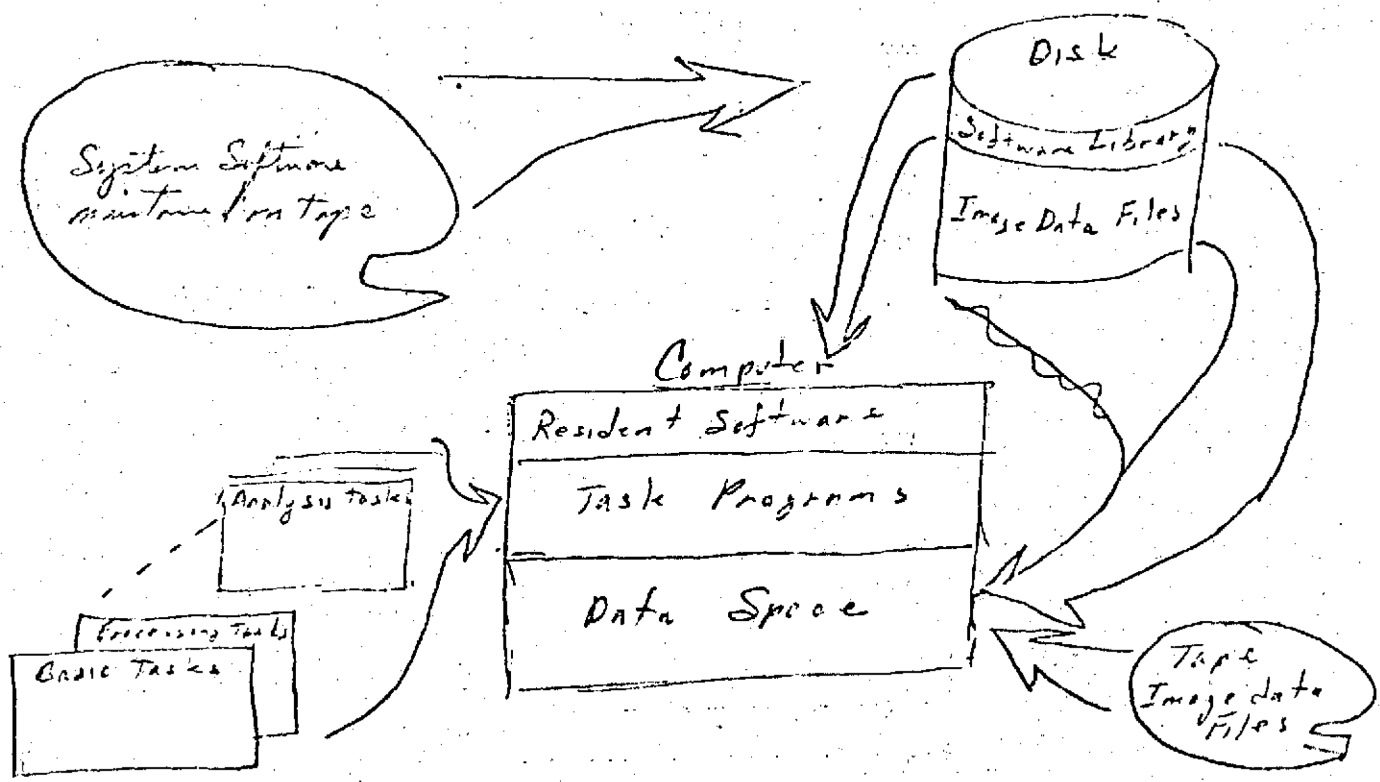

Fig. D.2.4-8 Modular LUS Software Organization

ORIGINAL PAGE IS
OF POOR QUALITY

Image data files are stored by image and band when on the disk, and can be used in different forms. For example, working files are required during date processing and would be in the form of raw pixel data, radiometrically corrected pixel data, or geometrically corrected data.

These files are exchanged from tape-to-disk-to-memory-to-tape during the correction operations. This type of overlay is necessary because one TM image contains about 29 M bytes or 15M 16-Bit computer words. Neither the computer memory nor the disk can hold the entire 6165 x 6165 pixel storage as a unit. The disk will almost hold one image, but some space for the software library is maintained on the disk for rapid use during the processor task overlay operations.

The more interesting software is that for the operational tasks. These are divided into three general areas: Basic, Processing, and Analysis. Basic task software is used to move data and task programs into and out of the computer memory, provide operator control of the LUS, and return information or data sets for review. Processing tasks are associated with the radiometric and geometric correction of pixel data, and image analyses or enhancement is performed with the analysis task software modules.

A general picture of the modular software operation is that the computer resident software performs basic functions that enables the processing and analyses task (or application) software to work within the LUS. It brings the needed task programs into the computer and moves pixel data to and from the disk, tape, or display, depending upon the task in progress. Table D.2.4-4 summarizes the task software so far considered for the LUS.

TABLE D.2.4-4 LUS TASK SOFTWARE SUMMARY

TASK TYPE/ IDENTIFICATION		FUNCTION	
Basic	/ B1	Initialize disk and computer software from tape	
	B2	TTY Operator Language	
	B3	CRT/Keyboard Operator Language	
	B4	Antenna System Control	
	B5	Program Track Change	
	B6	Acquisition Data to Tape/Sensor Calibration	
	B7	Display Image	
	B8	Basic Move Data, Label Data, Open Data File, Error Check. Read Label, Write Line, Display	
	B29	Message, etc.	
	B30	General Purpose, Read Bytes, Write Bytes, Store Bytes,	
	B45	Convert Bytes, etc.	
Processing	/ P1	Radiometric (Nearest Nabor)	/ 1 Band TM
	P2	Radiometric (Bilinear)	/ 1 Band TM
	P3	Radiometric (Cubic Convolution)	/ 1 Band TM
	P4	Radiometric	/ 3 Band TM
	P5	Radiometric (As above)	/ 3 Band TM
	P6	Radiometric	/ 3 Band TM
	P7	Radiometric	/ HRPI
	P8	Radiometric (As above)	/ "
	P9	Radiometric	"
	P10	Convert map coordinates from UTM to Geographic	
	P11	Convert map coordinates from Geographic to UTM	
	P12	GCP Fourier Transform	
	P13	Print Thematic Map	
	P14	Compound Image	
	P15	Superimpose Grid	
	P16	Change pixel scale factor (2048 x 2048 => 512 x 512)	
	P17	Generate Test Pattern	
	P18	Copy Color Image	
Analysis	/ A1	Enhance image contrast (intensity level conversion)	
(General Purpose)	A2	Compute intensity level frequency of occurrence and print histogram	
	A3	Digital filter for reduced blur (image enhancement)	
	A4	Image convolution	
	A5	Update geographic reference	
	A6	Correlate two images	
	A7	Correlate three images	
	A8	Correlate four images	
	A9	Spacial resection	
	A10	Rotate Image	
	A11	Translate Image	
	A12	Linear piecewise geometric transformation	
	A13	Change Detection (2 image cross correlation)	
	A14	Add, Subtract, linear combine two image analysis	
	A15	Haning, Haning convolution smoothing	

Detailed software design has not been accomplished. However, software development estimates are available for the software to control the LUS during data acquisition, move the data to tape, to disk, to radiometrically and geometrically correct the data and to display B & W and color images. Based on the use of experienced minicomputer programs with image handling experience, a completed top level software work can be accomplished within 36 man months of programmer effort. Estimating experienced programmer costs at $4K per man month (including overhead) the minimum software development cost is estimated at $144K. Considering basic software documentation and uncertainties in the estimating (including some contingency) at least $200K should be allocated for the basic software work.

No attempt is made currently to estimate the analysis task software costs because these are heavily dependent upon the particular bus operator's area of interest. Therefore, only a minimum software development cost is made at this time. The current estimated software cost is nonrecurring, however, and would add a minimum of $20K to each of 10 LUS's to $2.K to each 100 Units.

D.2.4.6 Centralized APDL and LDEL Costs

Centralized LUS software development and hardware costs are currently estimated from experience only; detailed estimation has not yet been accomplished. Based, however, on the hardware cost for the Enhanced II LUS, and considering costs of card and tape readers punches, high speed line printers, and other programming conveniences, at least two sets of hardware are necessary at estimated costs of $350K each.

Similarly, software costs for the APDL and LDEL can only be estimated from experience based upon systems of assured complexity. This experience indicates the minimum software development costs should equal the hardware costs with an additional 50 percent contingency and documentation cost.

Therefore, at this time, the APDL and LDEL hardware costs are estimated at $700K, and the initial software development and documentation costs are estimated at (1.35 X 700) $945K. These two costs total to an estimated of $1,645K.

D.2.4.7 - LUS RF/IF

System Requirements: The low cost ground terminals under consideration must be capable of receiving a 20 Mbps biphase modulated X-band carrier with a received signal level at the input to the antenna of approximately minus 140 $dBW/m^2/4$ kHz (the CCIR recommended maximum SPFD level). They must also be capable of tracking at a rate greater than 3^o/min when at elevation angles greater than 44^o.

System Design Options: The type of equipment of the LCGS includes:

(1) A 4 to 8 foot X-band reflector, feed and servo system capable of 3^o/min at elevation 44^o.

(2) A low noise uncooled paramp, a tunnel diode or an FET preamplifier.

(3) A manual, programmed or automatic tracking mechanism.

(4) A receiver (down-converter and demodulator) capable of 10^{-5} BER with a 12 -13 dB input SNR.

The configuration currently considered most prominent will yield a signal margin of approximately 3 dB and will consist of:

(1) A 4.0 to 8.0 foot antenna

(2) A low noise uncooled paramp

(3) A programmed tracking mechanism

(4) A receiver capbale of 10^{-5} BER with a 12 dB SNR input

A functional block diagram is given in Figure D.2.4-9.

Other system configurations are being studied. Most prominent among these is the use of a larger ground antenna (approximately 10 ft.) and FET low noise preamplifier. This configuration could lead to a cost saving of approximately $30K per system. Following careful consideration of all feasible system configurations, an LCGS configuration will be selected with the required cost/capability for maximizing local user access to the EOS.

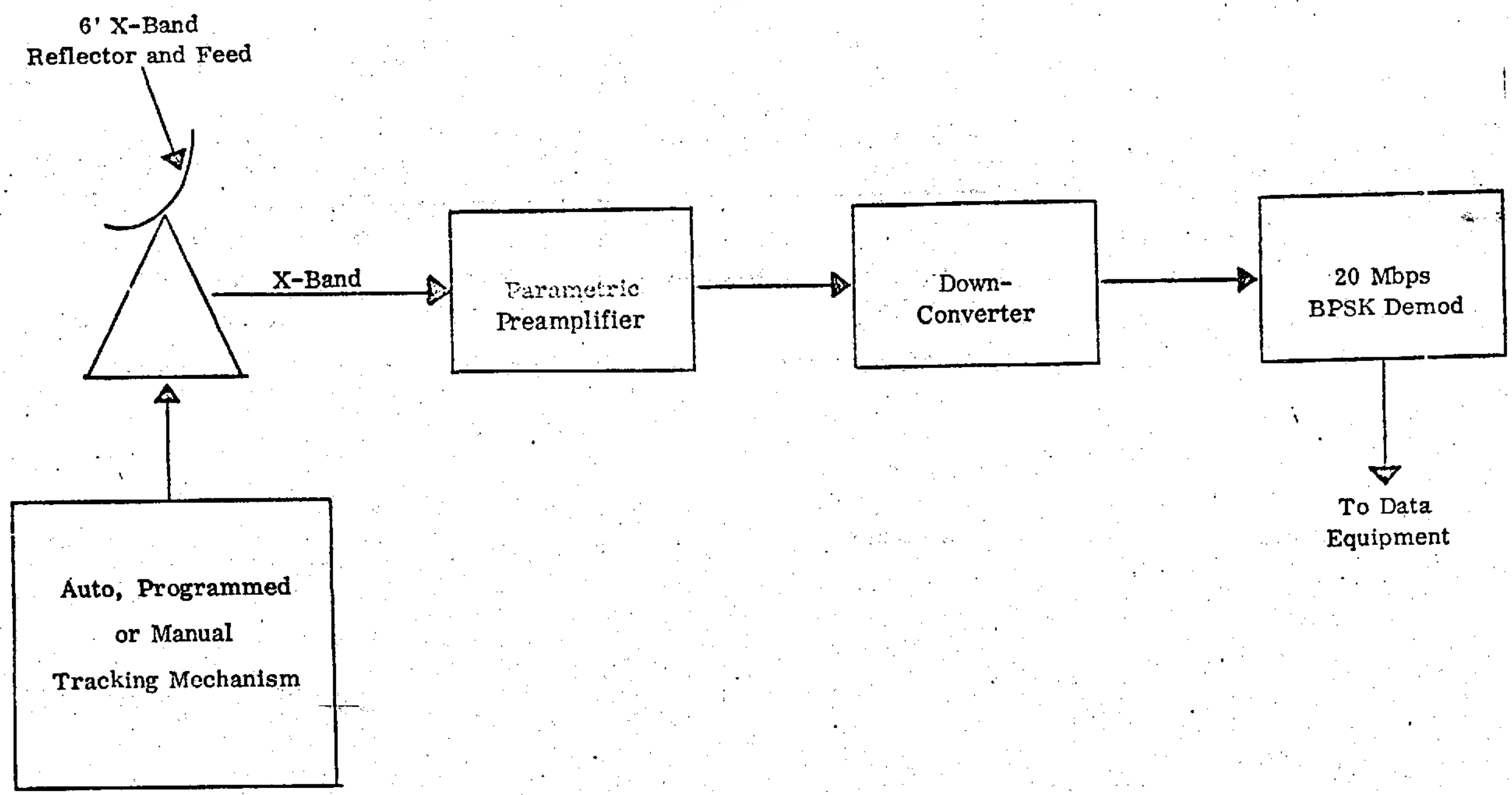

Figure D.2.4-9 Low Cost Ground System (20 Mbps) BPSK Local User Link
(Baseline Configuration)